Marshall Digital Scholar

2014

Cardiovascular Aging in the Female F344xBN Rat Model

Jacqueline C. Fannin
decker8@marshall.edu

Follow this and additional works at: http://mds.marshall.edu/etd

Part of the Circulatory and Respiratory Physiology Commons

Recommended Citation

Cardiovascular Aging in the Female F344xBN Rat Model

A dissertation submitted to
the Graduate College of
Marshall University

In partial fulfillment of
the requirements for the degree of
Doctor of Philosophy

in

Biomedical Sciences

by
Jacqueline C. Fannin

Approved by
Eric R. Blough, Ph.D., Committee Chairperson
Todd Green, Ph.D.
Richard Egleton, Ph.D.
Nalini Santanam, Ph.D.
Elsa Mangiarua, Ph.D.

Marshall University
May 2014

DEDICATION

To my wonderful Savior and Creator who has blessed me with the opportunity to study His

creation and to become an heir to His kingdom through His loving sacrifice.

For you formed my inward parts; you knitted me together in my mother's womb.

I praise you, for I am fearfully and wonderfully made

Wonderful are your works; my soul knows it very well.

Psalm 139:14

ACKNOWLEDGMENTS

Without the sacrifices or help from the following the completion of this dissertation would not have been possible. I owe my deepest gratitude to my loving husband and children. I know that there were many hours spent away from them in order to complete this dissertation. The sacrifice that they have made to help me achieve this goal will not be forgotten. This dissertation has taught me to not take for granted the time that I have with my loved ones as well as to appreciate the sacrifices of other scientists. My husband and children were my inspiration, motivation, as well as a refuge in the preparation for this dissertation. My parents and grandparents are also big contributors in helping to achieve my Ph.D. Similarly, since my first day of kindergarten to the defense of this dissertation my parents and grandparents have always been an inspiration and have provided me with the best opportunities for a quality education. My family has supported me mentally, physically, financially, as well as spiritually through the twenty one years of schooling I have completed thus far. I hope that I can provide the same love and support that my parents and grandparents have given me to my children's future.

Thirdly, I would like to deeply thank my advisor, Dr. Eric Blough. From the beginning of my research career he has encouraged me and helped me to fulfill my dream of having a career in biomedical sciences. He not only provided me with an excellent education and work environment but provided an example of a person having a successful career, great family as well as coworker relationships.

The love and support of my in-laws, friends, and colleagues has also been important in the completion of this dissertation. In the times that I needed someone to watch my kids so I could work on my dissertation I could always rely on my mother- and father-in-law, Robin and Bill

CONTENTS

LIST OF FIGURES

LIST OF TABLES

LIST OF SYMBOLS AND ABBREVIATIONS

4-HNE	4-hydroxynonenal
8-OHDG	8-hydroxy-2'-deoxyguanosine
AALAC	Association for Assessment and Accreditation of Laboratory Animal Care
ACE	Angiotensin converting enzyme
Ach	Acetylcholine
AIF	Apoptosis inducing factor
ALB	Albumin
ALB/GLOB	Albumin to globulin ratio
ALP	Alkaline phosphatase
ALT	Alanine aminotransferase
Amax/AVmax	Maximal aortic valvular blood flow velocity
AMPK	Adenosine monophosphate-activated protein kinase
AMY	Amylase
ANOVA	Analysis of variance
B6	C57Bl/6J mice
Bad	Bcl-2-associated death promoter
Bax	BcL-2-associated X protein
Bcl-xL	B-cell lymphoma-extra larger
BSA	Bovine serum albumin
BUN	Blood urea nitrogen
BUN/CRE	Blood urea nitrogen to creatinine ratio
BW	Body weight
Ca^{2+}	Calcium
cAMPK	Cyclic AMP-dependent protein kinase
Cat	Catalase
CDC	Center for disease control
COX-2	Cyclooxygenase 2

CRE	Creatinine
c-Rel (Rel)	Proto-oncogene c-Rel
CSA	Cross sectional area
CVD	Cardiovascular disease
Cx43	Connexin 43
DAPI	4', 6-diamindino-2-phenylindole
E/A	Early (E) and late (A) ventricular filling velocity ratio
ECHO	Echocardiogram
E-E'	Transmitral to mitral annular early diastolic velocity ratio
EF	Ejection fraction
EKG	Electrocardiogram
Emax	Slope of the left ventricular end-systolic pressure-volume relation
eNOS	Endothelial nitric oxide synthase
E-selectin	CD62 antigen-like family member E
ESV	End systolic volume
F344	Fischer 344 rat
F344xBN	Fischer 344/NNiaHSd x Brown Norway/BiNia
FS	Fractional shortening
FSH	Follicle stimulating hormone
Gata4	Gata transcription factor 4
GLU	Glucose
Glob	Globulin
Gpx	Glutathione peroxidase
Grx1	Glutaredoxin 1
GSH	Glutathione
H_2O_2	Hydrogen peroxide
HCN	Potassium/sodium hyperpolarization-activated cyclic nucleotide-gated ion channel
HE	Hydroethidine
HO$\cdot$	Hydroxyl radical

HOCl	Hypochlorous acid
HRP	Horseradish peroxidase
Hsp	Heat shock protein
HW	Heart weight
ICAM-1	Intercellular adhesion molecule 1
IKβ	Iκβ kinase
IKKα	Inhibitor of nuclear factor kappa-B kinase subunit alpha
IKKβ	Inhibitor of nuclear factor kappa-B kinase subunit beta
IL-1	Interleukin-1
IL-1β	Interleukin-1 beta
IL-2	Interleukin-2
IL-6	Interleukin-6
IL-8	Interleukin-8
iNOS	Inducible nitric oxide synthase
IVRT	Isovolumic relaxation time
IVS	Interventricular septum
JNK	c-Jun N-terminal kinase
K^+	Potassium
KDa	Kilodalton
Kg	Kilogram
KRB	Krebs-ringer bicarbonate buffer
LH	Luteinizing hormone
LPS	Lipopolysaccharide
LV	Left ventricle
LVID	Left ventricle internal diameter
LVM	Left ventricular mass
LVMd	Left ventricular mass diastole
LVMs	Left ventricular mass systole
LVPW	Left ventricular posterior wall

LVPWd	Left ventricular posterior wall diastole
LVPWs	Left ventricular posterior wall systole
MAPK	Mitogen activated protein kinase
MCP-1	Monocyte chemotactic protein-1
Mg	Milligram
MHz	Megahertz
Ml	Milliliter
M-mode	Motion mode
MnSOD	Manganese superoxide dismutase
MR	Mitral regurgitation
mRNA	Messenger ribonucleic acid
mtDNA	Mitochondrial deoxyribonucleic acid
MV decel	Mitral valve deceleration
MVmax	Mitral valvular blood flow velocity
N.A.	Not applicable
Na^+	Sodium
Na^+/K^+	Sodium to Potassium ratio
NADPH	Nicotinamide adenine Dinucleotide phosphate
NF-κβ	Nuclear factor-kappa beta
NF-Kβ (p52)	Nuclear factor-kappa beta p52
NF-Kβ1 (p50)	Nuclear factor-kappa beta 1 p50
NIA	National Institute of Aging
NO	Nitric oxide
N.T.	Not tested
O_2^-	Superoxide radical
ONOO-	Peroxynitrite
p44/42	Extracellular signal-related protein kinase
p450	Cytochrome p450
p53	Tumor protein 53

pAkt	Phosphorylated Akt
PBS	Phosphate buffered saline
PBS-T	Phosphate buffered saline with tween
Phos	Phosphorus
PI3K	Phosphoinositide 3-kinase
PKG-I	Protein Kinase G-I
PLA2	Phospholipases A2
PSR	Picrosirius red
PVC	Premature ventricular contraction
PVmax	Pulmonary valvular blood velocity
RelA (p65)	Transcription factor p65
RelB	Transcription factor RelB
ROO-	Alkyl-peroxyl radical
ROS	Reactive oxygen species
RV	Right ventricle
RVd	Right ventricle diastole
RyR2	Ryanodine receptor 2
S-1P	Sphingosine-1-phosphate
SD	Standard deviation
SDS-PAGE	Sodium dodecyl sulfate polyacrylamide gel electrophoresis
SEM	Standard error of the mean
SERCA	Sarco/endoplasmic reticulum Ca^{2+}
SHR	Spontaneously hypertensive rat
SOD	Superoxide dismutase
SP1	Specificity protein 1
TBIL	Total bilirubin
TNF-α	Tumor necrosis factor alpha
T-PER	Tissue protein extraction reagent
TSP-1	Thrombospondin 1

TUNEL	Terminal deoxynucleotidyl transferase dUTP nick end labeling
TVmax	Tricuspid valvular blood velocity
VAT	Ventricular activation time
VCAM-1	Vascular cell adhesion protein 1
VSMC	Vascular smooth muscle cells

ABSTRACT

Despite continued advances in medical care, cardiovascular disease (CVD) remains the leading cause of death for American women [1]. Although humans and non-human primates are the only mammals to experience menses, rodent models are commonly used to study age-associated cardiovascular alterations due to similar ovarian aging, low expense, and short lifetime to investigate cardiovascular aging. Previous studies have found that aging in the female rodent is characterized by increased ventricular apoptosis, elevations in oxidative-nitrosative stress, ventricular remodeling, increased collagen content, mild systolic and diastolic dysfunction, and reduced occurrence of arrhythmias compared to males [2-7]. Similarly, age-associated alterations in the female rodent aorta have been shown to include increased proliferation/migration of vascular smooth muscle cells (VSMC) and endothelial dysfunction [8, 9]. However, no study has investigated the age-associated alterations in the female heart and aorta of the National Institute of Aging (NIA) approved Fischer 344/NNiaHSd x Brown Norway/BiNia (F344xBN) rat model. The NIA has recommended the F344xBN due to its longer maximal life span, higher age for 50% mortality, and the fact that it exhibits a normal distribution of age-related pathologies at later ages [10, 11]. Here, we investigated the effects of aging on cardiovascular structure and function in the adult, aged, and very aged female F344xBN rats. Compared to adult hearts, increased age was associated with increases in oxidative-nitrosative stress, oxidative damage, (increases in hydroethidine (HE) staining, 4-hydroxynonenal (4-HNE), and nitrotyrosine expression), and activation of the mitochondrial-mediated apoptosis pathway (increased number of terminal deoxynucleotidyl transferase dUTP nick end labeling (TUNEL) positive nuclei, increased activation of caspases, and Bax/Bcl-2 ratio). Age related changes in cardiac structure consisted of an

increase in heart to body weight ratio, cardiomyocyte cross sectional area (CSA), posterior wall thickening, and left ventricle chamber dilatation. Coincident with these changes in cardiac structure and signaling, we also found that increased age was associated with evidence of diastolic dysfunction, alterations in heart rhythm intervals, and alterations in connexin 43 (Cx43) expression. The incidence of arrhythmias was not different with age; however, valvular dysfunction was increased. In the female F344xBN aorta there was an age-associated increase of intima-medial thickness and activation of p44/42 MAPK. Taken together, these results suggest that the female F344xBN rat may be an appropriate cardiovascular aging female rodent model in the absence of pathologies. (378 words)

CHAPTER 1

INTRODUCTION

Cardiovascular disease is the leading cause of death in the United States. The costs associated with treating CVD are expected to increase to $1.48 trillion by 2030 [12]. In addition to the modifiable risk factors (such as lipid levels, diabetes, sedentary lifestyle, etc.) aging, in and by itself, is thought to be a major risk factor for the development of CVD [13] as greater than 80% of cardiovascular deaths occur in adults 65 years of age and older[13, 14, 15]. Cardiovascular aging is associated with a loss of cardiomyocytes by apoptosis, hypertrophy of remaining cardiomyocytes, and increases in tissue fibrosis which can lead to systolic and diastolic dysfunction [16-20]. These age-associated changes can lead to a decline in cardiac function causing the elderly heart to fail [14, 15, 21].

It has been estimated that the costs of treating heart disease will increase 46% by 2025 as people continue to live longer and longer [22, 23]. Although the projected increase in CVD as well as its impact on healthcare cost is known, the effect of sex on cardiovascular risk is not well understood. Recent work has suggested that premenopausal women have a decreased risk of CVD compared to men of comparable age; however, this cardio-protective benefit appears to be lost in postmenopausal women [24, 25]. The decreased cardiovascular disease risk in premenopausal women may be due to age-associated sex differences in cardiac structure and function. For example, in healthy aging adults, left ventricular mass and fractional shortening is increased in women compared to men [26-29]. Age-associated sex differences were also found in the incidence of different cardiovascular pathologies. In the Framingham study, there was a

73

greater prevalence of left ventricular hypertrophy in women (69%) after 60 years of age compared to (15%) men. Aged females with aortic stenosis also had better maintenance of left ventricular systolic function and a lower incidence of collagen structural abnormalities [26]. The short and long term prognosis are worse for women after myocardial infarction, however, women have improved survival rates following non-ischemic cardiomyopathy [16-20, 30, 31].

The increase incidence of age-associated CVD has been attributed to the accumulation of free radical species known as reactive oxygen species (ROS) [32, 33].   The free radicals include superoxide anion ($O_2^{.-}$), hydroxyl radical (HO·), lipid radicals (ROO^-), nitric oxide (NO), and non-free radicals such as hydrogen peroxide (H_2O_2), peroxynitrite ($ONOO^-$), and hypochlorous acid (HOCl). Increased ROS levels (due to imbalance of ROS species to antioxidants) can cause oxidative stress that can damage cellular lipids, proteins and DNA which has been shown to lead to cell death [34, 35].

Cardiovascular disease research has mostly been focused on aging male animal models. Although women are also at an increased risk for CVD with aging, very few experimental studies have determined how aging affects the female heart and aorta. The purposes of this dissertation are (i.) to determine the effects of aging on F344xBN cardiac structure and function, oxidative-nitrosative stress, and apoptosis; and (ii.) to investigate how aging may affect aortic morphology and protein signaling. Age-associated alterations would suggest that this aging rodent model may model that seen in the aging human cardiovascular system.

SPECIFIC AIMS

Cardiovascular disease is the leading cause of death, morbidity, disability, functional decline, and healthcare costs in aging women [36]. It is anticipated that a better understanding of the role that aging plays in CVD will increase the quality of life in the aged. The long-term goal of this work is to improve our understanding of the age-associated alterations in the signaling pathways, structure, as well as function of the aging female heart and aorta to determine if the female F344xBN rat is an appropriate aging model to investigate therapeutic strategies to attenuate or reduce age-associated female cardiovascular dysfunction. The *hypothesis* of this dissertation is that the female F344xBN rat will exhibit age-associated alterations in cardiovascular structure and function. We plan to accomplish the goals and objective of this study by pursuing the following three *specific aims* and experimental design (Figure 1.1):

Specific Aim I: To determine if aging in the female F344xBN rat heart is characterized by alterations in heart weight, apoptosis, and oxidative-nitrosative stress.

> **Hypothesis:** The female F344xBN rat heart will exhibit age-associated increases in hypertrophy, apoptosis, and oxidative-nitrosative stress.

Specific Aim II: To determine if the heart of adult and aged female F344xBN undergo age-associated alterations in cardiac function.

> **Hypothesis:** Aging in the female F344xBN heart will be associated with increased systolic and diastolic dysfunction.

Specific Aim III: To determine if the aorta of adult and aged female F344xBN rats undergo age-associated alterations in morphology and signaling transduction.

Hypothesis: Aging in the female F344xBN aorta will be associated with increased intima-medial thickness, increased fibrosis, and activation of mitogen activated protein kinase (MAPK) signaling.

FIGURE 1.1
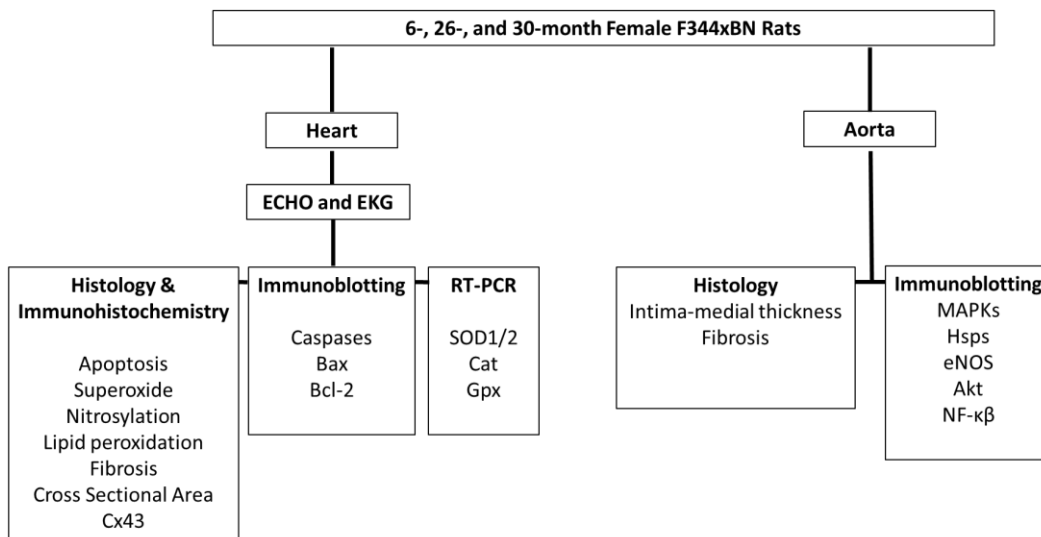
FIGURE 1.1: EXPERIMENTAL DESIGN TO STUDY AGE-ASSOCIATED ALTERATIONS IN THE FEMALE F344XBN HEART AND AORTA.

CHAPTER 2

REVIEW OF LITERATURE

The following chapter consists of the current literature review regarding this dissertation study. The areas to be covered include the following: aging and cardiovascular disease, aging female cardiovascular disease, aging cardiovascular structure and function, aging cardiovascular oxidative stress mechanisms, aging cardiac protein signaling, aging vascular aorta, aging aortic structure and function, and mechanisms of signal transduction in the aging aorta.

AGING AND CARDIOVASCULAR DISEASE

Aging is often thought of as a progressive disorder that decreases an organism's ability to maintain 'normostasis' and reproductive capacity [37]. The functional consequences of aging tend to be cumulative, organ-specific, as well as species-dependent. Aging is also strongly correlated with a higher incidence of several diseases including cancer, diabetes, Parkinson's disease, Alzheimer's disease, and dementia [37]. The majority of definitions of aging are based on calendar age [38]. The World Health Organization has devised a classification scheme in which it considers senility as those 60 years of age. Conversely, in the United States senility is typically defined as those greater than 65 years of age while gerontologists classify using the following three subgroups: younger older people (60-74 years), older people (75-85 years), and very old people (over 85 years) [38, 39].

Aging is considered a major independent risk factor for cardiovascular-related morbidity and mortality [37, 40-42]. According to the Center for the Disease Control (CDC), 12% of adults

have some form of CVD including hypertension, stroke, cardiomyopathies, or heart failure [37].

Of additional concern is the finding that the percentage of men and women presenting clinically

evident CVD increases to 70% over the age of 75 years [38, 39]. Cardiovascular disease deaths

over the last twenty years have been higher for women compared to men in the United States

making CVD the number one killer of women in the Western nations [26, 43-47]. In women,

almost 44% of total CVD deaths occurred in those above 85 years of age while 24% of total CVD

deaths were in men over 85 years [14, 36]. Although cardiovascular risk increases with age in

both sexes, the increase in age-associated risk is sharper in women (Figure 2.1) [45-48].

FIGURE 2.1

Prevalence of CVD in Aging Men and Women
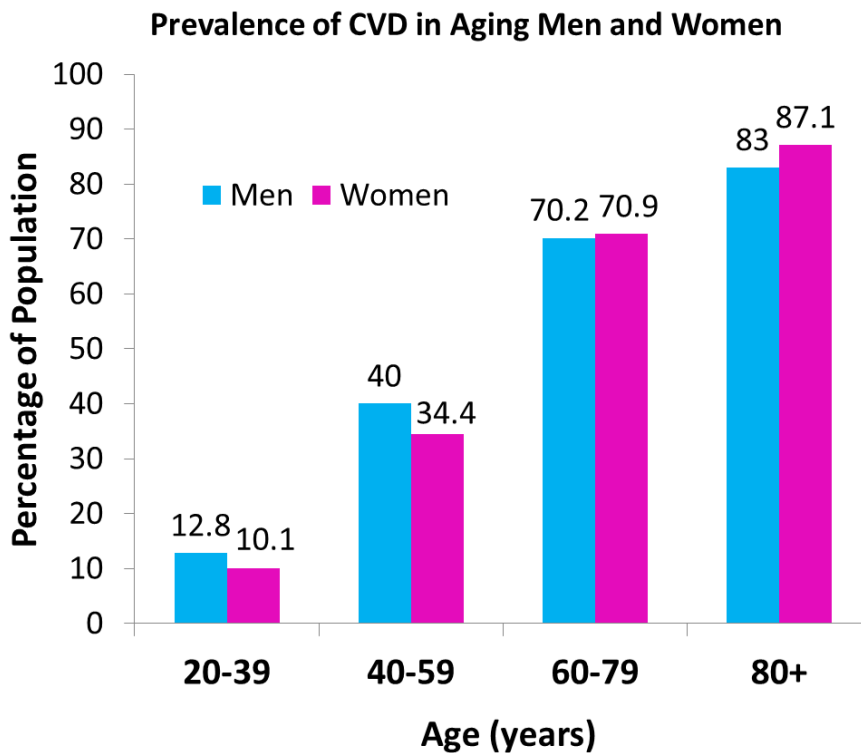
FIGURE 2.1: PREVALENCE OF CVD IN AGING MEN AND WOMEN ACCORDING TO THE AMERICAN HEART ASSOCIATION (2009).

Differences in pathophysiology, presentation, as well as the differences in age-associated cardiovascular function may explain the increased risk of CVD and death in women [44, 49, 50]. Indeed, whereas congestive heart failure in men is oftentimes due to systolic insufficiencies, congestive heart failure in women is often related to diastolic dysfunction [44-46, 50-53]. Similarly, the incidences of ischemia, cardiac failure, cardiac rupture, and ventricular remodeling have also been shown to differ between gender with aging and often lead to worse outcomes in women [20, 26, 27, 54-68].

Aging women appear to exhibit an "age window" during pre-menopause where women have a decreased risk of CVD compared to men of comparable age [24, 69]. This cardio-protective benefit appears to be lost over time as the risk of developing CVD in postmenopausal women is similar to that observed in men of a comparable age [25]. The reason(s) for this increase in CVD risk following menopause is currently unclear but may be related to changes in estrogen levels [70].

AGING FEMALE ANIMAL MODELS

In order to distinguish the physiological as well as molecular alterations that may cause this age-associated gender specific differences in CVD, an appropriate aging model is needed. Human aging research is limited due to cost, differences in lifestyle/history, and more importantly the time required for data collection and analysis of that particular system. There are a number of different animal models that can be used to acquire information on how aging affects the female cardiovascular system. The most common aging female animals studied are non-human primates and rodents. Non-human primates are the closest in regards to female human aging

due to the fact that they undergo menstrual sloughing of the endometrial lining. Although non-human female primates do experience some aspects of menopause in a manner similar to women (irregular cycles, hormone profiles, infertility, weight gain, blood and lipid profiles), non-human female primates differ in that there is a short postmenopausal lifespan, differences in hormone secretion timing, as well as seasonal menstrual cycles [71]. The use of non-human primates as aging models has been limited due to ethical concerns, complicated study logistics, and cost.

Conversely, rodents are widely used in aging research as they exhibit a relatively short lifespan and are genetically quite homogenous. Although rodents do not experience menses, they do experience ovarian aging. Ovarian aging in rodents has been determined to occur over the span of 24 months. In female rodents, reproductive maturity is typically reached at five months when there is an estrous cycle that lasts four to five days. During reproductive maturity, female rats exhibit periods of persistent estrous which consists of elevated and constant levels of estradiol, low levels of progesterone, lack of luteinizing hormone (LH) surges, and ovulation. Ovarian decline occurs between six to eighteen months depending on the rodent strain. This stage is characterized by low levels of estradiol and progesterone along with little or no developing follicles [72]. Between ten to twelve-months of age, increase in the irregularity of estrous cycles often occurs. Constant estrous usually takes place at about nineteen-months of age and is characterized by low to medium levels of serum estradiol, estrone, testosterone, androstenedione, progesterone, and very low levels of 20α-hydroxyprogesterone. In addition to these hormones, there is no preovulatory release of gonadotropin and prolactin. Luteinizing hormone was not changed but follicle-stimulating hormone (FSH) levels were found to be increased in the morning. After twenty four months, the levels of prolactin were increased in

8

aging female rats (Table 2.1).

TABLE 2.1: STAGES OF OVARIAN AGING IN LONG-EVANS FEMALE RATS AS DESCRIBED BY LU et al., (1979).

Age Months (m)	Stages of Ovarian Aging in Female Rat
5m	**Reproductive Maturity:** • Estrous cycle (4 – 5 days) • Elevated and constant levels of estradiol • Low levels of progesterone • Lack of hormone surges and ovulation
6 -8m	**Ovarian Decline:** • Decreased levels of estradiol and progesterone • Little or no follicles
10-12m	**Irregularity of Estrous Cycles**
19m	**Constant Estrous:** • Low to medium levels of serum estradiol, estrone, testosterone, androstenedione, and progesterone • Very low levels of 20α-hydroxyprogesterone • No preovulatory release of gonadotropin and prolactin • Increased levels of FSH
24m	**Prolactin:** • Increased levels of prolactin (abolished by ovariectomy) • Retained ability to develop follicles and corpora • Retained ability to secrete steroid hormones

Comparisons between aging research in female rodent models and humans can be complicated due to the differences in the mechanisms of ovarian/hormone aging in women and its potential impact on CVD. Although not fully understood, it is thought that the loss of the hormones estrogen and progesterone in aging women is due to the decrease in the ovarian follicular reserve [73, 74]. Conversely, aging female rats experience a persistent estrous due to a chronic anovulation, which consists of pseudopregnant/disestrus estrogen levels and high

progesterone levels from increased ovulation and the corpora lutea [73, 75]. Therefore, reproductive senescence in female rats consists of alterations in the hypothalamic-pituitary axis while reproductive senescence in women is classified as ovarian follicle depletion [73, 75].

OVARIECTOMY AND THE AGING CARDIOVASCULAR SYSTEM

In an effort to overcome the lack of menopause in rodents, the use of transgenic models, pharmacological acceleration of aging, and ovariectomy procedures are often performed to better mimic the hormone milieu seen in aging women. Ovariectomy is the removal of the ovaries, which induces a surgical menopause. The cessation of estrogen and progesterone, as well as the reduced production of testosterone, occurs after a surgical menopause. Surgical menopause leads to more severe and sudden symptoms compared to those observed during the natural menopause where ovaries produce lower levels of hormones over time. It is thought that surgery-induced menopause at the time or before natural menopause increases cardiovascular risk in rodents [76, 77].

Other differences have been observed in surgically-induced models of menopause compared to models of natural menopause. Bilateral oophorectomy is associated with different hormonal alterations including changes in estrogen production, reduced levels of progesterone and testosterone, as well as increases in gonadotropins (LH and FSH) compared to those that occur in women who experience natural menopause [78, 79]. Irrespective of age, estrogen levels are higher in women with intact ovaries than in women after bilateral oophorectomy [77, 80, 81]. Interestingly, both natural and surgically-induced menopausal rats exhibit increased FSH and decreased levels of estradiol and inhibin (A/B) [82]. Surgically-induced menopause has also been

shown to alter dopamine receptor affinity in the heart [82]. Other studies have found that the majority of women who undergo natural menopause exhibit differences in age-associated cardiovascular alterations when compared to those seen in surgically-induced menopausal women [73, 74]. It appears that the timing of the surgically-induced menopause may have an effect on the degree of cardiovascular alterations. For example, the elective bilateral removal of the ovaries at a young age is associated with an increased risk for CVD and premature death [77]. Ovariectomy is also associated with alterations in heart structure and function which include increases in cardiac interstitial space, cardiac fibrosis, heart weight, left ventricular weight, reduced cardiac contractility, increased evidence of oxidative stress, cardiac apoptosis, cytokine expression (TNF-α and IL-1β) as well as angiotensin converting enzyme (ACE) and angiotensin II type 1 receptor gene expression [83-87]. When estradiol treatment was given to ovariectomized rats, it prevented the reduction of cardiac contractility as well as the increase in apoptosis and cytokine expression but not elevations in oxidative stress [84, 87]. Taken together, these data suggest that the loss of ovarian function during aging may influence cardiovascular structure and function. Due to the complexities of the aging process, more studies are needed to distinguish whether observed differences are due to aging alone, hormone deprivation, or some combination of both. Due to the difficulties experienced using humans, aging research using rodent models may be an important consideration.

AGING CARDIAC STRUCTURE AND FUNCTION

Aging has been shown to impact many structural and functional aspects of the human heart. Echocardiography (ECHO; a serial noninvasive technique) has demonstrated age-

associated structural alterations including increases in left ventricular wall thickness, myocyte cell volume, a decrease in the number of cardiomyocytes, in addition to increases or no changes in the myocyte to collagen ratio [88, 89]. Age-associated changes in cardiac function include decreases in oxygen consumption, cardiac contractility, and ejection fraction (EF). Systolic function (the ability of the ventricles to contract) is usually preserved, while diastolic dysfunction (ability of the ventricles to fill) is commonly seen in aging humans as evidenced by increases in the diastolic function parameters, isovolumic relaxation time (IVRT) and mitral valve deceleration time (MV decel) [22, 90-96]. Myocardial stiffness, an important factor for diastolic dysfunction, has been shown to increase with advancing age, which may be associated with elevations in left ventricular end-diastolic pressure both at rest and with exertion [97]. Changes in the early to late filling velocity (E/A ratio), which is used to evaluate myocardial stiffness during diastole, also appear to increase with age [98, 99]. In addition to contractile alterations, other data has suggested that the aging heart also exhibits an increased incidence of ventricular arrhythmias, aortic valve sclerosis, and atrial fibrillation [22, 100].

Biochemical techniques have shown that aging is associated with the loss of cardiomyocytes and a compensatory hypertrophy of those myocytes that may remain [99, 101]. Within the cardiomyocyte, the mitochondria become larger and less efficient during aging [99, 102]. At the level of the sarcomere, aging is characterized by a prolonged contraction as well as relaxation due to age-associated changes in cardiac gene expression and calcium regulation [99, 103-105]. In the extracellular matrix surrounding the cardiomyocytes, aging is associated with an increase in collagen, fibrosis, and lipofuscin deposition [99, 106-108]. During exercise, older hearts also tend to increase heart rate to a smaller degree than that seen in the younger animals

which may be due to decrease catecholamine sensitivity or axonal degeneration of sympathetic neurons innervating the atria [99, 109, 110, 111].

RODENT CARDIAC STRUCTURE AND FUNCTION

Unlike that seen in humans, few studies have examined how aging affects cardiac structure and function in rodents. Research thus far has shown conflicting results with some studies demonstrating few or no signs of cardiac dysfunction [94, 112-113], whereas others have shown that the aging rodent heart is characterized by decreases in midwall fractional shortening and diastolic function as indicated by increase in isovolumetric relaxation time [94, 95, 112-115]. Age-associated changes in rodent cardiac structure include cardiomyocyte enlargement as well as reduced number of cardiomyocytes due to necrosis or apoptosis [13]. Other functional changes that have been noted include a prolongation of the action potential, increased cytosolic calcium transient time, increased number of L-type calcium channels, a slowed inactivation of the L-type current, and decreased outward potassium currents [13].

The F344xBN rat has been recommended for age-related studies by the NIA given that this hybrid rat lives longer and has a lower rate of pathological conditions than other inbred rat strains [10-11]. Similar to that seen in aging humans, Walker and colleagues, demonstrated that aging in the F344xBN rats was characterized by progressive diastolic and systolic left ventricular chamber dilatation; mild diastolic and systolic left ventricular hypertrophy; progressive age-associated decrements in resting left ventricular systolic function; and mild diastolic dysfunction, especially in very aged rats [94]. Other parameters of systolic function (ejection fraction (EF), fractional shortening (FS), AVmax, PVmax, MVmax, TVmax) in aged and very aged rats were not

statistically different from those in adult male rats, suggesting cardiac compensation may have taken place to obfuscate mild systolic declines. Most left ventricular structural and functional parameters did not differ significantly in aged and very aged rats, which suggested that most of the age-related changes have occurred or are well underway in the aged rats. In addition, the left ventricular hypertrophy observed in the adult rats appeared to be offset by increases in ventricular apoptosis and the loss of ventricular cardiomyocytes [94].

It has been postulated that age-associated increases in left ventricle mass (LVM), cardiomyocyte enlargement, decreases in cardiomyocyte number, and increases in extracellular collagen deposition may be responsible, at least in part, for the increase in arrhythmias seen with aging [116-119]. The aging rodent heart has been characterized as exhibiting a prolonged action potential, delays in total activation time, and decreases in anisotropic conduction velocity. In addition to changes in conduction velocity, aging is also characterized by the generation of abnormal activation patterns that vary in space and time. The molecular mechanisms underlying these alterations are not well understood but some researchers have posited that they may be due to age-associated increases in oxidative stress and fibrosis, as well as changes in ion channel expression [120]. Whether the molecular mechanisms that may be responsible for the age-associated alterations in cardiac structure and function may differ with animal gender is not well understood.

FEMALE RODENT AGING CARDIAC STRUCTURE AND FUNCTION

The increased risk of CVD in women may be due to differences in the type or magnitude of age-associated alterations in cardiac structure and function. Olivetti and colleagues have

demonstrated a small decrease in human heart weight with aging in males but not females [89, 121] Studies have also shown differences in animal model myocyte volume and diameter [89, 121]. Male non-human primates have also been shown to exhibit decreases in left ventricle/body weight, myocyte hypertrophy, and increases in the number of cells undergoing apoptosis when compared to that observed in their female counterparts [121]. Although a limited number of studies have looked at how cardiac structure and function change with age in a rodent, very few have directly investigated how sex may affect cardiac structure and function.

Boluyt and colleagues investigated how aging may affect cardiac and structure in female Fischer 344 (F344) rats using echocardiography. Aging female rat cardiac structural changes included a dilatation of the left ventricle between 13- and 22-months of age. This dilatation was characterized by increases in posterior and septal wall thickness during diastole at 22- and 30-months of age [2]. Aging in the female F344 was also associated with increases in collagen content and collagen cross-linking [4, 122-123]. In addition, Boluyt and colleagues demonstrated mild systolic dysfunction (decline in left ventricle EF, fractional shortening (FS), and velocity of circumferential fiber shortening) in 22-month old animals when compared to young adults and that these changes preceded the development of mild diastolic dysfunction [2, 124]. These authors suggested that this modest decline in systolic function was due, at least in part, to a shift in the amount of alpha and beta myosin heavy chains [2, 123]. Additional work, perhaps using other rodent models is needed in order to truly distinguish if these alterations are due to increasing age or if they are simply specific to the F344 strain.

ARRHYTHMIAS

Proper cardiac function is dependent upon the precise conduction of electrical impulses through the heart. The electrocardiogram (EKG), a readily performed and repeatable diagnostic tool, can measure and record the conduction system of the working heart in order to find abnormalities in cardiac conduction and to diagnose some forms of cardiovascular disease [125-130]. The EKG records a tracing of the depolarization and repolarization of the heart that can be separated into specific waves and intervals (Figure 2.2).

FIGURE 2.2
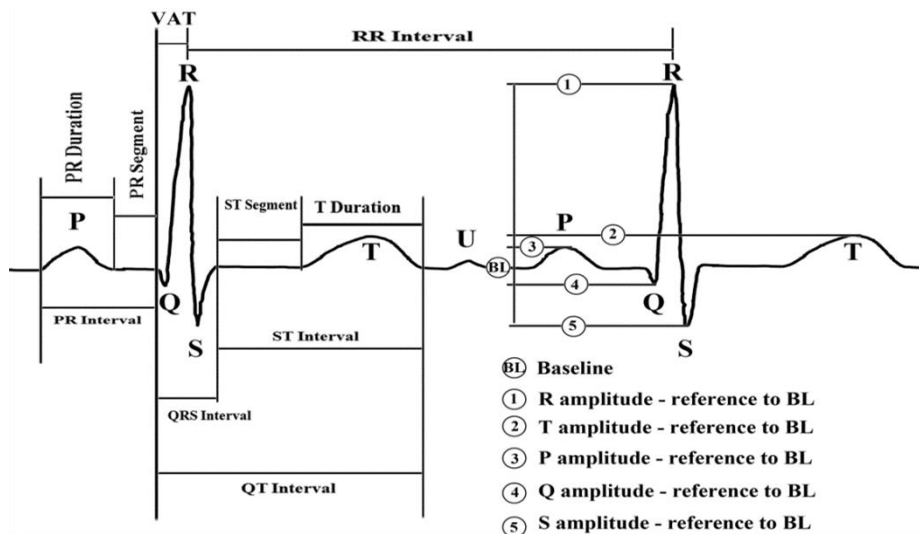
FIGURE 2.2. EKG TRACE ILLUSTRATING THE DIFFERENT WAVES AND INTERVALS IN A HEART RHYTHM.

Aging is considered a risk factor for ventricular arrhythmia [100, 119]. Mirroring the increase in the percentage of elderly is the incidence of atrial fibrillation [130-131]. Age-

associated increases in cardiac fibrosis as well as changes in gap junction morphology have been

hypothesized to cause changes in cardiac conduction in addition to the incidence of arrhythmias

and death [119, 132]. As humans age, there is an increase in the EKG abnormalities which are

associated with increased mortality [132-133]. Men tend to experience more atrial fibrillation,

early repolarizations, Brugada syndromes, and sudden cardiac death than women, while women

are more likely to be at risk to develop long QT syndrome-based arrhythmias as well as

bradycardia-induced torsades de pointes [134-135]. Although sex related differences in cardiac

electrocardiogram parameters have been observed, electrocardiogram abnormalities seem to

vary between studies. In men, there is an increase in QRS duration and sinus cycle length while

women tend to a have a higher heart rate upper limit [136-137].

Electrocardiogram analysis in elderly men and women have demonstrated large or

intermediate Q waves, left axis deviation, negative T-waves, complete right bundle branch block

as well as atrial fibrillation/flutter [138]. In aging men, the QRS complex has been found to be

narrowed while aged women have been shown to undergo a shifting of the QRS axis to the left

[139]. Other work has suggested that aging in men may be associated with a shortened QT

interval, increased PR intervals, and a prolongation of the QT interval [137, 140]. Conversely,

other research found that aging did not appear to alter EKG tracings in either men or women

[137].

Similar alterations in electrocardiogram parameters have also been found in aging

rodents. In Wistar rats, the PR and corrected QT intervals were found to increase with age [132].

Similarly, QRS duration has also been found to be prolonged in old rats [141]. Alterations in aging

electrocardiogram parameters have been shown to be rodent strain dependent and could only

be detected subsequent to heart failure at 19-months of age [142]. Very few studies have investigated electrocardiogram parameters in the aging female rodent. Gonadectomy appears to decrease the number of arrhythmias in male but not female rats [143]. Although not fully understood, these differences have been attributed to higher heart rates in male animals, longer QT intervals, as well as gender differences in ion channel expression [134-135, 144-148]. The exact mechanisms of the reduction of arrhythmias by estrogen are not fully understood but two potential indirect mechanisms have been proposed. One potential indirect mechanism may be related to the ability of estradiol to reduce the incidence of cardiac ischemia [149]. Other work has suggested that high levels of estradiol in female and male rats may directly reduce arrhythmias, possibly by causing a slowing of the inward calcium current [149, 150]. Although multiple studies have investigated EKG changes in aging rodents, these parameters have not been determined in the NIA approved aging F344xBN rat model.

CONNEXIN 43

Gap junction function is particularly important for the proper regulation of cardiac contraction (Figure 2.3). Changes in the expression, activation, and distribution of gap junction protein Cx43 may help to explain alterations in heart rhythm intervals during normal ventricular growth, age, and in some diseases [151-155]. It is thought that increases in Cx43 expression lower the susceptibility to lethal arrhythmias as decreased Cx43 expression has been shown to cause an increase in R-R interval and decreases in intrinsic sinus rate [119, 156-159]. The regulation of Cx43 in different disease states is not well understood. In the spontaneous hypertensive rat (SHR), Cx43 distribution appears altered compared to that seen in the normotensive animals

while Cx43 protein levels have been found to be increased, decreased, or unchanged in animals exhibiting heart failure and atrial fibrillation [157, 160-162]. In diabetic and ischemic hearts, Cx43 levels are unchanged, however, the distribution of Cx43 is altered and its phosphorylation is increased [159, 163, 164]. Other data suggests that alterations in Cx43 expression may work in conjunction with other molecules to regulate cardiac

FIGURE 2.3
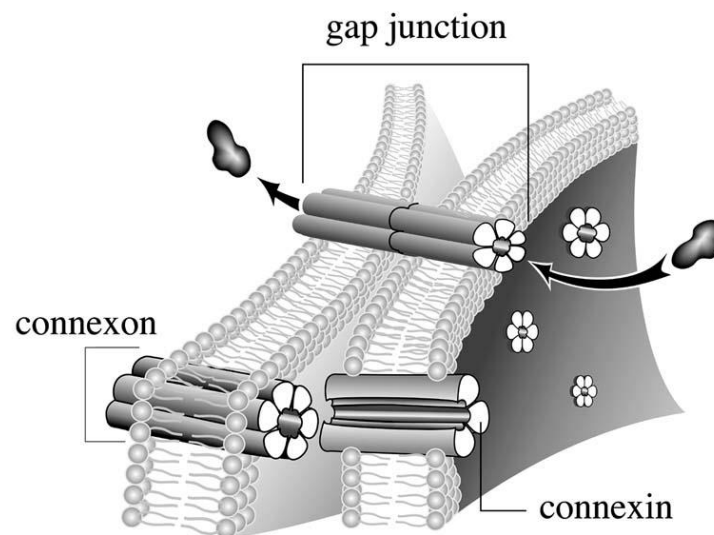
FIGURE 2.3: LOCATION AND STRUCTURE OF GAP JUNCTIONS IN THE CARDIOMYOCYTE MEMBRANE. (Photo credit: Landes Biosciences, 2004)

conduction given the finding that the sodium channel (Nav1.5) expression appears to parallel changes seen in Cx43 [165].

Similar to the differential regulation of Cx43 in different diseases, sex-associated differences in Cx43 have also been observed in aging males and female rats. Cx43 expression has

been shown to be increased in female hearts compared to male hearts [166, 167]. Age-associated sex differences in Cx43 may be regulated, at least in part, by the levels of female and male hormones given that previous work has shown that estrogen increases and testosterone decreases Cx43 expression [135, 168, 169]. Thus far, very few studies have investigated the effects of hormones, ovariectomy, as well as natural menopause on Cx43 expression. One study showed that estradiol administration increased Cx43 expression and phosphorylation during ischemia [170, 171]. These findings are consistent with the possibility that estradiol plays a role in the regulation of Cx43; however, no changes were found in Cx43 expression in the aged ovariectomized female rat heart [172]. Aging studies have also shown conflicting results with regards to the regulation of Cx43. Recent work has demonstrated that Cx43 expression is increased, decreased, or unchanged with aging [159, 173-175].

CARDIAC OXIDATIVE STRESS AND ANTIOXIDANTS

Oxidative stress and reactive oxygen species (ROS) have been implicated in the pathogenesis of several different diseases including Alzheimer's disease, Parkinson's disease, cancer, aging, and CVD [176-181]. ROS are molecules that contain oxygen with an unpaired electron. There are several different species of ROS, including superoxide anions, hydroxyl radicals, superoxide, hydrogen peroxide, and peroxynitrite.

Oxidative stress can result from an increase in oxidant generation or a decrease in the levels of antioxidants. The main source of ROS *in vivo* is aerobic respiration. ROS are also produced by the beta-oxidation of fatty acids, microsomal cytochrome P450 metabolism of xenobiotic compounds, stimulation of phagocytosis by pathogens or lipopolysaccharides (LPS), arginine

metabolism, and tissue specific enzymes [182]. Under normal conditions, ROS are cleared from the cell by the action of superoxide dismutase (SOD), catalase (Cat), or glutathione (Gpx) peroxidase [183]. If excessive, elevated cellular ROS can cause damage to cellular lipids, proteins, and DNA (Figure 2.4).

FIGURE 2.4
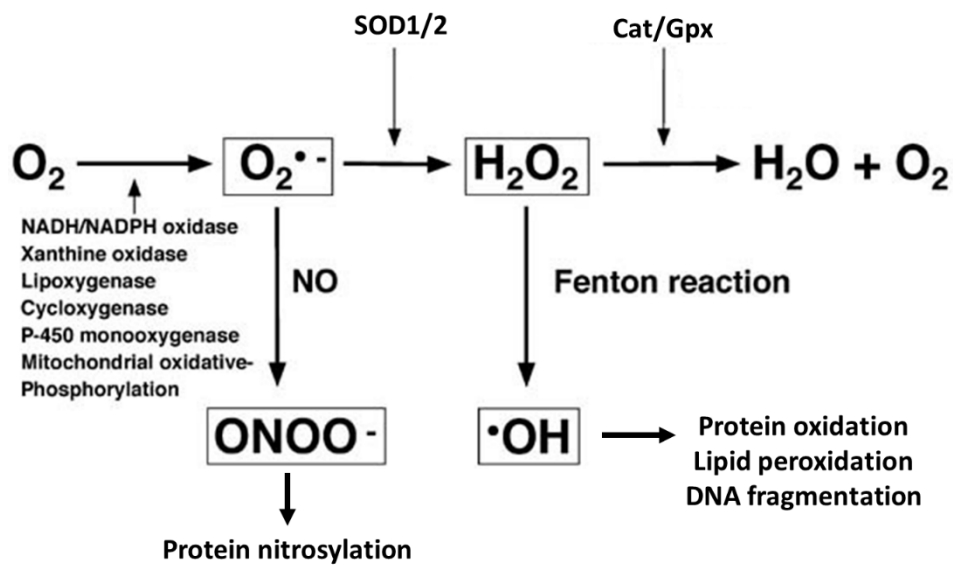
FIGURE 2.4: THE MECHANISM OF REACTIVE OXYGEN-NITROSATIVE SPECIES PRODUCTION AND OXIDATIVE-NITROSATIVE DAMAGE.

AGING RELATED CHANGES IN CARDIAC OXIDATIVE STRESS AND ROS-RELATED SIGNALING

Aging in the heart is associated with the accumulation of oxidative damage to lipids and proteins as well as decline in mitochondrial enzymes [184]. In addition, an increasing amount of mutations in mitochondrial DNA (mtDNA) have been gradually observed during aging [185]. The level of 8-OHDG mtDNA adducts and deletions increase exponentially with age [185]. In human and non-human primate muscle, liver, and brain tissue, complex IV and mitochondrial oxidative

21

phosphorylation enzyme activities decline with age. This decline in function is correlated with

the accumulation of mtDNA mutations, including deletions, and base substitutions [185]. De la

Asuncion and colleagues found increased levels of oxidized mitochondrial glutathione with aging

in rats and mice [186]. Similarly, aged male rat hearts exhibit an increase in superoxide, 4-HNE,

and nitrosative stress levels which appear to be highly correlated to increases in left ventricular

thickness [187]. The exact role that increased levels of oxidative stress may play in the

development and progression of age-associated CVD remains to be determined.

Compared to that observed in females, the hearts of aging male rats exhibited increases

in protein carbonylation, advanced oxidation protein products, nitrotyrosine, non-protein thiol,

reduced glutathione, and iron levels [5]. Although aging is associated with increases in oxidative

stress in both male and female hearts, female rat hearts exhibited lower mitochondrial hydrogen

peroxide production, oxidative damage, and greater mitochondria differentiation compared to

that seen in male animals [6]. It is thought that female rats have a higher mitochondrial

differentiation which is a metabolic adaptation to increase energy efficiency as it is associated

with their lower mitochondrial free radical production and oxidative damage [6]. In addition to

differences with sex, it is also likely that ROS levels vary with animal strain as female Wistar and

F344 rats exhibit lower ROS production and indices of oxidative damage than that seen in female

Sprague Dawley rats which may help to explain their greater mean life-span [188-190].

Reactive oxygen species are signaling molecules that activate signal transduction

pathways. One signaling pathway, MAPK signaling, that is involved in many of the age-associated

physiological changes (oxidative stress, hypertrophy, and apoptosis) as well as other cardiac

pathologies, is activated by ROS. The MAPK cascades are evolutionary conserved

serine/threonine protein kinases that regulate several important cellular functions including proliferation, differentiation, development, cell cycle, and cell death [191]. The major MAPK signaling pathways are the extracellular signal-regulated protein kinase cascade (p44/42), c-Jun amino-terminal kinase/stress-activated protein kinase cascade (JNK/SAPK), and the p38 cascade. Stimuli that include stress or injury typically activate the JNK and p38 MAPK kinases, while the p44/42 MAPKs are stimulated by mitogenic and growth factors [192, 193]. Work investigating MAPK signaling in aging human hearts have demonstrated reduced p38 MAPK activity/signaling in heart failure and impaired activation of MAPK target genes following increase in oxidative stress [194-196]. In the rodent heart, aging has been found to diminish and increase p44/42-, p38-, and JNK-MAPK activation [197-200].

It is well recognized that increases in cellular stress cause the upregulation of the heat shock proteins (Hsp) [201]. Hsp are also involved in cardiac hypertrophy, in response to vascular wall injury, ischemic preconditioning, and aging [202]. During aging there is an accumulation of damaged or misfolded proteins which may cause a burden on maintaining proteostasis [203-205]. An important function of heat shock proteins is to protect against age-related protein misfolding [204-207]. Studies in *C. elegans* and Drosophila have suggested that the overexpression of heat shock proteins increases lifespan [203, 208, 209]. In aged male F344 rats (24-months) it appears that aging decreases Hsp70 upregulation following chronic exercise and heat stress [210-212].

Similar to the MAPK proteins, the nuclear factor-κβ (NF-κβ) pathway is thought to play a role in cardiac remodeling, apoptosis, acute ischemia and reperfusion, unstable angina, as well as heart failure in both humans and rodents [213-218]. . The NF-κβ family consists of RelA (p65), c-Rel (Rel), RelB, NF-κβ1 (p50), and NF-κβ 2 (p52) (Figure 2.5). In the cytoplasm, p50 and p65 are

found as an inactive heterodimer due to the binding of the Iκβ kinase inhibitory proteins (Iκκα and Iκκβ). Cellular stimuli known to activate the NF-κβ pathway include ROS, tumor necrosis factor alpha (TNF-α), interleukin-1β (IL-1β), and bacterial LPS [219]. It has been shown that the Iκβs must first become phosphorylated and degraded before p50/p65 activation can occur [220-221].

Figure 2.5
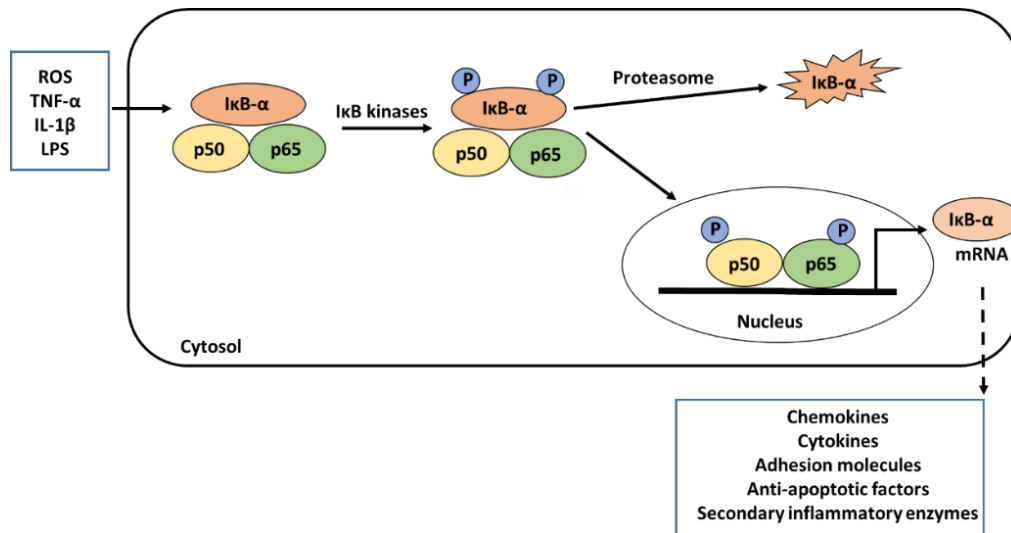
FIGURE 2.5: THE NF-KB SIGNALING PATHWAY.

The NF-κβ signaling pathway induces the transcription of chemokines, cytokines, adhesion molecules, and anti-apoptotic factors in response to increased levels of ROS, TNF-α, IL-1β, and LPS.

p50/p65 when phosphorylated (activated) then translocates into the nucleus to induce the transcription of chemokines (IL-8, MCP-1), cytokines (TNF-α, IL-1, IL-2, IL-6), adhesion molecules (ICAM-1, VCAM-1, E-selectin), acute phase proteins, antimicrobial peptides, secondary

inflammatory enzymes (COX-2, iNOS, PLA2, MnSOD), and anti-apoptotic factors [222-224]. Upon termination of the NF-κβ stimuli, p50/p65 binds to new Iκβs and the complex is translocated back to the cytoplasm. It is thought that the MAPK pathway works in concert with the NF-κβ pathway to increase transcription of inflammatory genes [222-223]. Recent work using transgenic mice has suggested that p50 deletion in increased cardiac inflammation and matrix metalloproteinase activity [225]. Conversely, other work has demonstrated that p50 deletion is associated with decreased matrix metalloproteinase expression and collagen deposition in cardiac tissue [226]. How aging may affect the regulation of NF-κβ pathway signaling is not well understood.

ACTIVATION OF ROS-RELATED SIGNALING IN THE FEMALE AGING HEART

Although the effects of estrogen on MAPK signaling have been studied in several pathological processes, e.g. breast cancer, migraines, and polycystic ovarian syndrome, little is known regarding how this molecule affects MAPK signaling in the heart. It is thought that differences in MAPK activation between male and females may be regulated, at least in part, by the influence of estrogen [227-229]. Estrogen has been shown to stimulate the activation of p44/42 MAPK and JNK MAPK in different model systems including cardiomyocytes, mammary cancer cells, pituitary tumor cells, tissue slices of the hippocampus, and endometriotic stromal cells [230-234]. In males as well as ovariectomized females where estrogen is removed, MAPK signaling is decreased after acute ischemia [227, 229]. In a model of cardiac pressure overload, estradiol treatment appeared to exhibit anti-hypertrophic effects by increasing the expression of atrial naturietic peptide (ANP) and inhibiting p38-MAPK activation [235]. Conversely, in ovariectomized female mice subjected to coronary ligation or transverse aortic constriction,

estradiol treatment had no effect on the activation of p38-MAPK [236]. How aging may affect MAPK signaling in the female heart has yet to be elucidated.

In addition to the regulation of MAPK proteins, there is evidence to suggest that gender also has an effect on the Hsp response. In hearts that were not exposed to increased cellular stress, male hearts have twice as less Hsp72 expression than that observed in the female heart. Conversely, ovariectomy was found to reduce Hsp72 levels in female hearts [237]. Estradiol treatment has also been found to increase Hsp27, Hsp70, Hsp72, and Hsp90 expression in the heart [238-242]. To our knowledge, no studies have looked at Hsp27, Hsp70, and Hsp90 in the aging female heart. More research is needed in order to determine how aging and gender affect the regulation of heat shock proteins in the cardiovascular system.

Aging female and male hearts show increased apoptosis, inflammation, as well as age-associated gender differences found in NF-κβ signaling [234, 243]. To our knowledge, only a few studies have investigated the changes in NF-κβ expression and activity in the aging female rat heart. Recent data has suggested that nuclear NF-κβ binding is increased in the brain, heart, and kidney of aged male as well as female mice even though the levels of p50 and p65 protein were not changed [244-245]. Whether age-related changes in NF-κβ activity are related to increased cardiovascular risk is not yet clear.

AGING HEART APOPTOSIS

Apoptosis or programmed cell death is a highly conserved and regulated cell response to inhibit the abnormal proliferation of cells [246]. Cardiomyocytes are not capable of self-regeneration and are terminally differentiated but can undergo apoptosis, necrosis, or autophagy

when unduly stressed [247]. Apoptosis is increased in many cardiovascular diseases such as dilated and ischemic cardiomyopathy, hypertrophic heart disease, and in arrhythmias [246, 248-251]. Increased age has been shown to cause apoptotic susceptibility in the heart following oxidative injury [252, 197]. Aging in the F344xBN heart is characterized by increases in the amount of cytochrome c, apoptosis inducing factor (AIF), Bax, rate of permeability transition pore opening, and fragmented DNA [253]. The age-associated increase in apoptosis appears to be due not only to the activation of pro-apoptotic molecules but also by decreases in anti-apoptotic NF-κβ, Bcl-xL, and Grx1 signaling [252]. Other work has demonstrated that the aging male F344xBN rat heart is characterized by increases in TUNEL positive nuclei, caspase-3 activation, caspase-dependent cleavage of alpha-fodrin, and diminished phosphorylation of protein kinase B/Akt (Thr308) [254]. The increase of apoptosis in the aging male F344xBN was highly correlated to age-associated increases in oxidative-nitrosative stress. Although not demonstrating cause and effect, these results suggest that the increased cellular ROS and cardiomyocyte apoptosis may play a role in age-related cardiac remodeling.

The incidence of cells undergoing apoptosis in the heart has been shown to differ with sex in humans, primates, and rodents. In humans, a higher number of TUNEL positive myocytes (indice of apoptosis) is seen in young males compared to females [89, 121, 255]. Similar to humans, aging does appears to increase cardiac apoptosis in male monkeys; however, there was no gender difference in apoptosis in male and female B6 mice in addition to the F344 rat [121,188, 190, 256, 257]. These results suggest differences in apoptosis regulation between species. How aging may affect cardiomyocyte apoptosis in the aging female F344xBN rat has, to our knowledge, not been investigated.

EFFECTS OF AGING ON AORTA STRUCTURE AND FUNCTION

Vascular aging, especially the aging aorta, also markedly increases the risk of cardiovascular disease in the elderly population [258, 259]. The aorta, the largest artery in the body, consists of smooth muscle, endothelial cells, fibroblasts, and extracellular matrix which

FIGURE 2.6
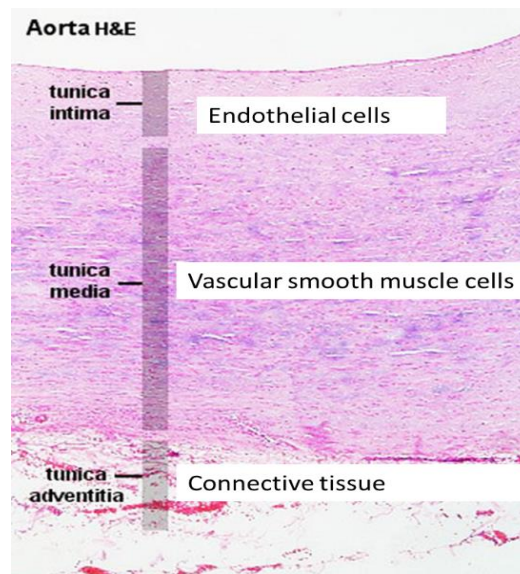
FIGURE 2.6: COMPOSITION OF THE THREE AORTIC LAYERS.

The location and the composition of the three layers of the aorta (tunica intima, tunica media, and tunica adventitia) are shown using a hematoxylin and eosin stain (H&E).

are distributed into three layers - the tunica adventitia, tunica media, and tunica intima (Figure 2.6) [260]. The outer layer of the aorta, the tunica adventitia is composed of collagen, which surrounds the tunica media. The tunica media is primarily composed of smooth muscle, elastic tissue, and extracellular matrix. The inner layer, the tunica intima, consists of a layer of

endothelial cells. Structural changes found in the aging vasculature include an enlarged lumen; intima-medial thickening; irregular shaped endothelial cells; migration and proliferation of VSMCs; increased deposition of extracellular matrix; increased expression of adhesion molecules; and alterations in the expression of metalloproteinases as well as cytokines [13, 42, 261-263]. Functional changes with age in the vasculature consist of impaired distensibility, increased stiffness, increased endothelial permeability, attenuation of β_2-adrenoceptor vasodilator response to agonists, and diminished response to adrenergic receptor stimulation [13, 264-267]. Like humans, rodents also appear to exhibit several age-associated changes in vascular structure and function including changes in intimal thickening, elevations in inflammation-associated molecule expression, and increased evidence of oxidative stress [13, 268-270].

Similar to that seen in other parts of the cardiovascular system, differences in aortic structure and function between genders have also been observed in the aging human and animals. In males, aortic wall and intimal-medial thickness are greater during aging than that observed in women; however, stiffness was not different between men and women [271]. Similarly, there were no differences in distensibility in the aging aorta between men and women [266]. Although the human aging aorta did not show increases in aortic stiffness, it has been documented that the increased vascular stiffness with aging is more prominent in male than female animal models [259, 272].

Abnormal proliferation and migration of VSMCs play important roles in the pathophysiology of atherosclerotic diseases [273, 274]. Previous studies have shown that VSMCs isolated from old animals replicate more actively than those obtained from young animals [274-276]. Similarly, aging has been shown to be associated with an increased proliferative response

29

of VSMCs after balloon angioplasty [277, 278].

EFFECTS OF AGING ON AORTIC ENDOTHELIAL CELL FUNCTION

Endothelial dysfunction is considered to be a common and early feature of vascular disease and impaired endothelium-dependent relaxation has been demonstrated in several animal models of hypertension, experimental diabetes, atherosclerosis, high salt diet, as well as aging [279-281]. The factors regulating endothelial dysfunction are likely complex and may vary between models and with aging. Nitric oxide is a vasodilator that is produced by endothelial nitric oxide synthase (eNOS) that plays a crucial role in blood pressure regulation. NO production is stimulated by shear stress, cyclic strain, acetylcholine (Ach), vascular endothelial growth factor, bradykinin, estrogen, sphingosine-1 phosphate (S-1P), hydrogen peroxide, and angiotensin II [282-285]. It is thought that eNOS activity is regulated by eNOS phosphorylation at Ser1177, Ser635, and Ser617 by phosphatidylinositol 3-kinase (PI3K)/Akt, adenosine monophosphate-activated protein kinase (AMPK), and cyclic AMP-dependent protein kinase (cAMPK) signaling [285, 286]. Given its important role in regulating vascular function it is not surprising that abnormalities in vascular NO production are thought to contribute to the pathogenesis of atherosclerosis and hypertension [287, 288]. Advanced age has also been found to be associated with impaired endothelial NO synthesis and endothelial dysfunction [289-292]. The mechanisms responsible for age-associated alterations in NO synthesis are not fully known but may include changes in activity or expression of eNOS; increased breakdown of NO due to oxidative stress/oxidative injury; changes in antioxidant defense systems; and decreased availability of eNOS substrate, L-arginine [293-299]. Although the activity of eNOS is generally thought to be

diminished with aging, the expression of eNOS has been shown to be decreased, increased, or

not changed in the aorta [8, 300, 301, 302]. In addition to changes in eNOS activity, decreased

NO availability during aging can also be caused by oxidative stress and alterations in eNOS

structure [282, 291, 299, 300, 303-306]. The regulation of eNOS function during aging may also

differ with sex. In aging male but not female mice, eNOS-dependent aortic relaxation is impaired

due to increased production of superoxide by nicotinamide adenine dinucleotide phosphate

(NADPH) oxidase [307]. Whether estrogen may also play a role in modulating eNOS activity is

currently unclear. Although estrogen has been shown to activate eNOS, estrogen studies in

animals have shown no effect or increased eNOS expression following estrogen treatment [8, 308,

309-312]. Conversely, in humans, estrogen replacement appears to be largely ineffective as a

means of decreasing CVD risk [309, 313-316]. To our knowledge no studies have investigated

eNOS expression or function in the aging female F344xBN.

SEX-RELATED DIFFERENCES IN AORTIC VSMCs WITH AGING

In women, the incidence of vascular dysfunction is thought to be related, at least in part,

to the cessation of ovarian hormone production [317, 318]. In VSMCs from young female Wistar

Kyoto rats, estrogen inhibited VSMC proliferation following stimulation with fetal calf serum

[319]. This effect was thought to be mediated by estrogen receptors [319]. Similar decreases in

VSMC proliferation with estrogen treatment following cell stimulation by growth factors or

mechanical stress have also been noted [317, 320, 321]. Like estrogen, progesterone is also

thought to inhibit the proliferation of aortic VSMC, most likely via its ability to inhibit DNA

synthesis [322]. Nonetheless, it should be noted that the effects of estrogen *in vivo* are likely

more complex than that seen in cell culture. For example, in aortas from diabetic female rats, estrogen failed to reverse the impaired basal release of NO and the abnormal relaxation to histamine [323]. The importance of estrogen in the regulation of vascular smooth muscle cells has also been suggested in estrogen receptor knockout models as well as estrogen deficient rodent models. In estrogen receptor knockout mice, there is a reduction in basal NO release as well as increased VSMC proliferation after injury [317, 324, 325]. In the estrogen-deficient aromatase-knockout [184] mouse, VSMCs exhibited abnormal proliferation and apoptosis in addition to slowed growth [317]. Although the effects of estrogen have begun to be investigated in animal models with different levels of estrogen, how alterations in estrogen levels during natural aging may affect aortic structure and function is not well understood.

AGING AORTA SIGNALING

The MAPK signaling pathways function regulates many processes in the aorta including VSMC proliferation, contraction, migration, differentiation, and cell survival [326-330]. Aging has also been shown to increase the activation (phosphorylation) of p44/42 and JNK MAPKs in the aorta while other work has shown that aging affects the ability of the aged aorta to activate p38 and JNK MAPK signaling following mechanical loading [331, 332]. In aged animals, the activation of p44/42 MAPK in vascular smooth muscle was increased compared to young animals [260, 273, 274].

Similar to that observed for the heart, age-associated changes in the expression/activity of NF-κβ were found in the vascular smooth muscle cells of the aorta. Aging has been found to increase the sensitivity of NF-κβ to glucose in aortic VSCM cells [333]. Other research has shown

that VSCM proliferation and NF-κβ activation stimulated by interlukin-1β was increased more in aged female rats than in young female rats [334]. In premenopausal women, receiving hormone treatment appeared to reduce NF-κβ activation [335] suggesting that estradiol reduces NF-κβ activation. How estrogen may inhibit NF-κβ activity is currently unclear but may be related to increased Iκβ levels or decreased levels of circulating TNF-α [335, 336].   Whether age-related changes in estrogen affect the activity of NF-κβ in the aging female aorta remains unclear.

CONCLUSION

The number one killer of women is CVD despite improved medical care and increased awareness/education [26, 43-47, 337-339]. Most cardiovascular deaths occur in women over 85 years of age [14, 36]. Aging is associated with an increased risk of developing cardiovascular disease such as myocardial infarction, stroke, atherosclerosis, peripheral occlusive disease, diabetes, and hypertension [340, 341]. Similar to that seen in humans, cardiovascular aging in rodents is characterized by cardiomyocyte loss, hypertrophy of the remaining cardiomyocytes, increased fibrosis, increased dilation of the lumen, thickening of the media and intima, increased stiffness, and endothelial dysfunction [13, 116, 117, 119, 339]. These structural changes adversely affect aging cardiovascular function by leading to systolic and diastolic dysfunction [114, 342]. In addition to structural and functional changes, there is also evidence that aging may also affect the regulation of several signaling pathways including the MAPK, NF-κβ, eNOS, Hsp, and apoptotic signaling in the heart and aorta [332, 343-346].   It is thought that age-associated increase in oxidative-nitrosative stress and damage may be a possible mechanism to explain alterations in cardiovascular structure, function, and signaling pathways [184, 187].

The exact role that increased levels of oxidative stress may play in the development and progression of age -associated CVD remains to be determined.

The effect of sex on cardiovascular risk has not been fully elucidated; however, data have suggested that pre-menopausal women have a decreased risk in CVD when compared to men of similar age [24, 69]. This cardio-protective benefit appears to be lost over time as the risk of developing CVD in post-menopausal women appears to be similar to that observed in men of a similar age [25]. Humans are the only species that undergo menopause. In order to overcome the difficulties found in aging female human and non-human primate research models (ethics, cost, and long lifespan), rodents may provide the best animal model to investigate age-related changes in cardiovascular structure and function. Although many studies have investigated cardiovascular aging in rodents, very few studies have investigated how aging may affect cardiovascular structure and function in an aged female rodent model (> 26-months) that does not exhibit an increased incidence of age-associated pathologies. Methods of surgically-induced menopause may also complicate age-related research findings given the sudden loss of hormones that are characteristic of this procedure. The NIA recommended male F344xBN rat model has been shown to exhibit many of the age-related changes in cardiovascular structure and function seen in the aged man; however, no study has investigated the age-associated alterations in the female F344xBN rat. In order to distinguish between changes in the cardiovascular physiology and changes that occur with aging, menopause, and their interaction, a better understanding of aging in the cardiovascular system is needed in a natural aging animal model. Whether aging in the female F344xBN rat is a fitting model for the age-related changes seen in human females is currently unclear and is the purpose of this dissertation research project.

CHAPTER 3

THE EFFECTS OF AGING ON INDICES OF OXIDATIVE STRESS AND APOPTOSIS IN THE FEMALE F344xBN RAT

Oxidative-nitrosative stress may play a role in age-associated cardiovascular disease as implied by recent studies. However, limited research has been conducted using aged female rodent models. This chapter details the findings related to the age-associated alterations in cardiac ROS, oxidative-nitrosative damage, and apoptotic signaling outlined in Specific Aim 1.

ABSTRACT

Oxidative-nitrosative stress may play a role in age-associated CVD as implied by recent studies. However, limited research has been conducted using aged female rodent models. In this study, we examined hearts obtained from 6-, 26-, and 30-month old female F344xBN rats in order to examine how aging affects levels of cardiac oxidative-nitrosative stress and apoptosis. Oxidative (superoxide anion and 4-HNE) and nitrosative (protein nitrosylation) stress markers were increased 180 ± 17 %, 110 ± 3 %, and 14 ± 2 %, respectively in 30-month hearts compared to the hearts of 6-month female rats. Coincident with these changes in oxidative-nitrosative stress, aging was also found to be associated with increases in the number of TUNEL-positive cardiomyocytes, alterations in the Bax/Bcl-2 ratio, and elevated cleavage of caspase-3. Regression analysis demonstrates significant correlation in the age-associated changes markers of oxidative–nitrosative stress with changes in apoptotic signaling. The findings from this descriptive study imply that age-associated increases in mitochondrial-mediated apoptosis may

be associated with the increase in oxidative-nitrosative stress in the aging F344xBN female heart.

INTRODUCTION

Aging is thought to be a major risk factor for CVD, and is associated with a loss of cardiomyocytes by apoptosis, and increases in tissue fibrosis which can lead to systolic and diastolic dysfunction [89, 101, 116, 347, 348]. The effect of sex on cardiovascular risk has not been fully elucidated; however, data have suggested that pre-menopausal women have a decreased risk in CVD when compared to men of similar age [24, 69]. This cardio-protective benefit appears to be lost over time as the risk of developing CVD in post-menopausal women appears to be similar to that observed in men of a similar age [25]. The reason(s) for the increased risk of developing CVD following menopause is unclear but may be related to changes in estrogen levels. Recent work has shown that pre-menopausal females appear to exhibit reduced levels of ROS [349]. Similarly, levels of oxidative-nitrosative stress are reduced in pre-menopausal rats or estrogen treated rats due to increases in either antioxidant enzyme activity or increases in potential ROS scavenging [350]. Other studies have demonstrated that the mitochondria-mediated pathway of apoptosis was activated in the heart in ovariectomized rats and this appeared to occur coincident with decreased antioxidant enzyme activity and increased indices of oxidative stress [83, 351]. Although these data are suggestive of estrogen playing a protective role in the cardiovascular system, how the natural loss of estrogen with aging affects cardiac ROS levels is not well known.

Aging in the male F344xBN rat has been found to be associated with declines in cardiac function, increased markers of oxidative-nitrosative stress, and increased cardiomyocyte

apoptosis [187]. Whether these changes are also present in the aging female F344xBN heart is currently unclear. Herein, we examine the effects of aging on indices of oxidative-nitrosative stress and apoptosis in 6-, 26-, and 30-month old female F344xBN rats. Similar to that seen in the aging males, we hypothesized that aging in female F344xBN animals would be characterized by increases in oxidative-nitrosative stress and cardiomyocyte apoptosis. The data presented in this descriptive report support this notion and are consistent with the possibility that age-related increases in oxidative-nitrosative stress in the female F344xBN heart could be responsible, at least in part, for the increased cardiomyocyte apoptosis observed in the aging heart.

MATERIALS AND METHODS

Materials

Protein kinase B (Akt) Akt [#9272], phosphor-Akt(Ser473) [#9271], phosphor-Akt(Thr308) [#9275], Bcl-2 (50E3) [#2870], caspase-12 [#2202], caspase-3 [#9662], cleaved caspase-3 Asp175 [#9661], HSP27 [#2442], HSP90 (#4877), nitrotyrosine [#9691], GAPDH [#2118], 3T3 Control Cell Extracts [#9203], mouse secondary [#7076], rabbit secondary [#7074] and biotinylated protein ladder [#7727] were from Cell Signaling Technology (Beverly, MA). The antibody for HSP70 [#sc-1060], HeLa whole cell lysate [sc-2200], and L6 +IGF Cell Lysate [sc-24127] were purchased from Santa Cruz Biotechnology Inc. (Santa Cruz, CA). Precast 10% and 15% PAGEr Gold Precast Gels were from Lonza (Rockland, ME), Precision Plus Protein Dual Color Standards [#161-0374] were obtained from Bio-Rad (Hercules, CA,) and ECL western blot detection reagent was from Amersham Biosciences (Piscataway, NJ). Restore western blot stripping buffer was purchased from Pierce (Rockford, IL), and the In Situ Cell Death Detection Kit was procured from Roche

Applied Science (Mannheim, Germany). All other chemicals were obtained from Sigma (St. Louis, MO).

Animals

All animal procedures were conducted under the Animal Use Review Board of Marshall University using the criteria outlined by the Association for Assessment and Accreditation of Laboratory Animal Care (AALAC) as proclaimed in the Animal Welfare Act (PL89-544, PL91-979, and PL94-279). Adult (6-months of age, n = 9), aged (26-months, n = 8), and very aged (30-months, n = 8) female F344xBN rats were obtained from the NIA (Bethesda, MD). Two rats per cage were housed in AALAC approved vivarium with a 12 h: 12 h light-dark cycle at $22 \pm 2°C$. Food and water were provided *ad libitum* (LabDiet 5001, PMI Nutrition International, LLC, Brentwood, MO). Animals were allowed to recover from shipping for at least two weeks before experimentation and monitored daily. Rats were removed from the study if they demonstrated signs of failure to thrive such as precipitous weight loss, disinterest in environment, or unexpected gait alterations.

Heart Collection

Rats were anesthetized with an intraperitoneal injection of ketamine (40 mg/kg) and xylazine (10 mg/kg) and supplemented as necessary for reflexive response. Hearts were removed following midline laparotomy, placed in Krebs-Ringer bicarbonate buffer (118 mM NaCl, 4.7 mM KCl, 2.5 mM $CaCl_2$, 1.2 mM KH_2PO_4, 1.2 mM Mg SO_4, 24.2 mM $NaHCO_3$, and 10 mM a-D-glucose; pH 7.4; equilibrated with 5% CO_2/95% O_2 at 37°C), massaged to remove any remaining blood, and quickly weighed before snap freezing in liquid nitrogen.

38

Histological and Immunohistochemical Analysis

Hearts were sectioned (8 µm) onto poly-lysine coated slides using an IEC Minotome Cryostat. The oxidative fluorescent dye, hydroethidine, was used to visualize superoxide *in situ* as previously described [187].   Digitized images were used to determine average pixel intensity of six randomly positioned regions (1000 µm^2) per cross section to calculate the intensity of fluorescent ethidium-stained nuclei. Eight images per section were analyzed with ≥ 500 nuclei per section examined.

Nitrotyrosine immunoreactivity was visualized with immunofluorescence as detailed by the manufacturer. Briefly, sections were washed three times using a phosphate buffered saline with 0.5% Tween 20 (PBS-T) at pH 7.5. Sections were incubated in a humidified chamber at 24°C for 1 h in a blocking solution (5% bovine serum albumin (BSA) with the nitrotyrosine antibody (1:1000 in PBS-T) and then washed three times with PBS. Immunoreactivity was visualized following additional incubation for 30 min with FITC labeled anti-rabbit IgG (1:200) and counterstaining with 4, 6-diamidino-2-phenylindole (DAPI; 1.5 µg/ml). Images were recorded using an Olympus fluorescence microscope (Melville, NY) at 20X.

In situ TUNEL Staining

Cross-sections (8 µm) were fixed with 4% paraformaldehyde, washed with PBS (pH 7.4), and then permeabilized using 0.1% Triton X and 0.1% sodium citrate for 2 min at 4°C before TUNEL staining. Sections were counter-stained for dystrophin immunoreactivity to illuminate the muscle membrane as outlined previously [352].   Terminal deoxynucleotidyl transferase (TdT) and

fluorescein-dUTP (TUNEL reaction mixture) was added to the sections before incubation in a dark

humidified chamber at 37°C for 60 min. After rinsing with PBS, sections were mounted and

counterstained with DAPI to visualize nuclei. Three randomly selected regions from each cross-

section were digitally recorded with a CCD camera (Olympus, Melville, NY) to visualize TUNEL

positive nuclei using an Olympus fluorescence microscope (Melville, NY) with a 20X objective.

Control experiments performed in parallel using DNase 1 or without TdT were used to verify

specificity of labeling.

Isolation of Protein Isolates

Heart samples were pulverized using a mortar and pestle in liquid nitrogen to a fine

powder and weighed. TPER Lysis Buffer (10 μL/mg tissue; Pierce, Rockford, IL, USA) containing

protease (P8340, 10 μL/mL Sigma-Aldrich, Inc., St. Louis, MO, USA) and phosphatase inhibitors

(P5726, 10 μL/mL, Sigma-Aldrich, Inc., St. Louis, MO, USA) was added to each sample and the

samples homogenized for 45 s. After incubation on ice (30 min), this procedure was repeated

and the samples were then centrifuged at 14,000 x g at 4°C for 5 min. After centrifugation, the

supernatants were removed and the protein concentration of each sample was determined in

duplicate using the Pierce Reagent Assay (Pierce, Rockford, IL). Samples were diluted to a

concentration of 1.5 μg/mL in SDS-loading buffer and boiled for 5 min. Thirty micrograms of

protein from each sample were separated using 10% or 15% SDS-PAGE gels.

Immunoblot Analysis

Proteins were transferred using standard conditions onto Hybond nitrocellulose

membranes after electrophoresis [353]. *Rapid Stain* (G-Biosciences, St. Louis, MO) was used to verify the transfer of protein, equal protein loading between samples, and for normalization between gels. Before incubation with primary antibody, membranes were blocked using 5% milk TBS-T for 1 hour, and then incubated with primary antibody overnight (1:1000). After extensive washing in TBS-T, membranes were incubated with horseradish peroxidase-(HRP)-labeled IgG secondary antibodies for 1 h. Protein bands were visualized with ECL western blotting detection reagent before densitometry using a flatbed scanner (Epson Perfection 3200 PHOTO) and the AlphaEaseFC imaging software. The integrated optical densities were kept within a linear and non-saturated range by adjusting the exposure time.

Statistical Analysis

Results are presented as mean ± standard error of the mean (SEM). The SigmaStat 11.2 statistical program was used to perform one-way analysis of variance (ANOVA) for overall comparisons as well as to determine group differences using the Student-Newman-Keuls *post hoc* test where applicable. A ($p < 0.05$) was accepted as the level of significance.

RESULTS

Superoxide production, markers of ROS stress, and protein nitrosylation are increased with aging

Compared to 6-month old animals, body weight (BW) and heart weight (HW) were significantly higher in the 26- and 30-month old rat ($p < 0.05$) (Table 3.2). Hydroethidine which emits fluorescence upon oxidation by superoxide to ethidium bromide, was used to semiquantitatively determine superoxide production in heart tissue sections from each age

group. Compared to 6-month old animals, ethidium fluorescence was 239% and 180% higher in 26- and 30-month female hearts, respectively ($p < 0.05$, Figure 3.1). In a similar fashion, aging increased tyrosine nitration in the 26- and 30-month old animals ($p < 0.05$, Figure 3.2). The modification of proteins due to lipid peroxidation was examined using 4-HNE, a lipid peroxidation metabolite. Compared to 6-month old animals, 4-HNE levels were 71% and 110% higher in the 26- and 30-month hearts ($p < 0.05$, Figure 3.3).

Age-associated cardiomyocyte apoptosis in the female F344xBN heart was associated with caspase activation and changes in the Bax/Bcl-2 ratio

Similar to previous work, TUNEL staining was performed to determine if aging was associated with evidence of increased DNA fragmentation which is suggestive of cellular apoptosis [197, 254, 354, 355]. Compared to that observed in the 6-month animals, the number of TUNEL positive nuclei appeared to be increased in 26- and 30-month hearts (Figure 3.4). Because caspase-3 activation is an important step in the initiation of DNA fragmentation / apoptosis, we next examined if aging was associated with increased caspase-3 cleavage. With aging, total caspase-3 expression was 19% and 29% lower in the 26-month and 30-month hearts, respectively ($p < 0.05$, Figure 3.5). Consistent with these data, this decrease in total caspase-3 levels was paralleled by increases in the amount of cleaved caspase-3 (19- and 17-kDa fragments) of 167% and 290% at 30-months ($p < 0.05$; Figure 3.5). To confirm these findings, we next examined the ratio of Bax (pro-apoptotic) to Bcl-2 (anti-apoptotic). It is thought that Bax promotes apoptosis by forming a homodimer, which becomes inserted into the mitochondrial membrane where it forms a pore that potentiates the release of cytochrome-C from the

mitochondria. With aging, Bax expression was 15% higher at 30-months when compared to that observed in the 6- and 26-month old animals (Figure 3.6). Conversely, the amount of Bcl-2 protein was 13% lower in the 26-month old animals (Figure 3.6). As expected from these data, the Bax/Bcl-2 ratio was 19% higher in 30-month animals compared to that observed for the 6- and 26-month age groups ($p < 0.05$, Figure 3.6).

DISCUSSION

The F344xBN rat exhibits less age-associated pathologies and an increased longevity in comparison to other rat models [10, 11]. Although previous data has demonstrated increased levels of apoptosis and oxidative stress are associated with aging in the male heart, to our knowledge this is the first investigation to examine if these phenomena occur in the naturally menopausal aging female rat model [187, 254]. Herein, we observed evidence of increased superoxide, protein nitrosylation, and lipid peroxidation with aging (Figures 3.1 – 3.3). Why aging may increase ROS levels is not yet fully understood, however, recent data has suggested that alterations in enzymatic activity of the xanthine and NADPH oxidoreductases, the mitochondrial electron transport chain, nitric oxide synthase activity, and lipoxygenase/cyclooxygenase may function as potential contributors [356, 357]. In addition to ROS production, it is thought that the amount of ROS present in the cell at any one time is determined, at least in part, by the balance between ROS generation and breakdown. The antioxidant enzymes, SOD, Cat, and Gpx, are thought to remove ROS thereby functioning to prevent excessive accumulation of ROS [183, 350, 358]. Recent studies have found that antioxidant activity is increased or decreased with age in the rodent heart [359, 360]. Adding to the confusion, we did not find any age-associated

alterations in the messenger RNA (mRNA) expression of SOD1, SOD2, Cat, and Gpx in the female

F344xBN heart (data not shown). Whether age-associated dysregulation in the amount of ROS

produced, decreases in the abundance of antioxidant enzyme expression, or a combination of the

two are responsible for our findings of elevated indicators of ROS in the aging rat heart is currently

not known. Future studies designed to directly examine the regulation of some, or several of the

ROS generating and buffering pathways will be required to extend our understanding of the

relationship between aging and cardiac ROS regulation.

Elevated levels of superoxide are oftentimes associated with increased nitrosative stress

given that superoxide can react with nitric oxide to form peroxynitrite. Peroxynitrite, in turn, can

cause tyrosine nitration and the measurement of nitrosylated tyrosine residues is thought to be

an established marker for nitrosative stress [361]. Similar to that seen in the aging male F344xBN,

we found that aging in the female heart was associated with increased protein tyrosine

nitrosylation (Figure 3.2) [187]. This latter finding is different from previous work using the female

Long-Evans/Wistar rat, which found no change in 3-nitrotyrosine levels with cardiac aging [362].

The reasons for differences between the current study and previous is not entirely clear but may

be related to differences in the animal strain used and/or animal age as the Long-Evans/Wistar

hybrid rats were only 24-month of age at time of sacrifice as opposed to the 26- and 30-month

old animals used in the present study.

Similar to our analysis of nitrosative stress, and like that seen in the aging male F344xBN,

we also observed that aging was associated with increased 4-hydroxynonenal (4-HNE) reactivity

(Figure 3.3) [187]. It is thought that 4-HNE levels are a marker of lipid peroxidation and that

increased levels of 4-HNE can result in alterations in lipid signaling and enzyme inactivation [363].

44

Studies have shown that production of 4-HNE occurs primarily from the mitochondria, and that the mitochondria are the primary target for lipid peroxidation damage [364]. This damage to the mitochondria, if extensive, can lead to alterations in ROS production and the release of cytochrome-C from the mitochondria. To investigate this possibility, we next examined if aging was associated with increased evidence of cellular apoptosis. Similar to that seen in the aging male F344xBN hearts, TUNEL staining suggested the possibility of increased DNA fragmentation with aging in the female F344xBN heart (Figure 3.4) [254]. In an effort to elucidate the mechanism of apoptosis, we next investigated the effects of aging on the expression of proteins involved in apoptotic signaling. It is thought that the mitochondrial-mediated apoptotic pathway employs the activation of caspase-3 [365]. Here we demonstrate that caspase-3 cleavage was increased with age in the female F344xBN heart (Figure 3.5). In a similar fashion, we also found an increase in Bax expression and the ratio of Bax/Bcl-2 with aging (Figure 3.6). Taken together, and like that previously proposed in the aging male F344xBN heart, these data suggest that age-associated increases in cellular apoptosis are mediated, at least in part, by the mitochondrial pathway.

To examine the degree of relationship between the different dependent variables, we calculated the correlation between age, heart weight, number of TUNEL positive cardiomyocytes, HE levels, nitrotyrosine, and 4-HNE. Very high correlation was observed between aging as well as superoxide production, levels of nitrosative-stress marker, and nitrotyrosine (Table 3.2A). Although the exact mechanism(s) cannot be concluded from this data, these findings are consistent with the possibility that the age-associated increases in superoxide production may lead to increased oxidative-nitrosative damage that include elevations in the amount of proteins undergoing 4-HNE and nitrotyrosine modification. Interestingly, we also found that age-

45

associated increases in oxidative-nitrosative damage were highly correlated with activation of the mitochondrial-mediated pathway of apoptosis (Table 3.2B). Whether increases in age-related oxidative damage, as suggested by our nitrotyrosine and 4-HNE data, are responsible for initiating cellular apoptosis is currently unclear and beyond the scope of the present study. Nonetheless, the data of the present study demonstrate that aging in the female F344xBN heart is characterized by increased levels of oxidative stress and pro-apoptotic signaling (Figure 3.9). Whether these biochemical changes result in adaptations in cardiac function is currently unclear and is the focus of ongoing experimentation (Figure 3.7).

TABLE 3.1: THE HEART AND BODY WEIGHTS OF AGING F344XBN FEMALES.

An asterisk (*) and a cross (†) indicate significant differences from the adult (6-month) and aged (26-month) values respectively ($p < 0.05$), n = 8 or 9 hearts per age group.

Group	Body WT (g)	Heart WT (g)	HW/BW ratio (x100)
6m	230.5 ± 5.3	0.76 ± 0.03	0.330 ± 0.009
26m	274.0 ± 4.9*	0.95 ± 0.01*	0.334 ± 0.019
30m	321.3 ± 7.2*†	1.12 ± 0.05*†	0.351 ± 0.011

TABLE 3.2A: THE REGRESSION ANALYSIS OF EXPRESSION LEVELS OF SPECIFIC PROTEINS AND AGE, HE STAINING INTENSITY, PROTEIN NITROTYROSINE LEVELS, 4-HNE LEVELS, HEART WEIGHT, AND TUNEL STAINING INTENSITY OF 6-, 26-, AND 30-MONTH FEMALE F344XBN HEARTS. The following symbols indicate (*) low correlation ($p < 0.05$), (**) moderate correlation ($p < 0.05$), (***) high correlation ($p < 0.05$). P values are found in parentheses below R values. Numbers within parentheses near name of protein indicate protein size in kDa. N.T. (not tested).

	Age	Heart Weight	TUNEL	HE	Nitro-tyrosine	4-HNE
Independent Variable						
Age	N.T.	0.899*** (<0.001)	0.690 (0.40)	0.965*** (<0.001)	0.849*** (0.004)	0.969*** (<0.001)
HE	0.965*** (<0.001)	0.802** (0.009)	0.722* (0.028)	N.T.	0.767* (0.016)	0.905*** (<0.001)
Heart Weight	0.286 (0.455)	N.T.	0.478 (0.193)	0.802** (0.009)	0.911*** (<0.001)	0.448 (0.226)
TUNEL	0.690 (0.40)	0.478 (0.193)	N.T.	0.722* (0.028)	0.597 (0.090)	0.718* (0.029)
Nitro-tyrosine	0.849** (0.004)	0.911*** (<0.001)	0.597 (0.09)	0.767* (0.016)	N.T.	0.907*** (<0.001)
4-HNE	0.969*** (<0.001)	0.924*** (<0.001)	0.718* (0.029)	0.905*** (<0.001)	0.907*** (<0.001)	N.T.

TABLE 3.2B: THE REGRESSION ANALYSIS OF EXPRESSION LEVELS OF SPECIFIC PROTEINS AND AGE, HE STAINING INTENSITY, PROTEIN NITRO-TYROSINE LEVELS, 4-HNE LEVELS, HEART WEIGHT, AND TUNEL STAINING INTENSITY OF 6-, 26-, AND 30-MONTH FEMALE F344XBN HEARTS. The following symbols indicate (*) low correlation ($p < 0.05$), (**) moderate correlation ($p < 0.05$), (***) high correlation ($p < 0.05$). P values are found in parentheses below R values. Numbers within parentheses near name of protein indicate protein size in kDa. N.T. (not tested).

	Age	Heart Weight	TUNEL	HE	Nitro-Tyrosine	4-HNE
Apoptotic Signaling						
Bax	0.263 (0.493)	0.331 (0.385)	0.526 (0.146)	0.111 (0.835)	0.738 (0.094)	0.478 (0.338)
Bcl-2	0.473 (0.199)	0.356 (0.346)	0.981** (0.009)	0.862* (0.027)	0.394 (0.439)	0.637 (0.174)
Casp-9 (51kDa)	0.748 (0.848)	0.326 (0.392)	0.528 (0.144)	0.262 (0.615)	0.554 (0.254)	0.447 (0.347)
Casp-9 (40kDa)	0.782* (0.013)	0.651 (0.058)	0.676* (0.046)	0.837* (0.038)	0.640 (0.171)	0.847* (0.033)
Casp-9 (38kDa)	0.927*** (<0.001)	0.811** (0.008)	0.659 (0.054)	0.923** (0.009)	0.705 (0.118)	0.924** (0.008)
Casp-9 (17kDa)	0.800* (0.01)	0.820** (0.007)	0.665 (0.051)	0.605 (0.203)	0.905* (0.013)	0.865* (0.026)
Casp-3	0.878** (0.007)	0.928*** (<0.001)	0.537 (0.136)	0.940** (0.005)	0.887* (0.019)	0.974*** (<0.001)
Casp-3 (19kDa)	0.612 (0.08)	0.664 (0.051)	0.590 (0.094)	0.421 (0.406)	0.863* (0.027)	0.737 (0.094)
Casp-3 (17kDa)	0.683* (0.043)	0.740* (0.023)	0.598 (0.089)	0.511 (0.301)	0.894* (0.016)	0.804 (0.054)
Akt	0.409 (0.275)	0.899*** (<0.001)	0.474 (0.197)	0.236 (0.653)	0.201 (0.703)	0.052 (0.923)
p-Akt(Ser473)	0.560 (0.117)	0.336 (0.337)	0.690* (0.040)	0.852* (0.031)	0.372 (0.467)	0.634 (0.176)
Heat Shock Proteins						
Hsp70	0.205 (0.597)	0.264 (0.492)	0.536 (0.274)	0.018 (0.963)	0.137 (0.725)	0.134 (0.731)
Hsp90	0.094 (0.809)	0.084 (0.830)	0.132 (0.803)	0.145 (0.710)	0.117 (0.764)	0.058 (0.883)

FIGURE 3.1
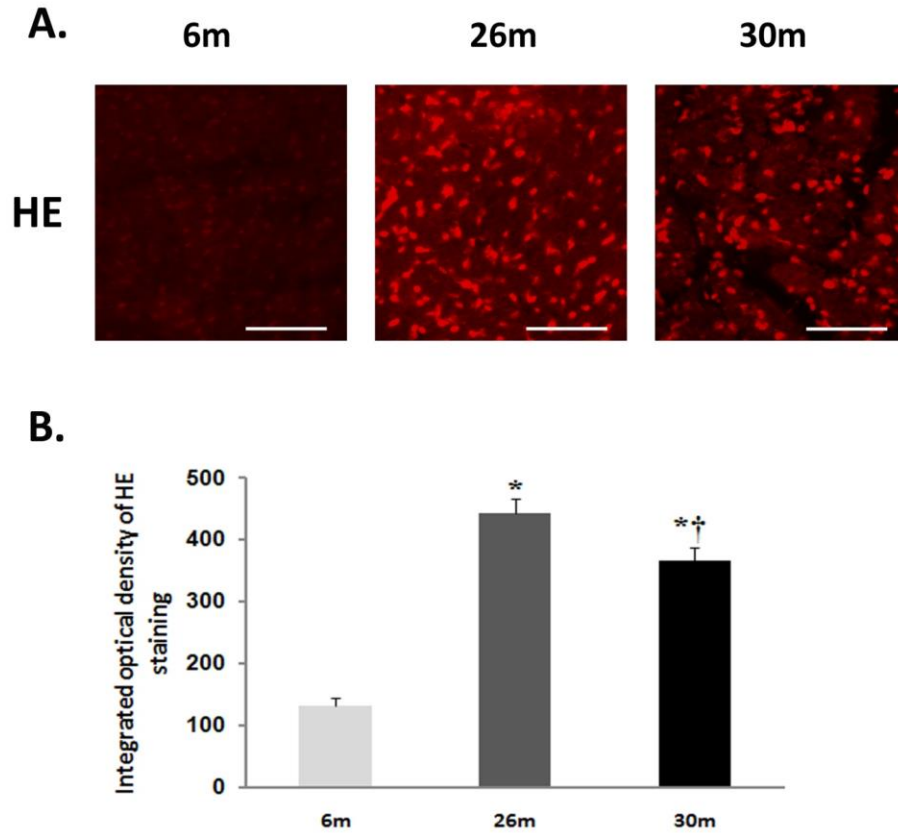
FIGURE 3.1: INCREASED SUPEROXIDE LEVELS IN THE AGING FEMALE F344XBN HEART.

A. The detection of superoxide using the formation of dihydroethidium from hydroethidine staining in 6-, 26-, and 30-month female F344xBN rat hearts. Scale bar = 100 μm.

B. Cardiac superoxide levels were quantified by the intensity of fluorescent Et-stained nuclei and these results were reported as the integrated optical density of pixel by micrometer. Significant differences are indicated by an asterisk (*) and a cross (†) from the adult (6-month) value and aged (26-month) value, respectively ($p < 0.01$).

FIGURE 3.2
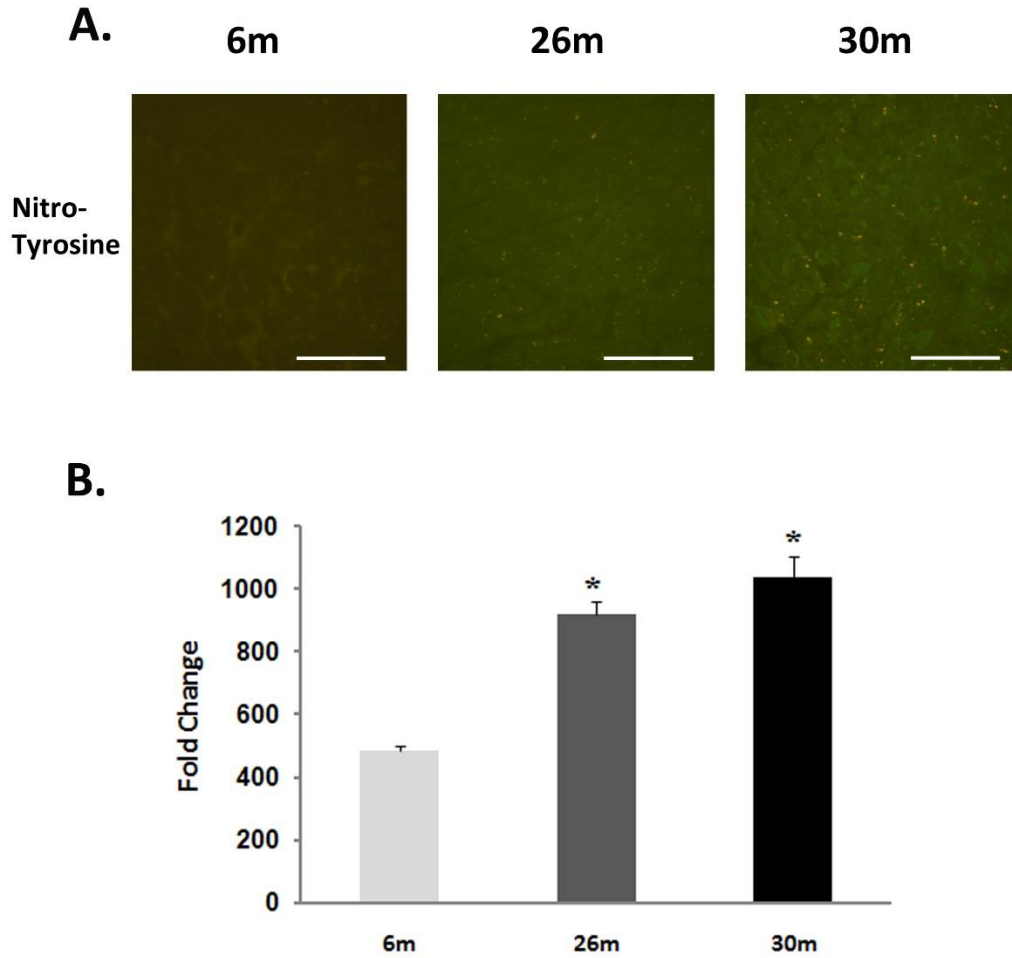
FIGURE 3.2: AGING INCREASES THE NITROSYLATION OF TYROSINE RESIDUES.

A. Immunohistochemical staining of 6-, 26-, and 30-month female F344xBN hearts to determine the nitrosylation of tyrosine residues. Scale bar = 100 μm. **B.** Immunoblot analysis of protein tyrosine nitration in the aging female F344xBN hearts. Results were reported as fold change. Significant differences are represented by an asterisk (*) and a cross (†) from the adult (6-month) value and aged (26-month) value, respectively ($p < 0.05$).

FIGURE 3.3

A. 6m 26m 30m

4-HNE

B.
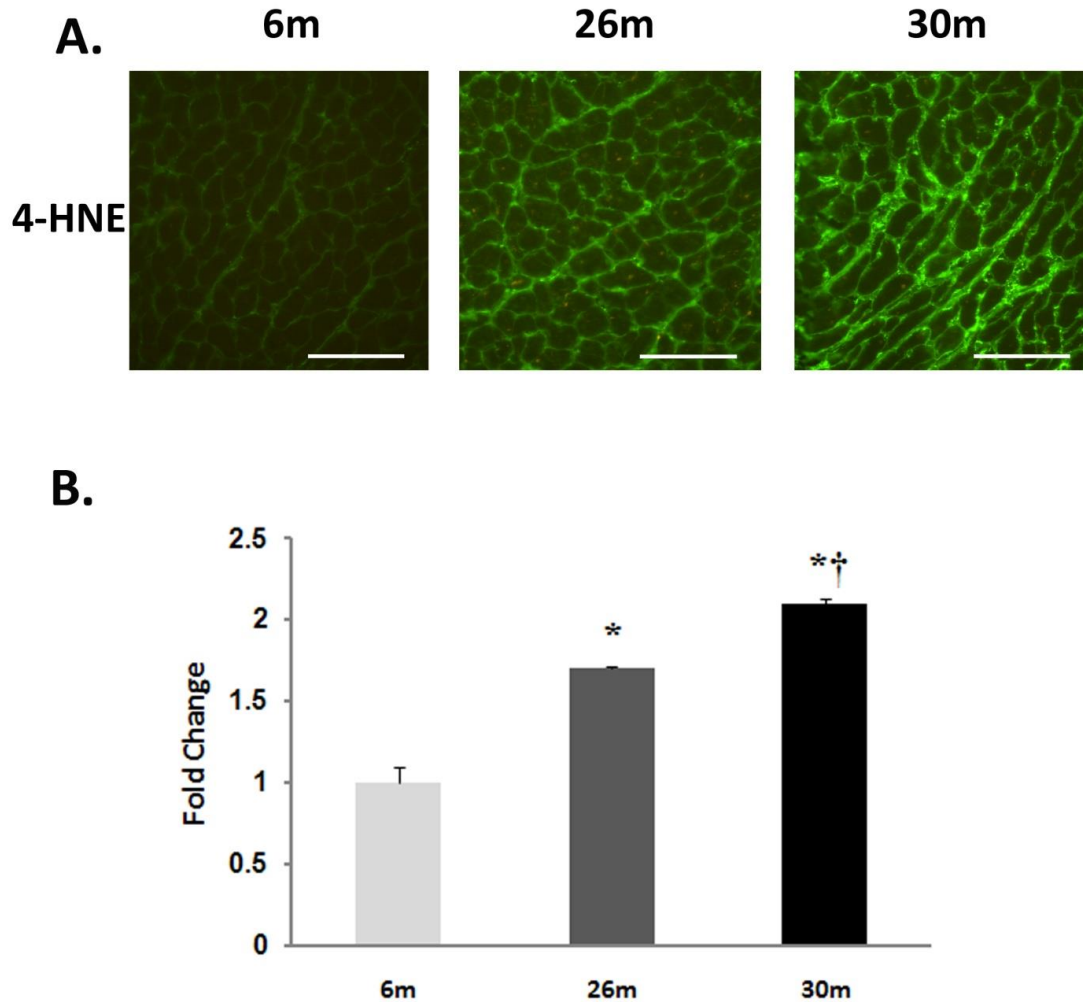
FIGURE 3.3: LIPID PEROXIDATION INCREASES WITH AGE IN THE FEMALE HEART.

   A. Immunohistochemical analysis of 4-HNE levels in the 6-, 26-, and 30-month female

F344xBN heart. Scale bar = 100 μm. **B.** The quantification of 4-HNE levels determined by

immunoblotting. The results were reported as fold change of the 6-month value. Significant

differences are represented by an asterisk (*) and a cross (†) from the adult (6-month) value and

aged (26-month) value, respectively ($p < 0.05$).

FIGURE 3.4
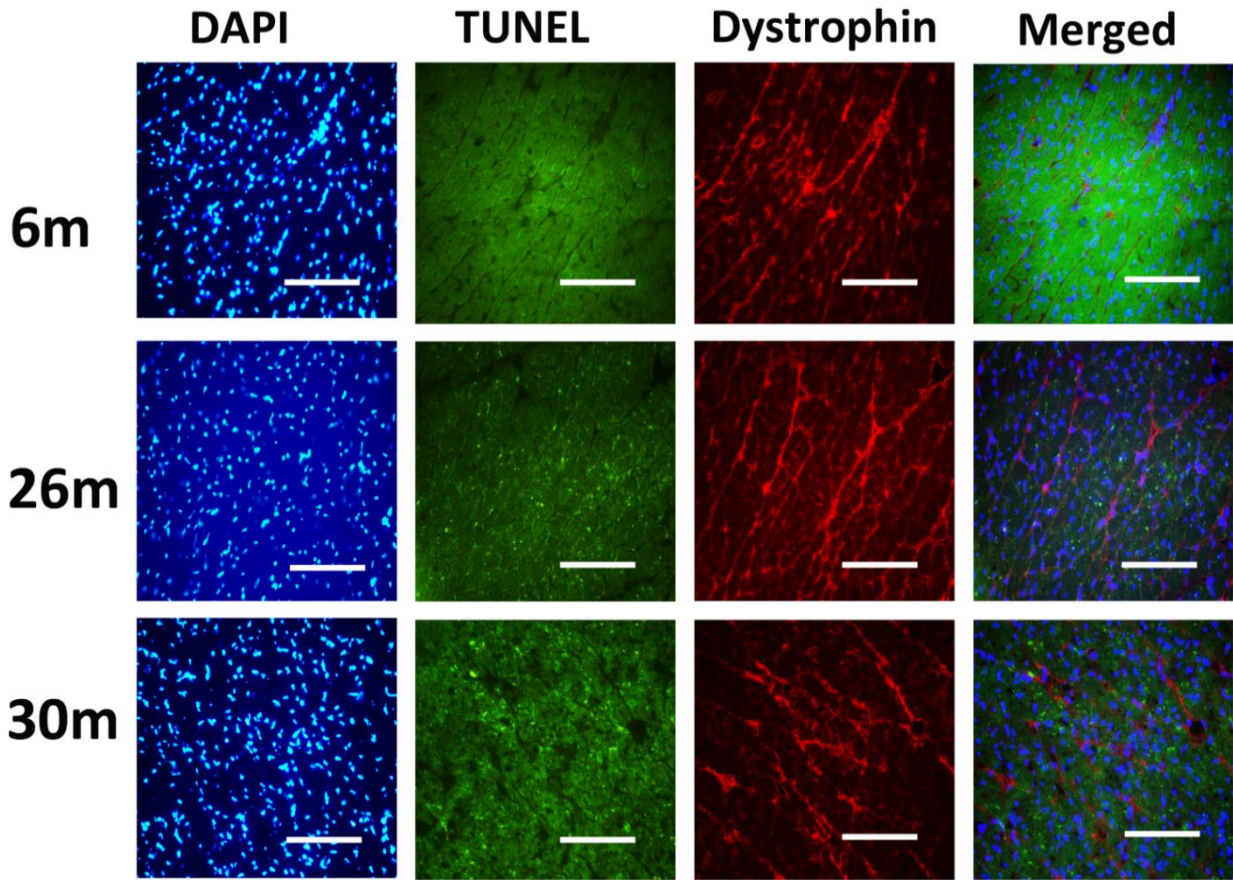
FIGURE 3.4: INDICES OF APOPTOSIS INCREASE IN THE AGING FEMALE HEART.

All cardiomyocyte nuclei were stained with 4', 6-diamidino-2-phenyllindole (DAPI) and nuclei with DNA fragmentation, an indice of apoptosis, were visualized with TUNEL staining. The mouse monoclonal antibody dystrophin (C-terminus) was used to visualize cardiomyocyte borders. Scale bar = 100 μm.
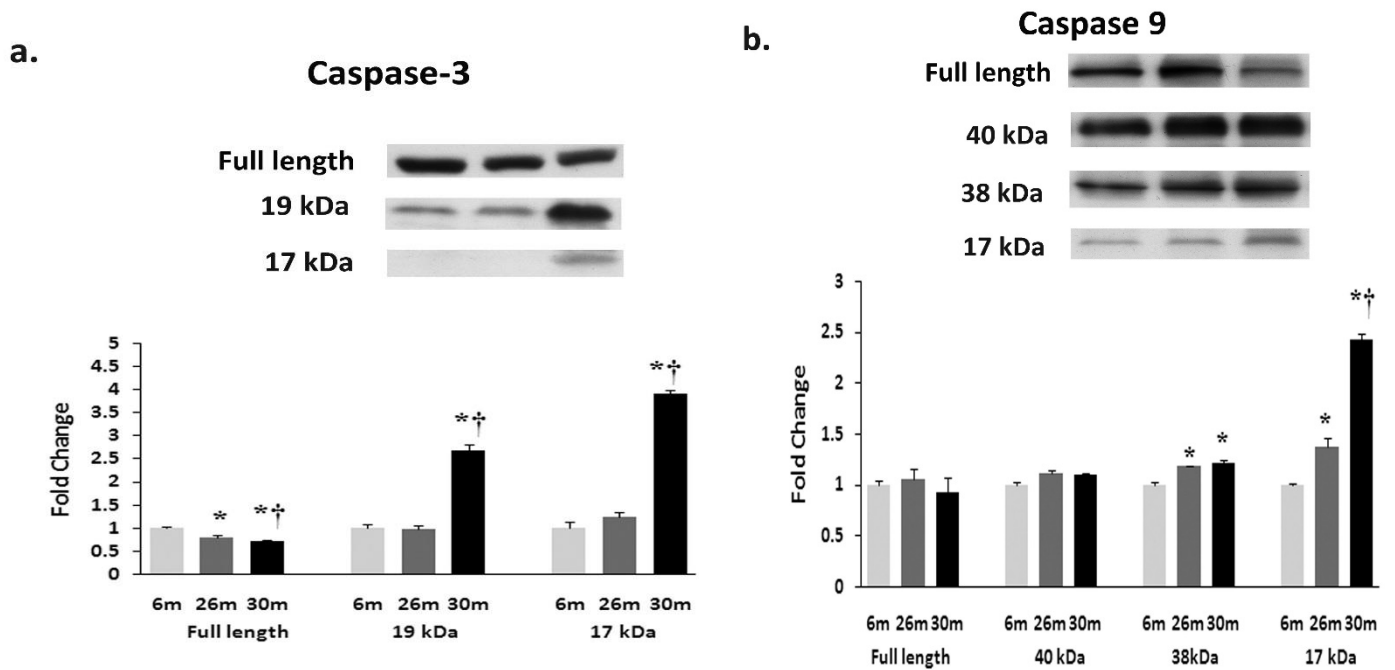
FIGURE 3.5

FIGURE 3.5: AGING ALTERS THE EXPRESSION AND ACTIVATION OF CASPASE-3 AND CASPASE-9.

Expression of caspase-3 (**a**) and caspase-9 (**b**) in heart tissue of female F344xBN rats as determined by immunoblot analysis. Caspase levels were normalized to amount of protein loaded into each lane. Representative immunoblot images are shown for each group. Data are reported as mean ± SEM. (*) represents significant difference from 6-month age group ($p < 0.05$). (†) represents significant difference from 26-month group ($p < 0.05$).

FIGURE 3.6
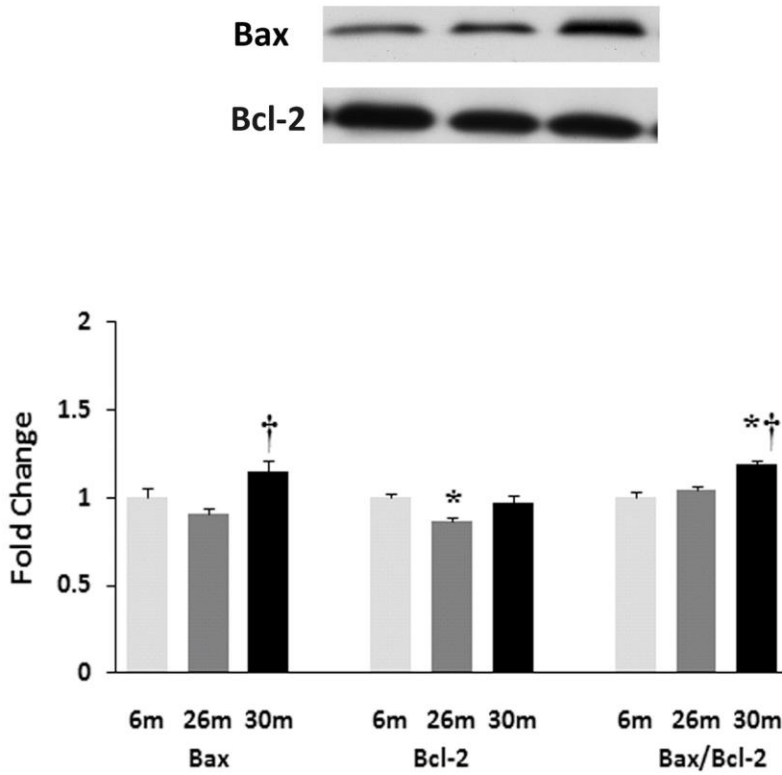
FIGURE 3.6: AGING AFFECTS THE EXPRESSION AND/OR REGULATION OF APOPTOTIC REGULATORS BAX AND BCL-2.

Bax and Bcl-2 expression of female F344xBN rat hearts with age as measured by immunoblot analysis. Bax and Bcl-2 expression was normalized to amount of protein loaded into each lane. Bax and Bcl-2 ratio is given for each group. Representative immunoblot images are shown for each group. Data are reported as mean ± SEM. Significant differences from 6-month group ($p < 0.05$) are represented by an (*). (†) represents significant difference from 26-month group ($p < 0.05$).

FIGURE 3.7
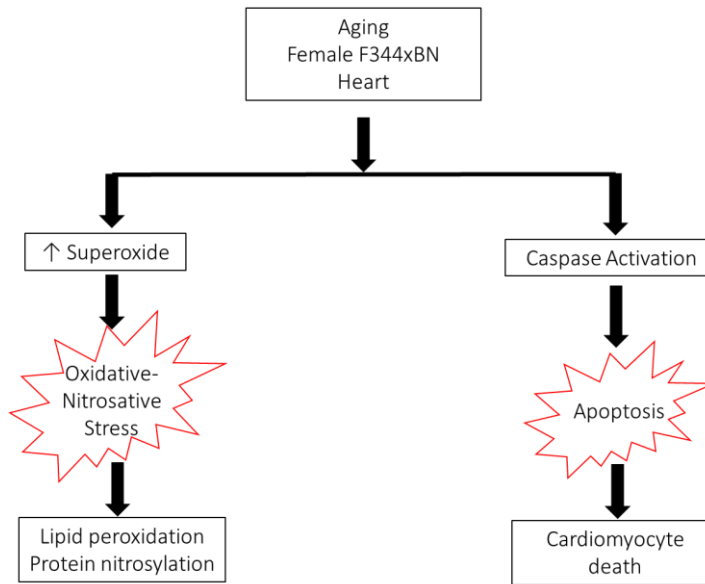
FIGURE 3.7: SUMMARY OF FINDINGS IN THE AGING FEMALE F344XBN HEART.

Aging in the female F344xBN heart involved increased oxidative-nitrosative stress and

damage in addition to increased mitochondrial mediated apoptosis.

CHAPTER 4

AGE-ASSOCIATED ALTERATIONS OF CARDIAC STRUCTURE AND FUNCTION IN THE
FEMALE F344XBN RAT HEART

In Chapter 3, the results showed that there was an age-associated increase in oxidative-nitrosative stress and damage as well as apoptotic signaling. According to the free radical theory of aging as well as previous studies, the accumulation of oxidative-nitrosative stress leads to cardiac dysfunction through alterations in cardiac structure and function. This chapter investigated the age-associated alterations in cardiac structure and function in the female F344xBN outlined in Specific Aim II.

ABSTRACT

The F344xBN rat model exhibits an increased life span and fewer age-associated pathologies compared to commonly used F344. How aging may affect cardiac structure and function in these animals, has to our knowledge, not been investigated. Echocardiography was performed on female F344xBN rats at 6-, 26-, and 30-months of age using a Phillips 5500 Echocardiography system. Before sacrifice, electrocardiograms were measured in the female F344xBN in order to determine heart rhythm interval changes. Aging was associated with an increase in heart to body weight ratio, cardiomyocyte CSA, posterior wall thickening, and left ventricle chamber dilatation. Aging was associated with slight evidence of diastolic dysfunction. Alterations in heart rhythm intervals were associated with alterations in the spatial distribution of Cx43. The incidence of arrhythmias was not different with age; however, valvular dysfunction

was increased. These data suggest that aging in the female F344xBN rat heart is associated with changes in cardiac structure as well as function. Further investigation regarding other parameters of cardiac biochemistry and function is needed to better understand the normal compensated cardiovascular aging process in the female F344xBN.

INTRODUCTION

Aging is associated with an increased risk of developing myocardial infarction, stroke, atherosclerosis, peripheral occlusive disease, diabetes, and hypertension [340, 341]. Similar to that seen in humans, aging in rodents is characterized by cardiomyocyte loss, hypertrophy of the remaining cardiomyocytes, and increased fibrosis [13, 116, 117, 119]. These structural changes adversely affect aging cardiac function by prolonging contraction and relaxation leading to systolic and diastolic dysfunction [114, 342].

The F344xBN rat has been recommended by the NIA for aging studies due to its increased life span and the presence of fewer age-associated pathologies when compared to other rodent models [10, 11]. It has been demonstrated that male F344xBN animals undergo similar age-associated changes in cardiac structure and function to those seen in humans. Whether female F344xBN animals exhibit similar alterations has, to our knowledge, not been examined.

Normal cardiovascular aging can lead to structural changes in addition to decreased Cx43 expression or increased heterogeneity which can lead to electrical abnormalities by disrupting normal myofiber organization as well as slowing conductance [172, 366]. Such changes in electrical conductance, electrolyte imbalance, and altered ion channels have been linked to various forms of cardiac disease and rhythm disturbances [119, 367, 368]. These adaptations are

capable of resulting in secondary cardiac dysfunction, which can include alterations in cardiac rhythm. To our knowledge such changes have not been investigated in the female F344xBN. These changes, if present, in a non-pathological model of female aging may provide insight into the normal compensated cardiovascular aging process within the female heart [10].

The purpose of this study was to examine how aging affects the structure and function of the female F344xBN rat heart and to determine if changes in tissue structure and function, if present, are associated with changes in electrocardiographic measures and Cx43 heterogeneity of distribution. We hypothesize that alterations in cardiac structure and Cx43 heterogeneous distribution in the female F344xBN heart will be associated with cardiac dysfunction and heart rhythm interval changes.

MATERIALS AND METHODS

Animals

All procedures were performed in accordance with the Guide for the Care and Use of Laboratory Animals as approved by the Council of the American Physiological Society and the Animal Use Review Board of Marshall University. All procedures were conducted in strict accordance with the Public Health Service Animal Welfare Policy. Virgin adult (6-month), aged (26-month), and very aged (30-month) female F344xBN rats were obtained from the NIA and housed two per cage in an AAALAC approved vivarium. Animal ages were chosen based on survivability curves from the National Institute of Aging to approximate females in the third, seventh, and eighth decade of life. Given that previous data have demonstrated a complete loss of cyclicity at 16 months of age, the estrous phase was not monitored (PMID 17460359). Housing

59

conditions consisted of a 12 h-12 h light-dark cycle and temperature was maintained at 22 ± 2˚C.

Animals were provided with food and water *ad libitum*. Rats were allowed to recover from

shipment for at least two weeks before experimentation during which time the animals were

carefully observed and weighed weekly. Any of the rats showing signs of failure to thrive, such as

precipitous weight loss, disinterest in environment, or unexpected gait alterations were excluded

from the study.

Echocardiographic procedures

Rats (6-, 26-, and 30-month) were anesthetized using a cocktail of ketamine (40 mg/kg)

and xylazine (10 kg/mg) which was injected into the intraperitoneal cavity in order to perform

echocardiograms. Echocardiographic procedures were done as previously described by Walker

and colleagues [94]. In order to prevent disturbances of ultrasound waves, the ventral thorax was

shaved and the rats were placed either on their backs or left side and covered with ultrasonic

transmission gel. A Phillips 5500 Echocardiographic system with a 12 MHz transducer was used

to take two-dimensional echocardiographic measurements, two-dimensional guided motion

mode (M-mode), Doppler M-mode, and parasternal long- and shot-axis views. Parasternal long-

and short-axis views were used to determine two-dimensional cardiac structural measurements.

The echocardiographic views were then used to position the M-mode echocardiographic line.

Valvular blood flow velocities were evaluated using pulse wave Doppler with the probe toward

the apex (x-axis) and the depth along the y-axis (long axis procedure). Positioning the probe

toward the left ventricle and across the heart during short axis procedures made it possible to

evaluate wall structure in order to calculate EF and FS during systole. A digital echocardiographic

analysis system was used to analyze M-mode displays. All echocardiography procedures and parameters were measured by the same echocardiogram technician to limit inter-observer variability.

Left ventricular mass (LVM) was calculated according to the following equation on the basis of previous reports demonstrating a good correlation (r = 0.78, SEE = 0.124, P < 0.0001) between calculated and postmortem LVM [369, 370].

$$LVM= 1.04(IVSd+LVIDd+PWTd)^3-LVIDd^3 \text{ [371]}$$

Serum Collection

During tissue collection blood was collected by cardiac puncture into a BD Vacutainer serum collection tube. The blood was centrifuged at 800 x g for 15 minutes to separate serum. The serum was collected and used to measure serum parameters using an Abaxis VetScan analyzer (Abaxis, Union City, CA). The following parameters were determined: non-fasting serum glucose (GLU), alanine aminotransferase (ALT), alkaline phosphatase (ALP), blood urea nitrogen (BUN), albumin (ALB), calcium (Ca^{2+}), creatinine (CRE), amylase (AMY), globulin (GLOB), potassium (K^+), sodium (Na^+), phosphorus (PHOS), total bilirubin (TBIL), and total protein [372].

Heart Collection

Rats were anesthetized with an intraperitoneal injection of ketamine (40 mg/kg) and xylazine (10 mg/kg) and supplemented as necessary for reflexive response. Before heart collection, a three lead EKG was performed on all animals using the Biopac Student Lab software (BIOPAC Systems, Inc., Microsoft). After completion of the EKG, the heart was removed after a

midline laparotomy and placed in Krebs-Ringer bicarbonate buffer containing the following: 118 mM NaCl, 4.7 mM KCl, 2.5 mM CaCl$_2$, 1.2 mM KH$_2$PO$_4$, 1.2 mM MgSO$_4$, 24.2 mM NaHCO$_3$, and 10 mM a-D-glucose (pH 7.4) equilibrated with 5% CO$_2$/95% O$_2$ and maintained at 37°C. Isolated hearts were quickly massaged to remove any blood from the ventricles, cleaned of connective tissue, weighed, and immediately snap frozen in liquid nitrogen.

Electrocardiographic analysis

EKGs collected from the aging female rats were analyzed using BioPac Student Lab PRO software. All animals were evaluated for any electrical anomalies in all three leads. Lead II was used to evaluate changes in EKG parameters, a 6 rhythm section of the EKG was used to obtain data for comparison of ventricular acceleration time (VAT), heart rate, ST interval, T amplitude, QRS interval, QT interval, PR interval, T duration, T-T interval, R+S amplitude, S amplitude, R amplitude, Q amplitude, and P amplitude. Mean electrical axis was calculated from leads I and III after calibration of 2 cm/mV using the following formula derived by Singh and Athar [373, 374].

$$\tan\theta = \frac{I + 2III}{\sqrt{3}I}$$

Heart rate was determined by the average intervals between R waves on lead II.

Determination of myocyte cross sectional area and histological analysis

An IEC Minotome Cryostat was used to section (8 µm) frozen hearts (n = 4) on poly-lysine coated slides. To determine morphology, heart sections were stained with hematoxylin and eosin stain. Picrosirius red staining (PSR) was employed to examine collagen. The collagen area fraction

of the PSR-stained tissues was determined using Image J software.

Immunostaining for dystrophin (NCL-DYS2, Novocastra Vector Laboratories, Burlingame, CA) and connexin-43 (Cell Signing Technology #3512, Danvers, MA) was visualized by immunofluorescence as outlined by the antibody manufacturer. A phosphate-buffered saline (PBS) containing 0.5% Tween-20 (PBS-T) at pH 7.5 was used to wash sections three times before incubating for 30 min in a blocking solution (5% BSA). The dystrophin antisera diluted in PSB-T (antibody dilution of 1:100) was added to sections for 1 h in a humidified chamber at 24°C. After incubation the sections were washed three time with PBS, and incubated again for 30 min in a humidified chamber at 24°C with a secondary antibody solution containing a FITC anti-rabbit IgG (1:200) and DAPI (1.5 μg/ml) in order to visualize cell nuclei. Sections were washed a final time with PBS before mounting. The epifluorescence of specimens was visualized using an Olympus fluorescence microscope (Melville, NY, USA) fitted with a 40X objective. Images were recorded digitally using A CCD camera and the Olympus MicroSuite™ Basic from Olympus America (Melville, NY, USA) were used to digitally record and analyze images, respectively. The CSA of the cardiac myocytes was determined by measuring the area within the dystrophin positive staining.

Statistics

Results are given as mean ± SEM. Statistical analyses were performed using Sigma Stat 3.5 statistical software (Systat Software, Inc.). Age comparisons between echocardiographic structural, functional parameters, and morphologic indices were evaluated by One Way ANOVA with the Student-Newman-Keuls *post hoc* test for parametric normally distributed data or Kruskal-Wallis One Way Analysis of Variance on Ranks with a Dunn's *post hoc* test for none

parametric distributions. Linear regression analysis was performed with dependent variables against the independent variables age, correlation were ranked as low correlation (0.3 to 0.7), moderate correlation (0.5 to 0.7), high correlation (0.7 to 0.9), very high correlation (0.9 to 1) between parameters (supplemental data).   The level of significance accepted *a priori* was $\leqslant$ 0.05.

RESULTS

Cardiac function is preserved in the aging female F344xBN rat

Compared to 6-month old animals, heart and body weight was higher at 26-months (72 ± 2 mg vs. 95 ± 2 mg, p < 0.001; 235.3 ± 1.7 g vs. 296.4 ± 6.5 g; *p* < 0.05) and 30-months (104 ± 4 mg, *p* < 0.05); 235.3 ± 1.7 g vs. 315.6 ± 8.6 g; *p* < 0.05) (Table 4.1). Compared to 6-month old animals, cardiac myocyte CSA was 20 ± 1.9 % and 28 ± 2.3 % higher in the 26- and 30-month old animals, respectively (*p* < 0.05) (Figure 4.2). Histological analysis using picrosirius red staining demonstrated a significant age-related decrease in collagen reactivity (Figure 4.2, *p* < 0.05). Immunohistochemical staining of the aging female heart suggested alterations in Cx43 localization from the cell ends to the lateral margins (Figure 4.3). Alignment of the Cx43 staining appears to be uniform, localized, and linear within the 6 month tissues sections, as would be expected because of Cx43 localization along the intercalated disk. The linearity of the staining appears to become less uniform and diffuse with aging which may indicate alteration in Cx43 distribution within the cardiac myocyte. In addition to changes in Cx43 immunoreactivity, aging also appeared to be associated with changes in cardiac rhythm. In particular, aging appeared to be characterized by the presence of hyper-acute T waves, a long PR interval, a long P wave

duration, tall P waves, and significant Q waves (Figure 4.3, Table 4.4). No evidence of arrhythmias was observed in any age group.

No age-associated changes in transmitral to mitral annular early diastolic velocity ratio (E-E') ratio was found in the female F344xBN rats. Left ventricular IVRT was significantly higher in 26-month old animals (0.036 ± 0.005 sec) compared to that seen in the 6-month old animals (0.015 ± 0.002 sec; $p < 0.05$). Mitral valve deceleration time demonstrated no significant change with age. Mitral valve Emax was significantly lower at 26- (61.5 ± 1.5 cm/sec) and 30-months (55.4 ± 1.4 cm/sec) when compared to that seen in the 6-month old animals (78.0 ± 3.3 cm/sec; $p < 0.05$). Mitral valve Amax levels were lower at 30-months (35.1 ± 1.6 cm/sec) when compared to 6-months (41.5 ± 1.3 cm/sec; $p < 0.05$). No significant changes were found in MV E/A ratio with age (Table 4.3).

Compared to 6-month animals, EF was significantly higher at 26-months (82 ± 1.0 % vs. 74 ± 0.9 %; $p < 0.05$).   Fractional shortening was lower at 30-months (41.5 ± 1.7 %) when compared to that observed in 26-month old animals (45.6 ± 1.0 %; $p < 0.05$). End systolic volume (ESV) was significantly lower at 26-months (0.082 ± 0.005 mL) when compared to 6-month old animals (0.143 ± 0.017 mL; $p < 0.05$).   However, heart rate was unaltered with age (Table 4.2).

Aging increases septal and posterior wall thickness and valvular insufficiency in the female F344xBN heart

Compared to 6-month old animals, left ventricular septal thickness (IVS) during systole was higher in 26-month old animals (0.193 ± 0.008 cm vs. 0.253 ± 0.003 cm; $p < 0.05$). Left ventricular internal dimension during systole (LVIDs) significantly increased at 26-months (0.331

± 0.009 cm) compared to 6-month (0.378 ± 0.017 cm; $p < 0.05$). During diastole LVID demonstrated no significant change. Left ventricular posterior wall thickness (LVPW) during systole and diastole was significantly increased at 30-months (LVPWs: 0.288 ± 0.009 cm; LVPWs: 0.189 ± 0.008 cm) compared to 6-months (LVPWs: 0.193 ± 0.002 cm; LVPWd: 0.153 ± 0.010 cm; $p < 0.05$). No changes were found in right ventricular dimension (RVd) during diastole or left ventricular mass with age (Table 4.4).

The incidence of tricuspid, mitral, and pulmonary valve insufficiency was higher in 26- and 30-month female hearts relative to that observed in 6-month animals. The presence of aortic insufficiency with age was only seen in the 30-month age group (Figure 4.5).

Aging is associated with alterations in serum glucose and electrolytes in the female F344xBN rat

In the aging female F344xBN non-fasting serum glucose levels were significantly decreased at 30-month (323.7 ± 13.3 mg/dl) compared to 6-month (372.8 ± 16.0 mg/dl) female F344xBN rat. Serum levels of ALP, BUN, PHOS, and potassium (K^+) significantly decreased at 26- and 30-months compared to that observed in the 6-month old animals. TP, GLOB, and CRE increased significantly at 30-months (6.3 ± 0.1 g/dl; 2.12 ± 0.1 g/dl; 0.4 ± 0.03 mg/dl) compared to 6-months (5.8 ± 0.05 g/dl; 1.56 ± 0.12 g/dl; 0.3 ± 0.002 mg/dl). In the 26-month old female F344xBN rat serum calcium (Ca^{2+}, 11.2 ± 0.1 mg/dl) levels were significantly increased compared to 6-month female rats (10.7 ± 0.09 mg/dl). No significant changes were found in serum ALB, ALT, sodium, and TBIL with age in the female F344xBN. Significant increases of calcium to phosphate (Ca^+/PHOS) and sodium to potassium (Na^+/K^+) ratios were observed in the 26- and 30-month age groups when compared to 6-month animals ($p < 0.05$). Compared to 6-month animals, BUN/CRE

and the albumin to globulin (ALB/GLOB) ratios were lower in the 26- and 30-month age groups (Table 4.5, $p < 0.05$).

DISCUSSION

The purpose of this study was to examine how the aging process affects the cardiac structure and function in the female F344xBN rat. Similar to previous work using male animals, our data indicated that aging in these animals is associated with an increase in the thickness of the septal and posterior walls between 6- and 30-months of age [94]. In addition to these changes, we also observed that aging was associated with increases in average cardiomyocyte muscle fiber CSA (Figure 4.2) and a trend towards increased left ventricular wall thickness (Table 4.4). These data, taken together, are consistent with the efforts of Boluyt and colleagues who noted an increase in thickness of septal and posterior walls at 30-months in the aging F344 model [2]. Unlike this study, previous echocardiography studies in humans, male F344xBN rats, and female F344 rats (at 30-months of age) have shown that LVM in female F344 rats is increased with age [26, 89, 94, 114]. Why discrepancies may exist between studies is currently unclear but may be related to differences in experimental design, differences across species, rat strain or in the time points chosen for examination. Future experiments perhaps using older female F344xBN rats may be useful for clarification.

Aging is oftentimes associated with an increased risk of diastolic dysfunction which appears to exhibit a greater incidence in women compared to men [375]. Diastolic problems oftentimes, but not always, precede the development of systolic dysfunction [375]. In humans, diastolic dysfunction is defined by abnormal ventricular relaxation and filling that is characterized

by a low E wave velocity, a high A wave velocity, prolonged deceleration time, and prolonged IVRT [375]. In the present study, we observed age-related decrease in E', increases in left ventricular relaxation time and a trend in MV decel time in the female F344xBN heart. Nonetheless, we did not find any changes in the E/A ratio with age. Conversely, Boluyt and colleagues, using aged female F344 animals, demonstrated increases in left ventricular IVRT, decreases in the E wave, and an increased A wave velocity [2]. Similar to previous findings by Boluyt and colleagues who used the aging female F344 model, we observed age-related increases in left ventricular relaxation time, decreased E' wave velocity, and a trend in MV decel time but no change in the E/A ratio with aging in the female F344xBN heart [2]. Taken together, these data suggest that aging in the female F344 and F344xBN rats, like that seen in humans, is often characterized by alterations in diastolic function.

Like prior work done in the F344 rat strain, aging in the female F344xBN rat did not appear to significantly impair systolic function [2, 118]. Similar to that observed in the aging F344 animals, we also noted a slight increase in ejection fraction at 26-months although this parameter must be interpreted with caution since animals at this time point also exhibited increased evidence of valvular regurgitation [2]. Interestingly, work by Forman and colleagues reported that F344 males had a higher occurrence of mitral regurgitation (MR) than that seen in their female counterparts which may help explain the differences in function between the sexes [118]. This finding is consistent with previous work from our laboratory which demonstrated a higher percentage of MR with age in male F344xBN (unpublished data). Why differences may exist between aged male and female F344xBN rats will require further investigation.

Probabilities of survival curves generated by the NIA were used in the current study in an

effort to approximate aging humans in the 3rd, 7th, and 8th decade of life. It is likely that aging in

the female F344xBN does not closely mimic the changes seen in aging women at similar time

points along the aging spectrum. Why aging in female rodents might differ from that seen in

humans is likely complex and poorly understood but may be related to dissimilarities in hormonal

regulation during aging. Previous data has demonstrated that the F344xBN estrous cycle ceases

at 16 months of age which suggests that the 26- and 30-month old animals used in the present

study are likely to represent animals that are moderate and late post-menopausal [376]. Unlike

that seen in humans, this loss in function is characterized as persistent estrous with maintained

levels of estrogen, lower levels of progesterone, the absence of LH surges, and ovulation. This

initial decline, in turn, is followed by the final stage where aged female rodents have low levels of

plasma estradiol, progesterone, and (no or little) developing ovarian follicles [377]. Whether

estrogen, if present, may have blunted the age-associated changes typically seen in male animals

is currently unclear.

Age-associated alterations in heart rhythm in the female F344xBN heart

Unlike the aging male F344xBN rats, no evidence of arrhythmias were detected with age

in the female F344xBN [94]. Nonetheless, our data suggest that aging in the female F344xBN is

associated with changes in heart rhythm including increases in the VAT, ST interval, T amplitude,

QRS interval, QT interval, T duration, Q amplitude, P amplitude, and a shift in the mean electrical

axis with age (Table 4.2), increase in heart weight, myocyte CSA, and LVM. Alterations in heart

rhythm intervals such as increased PR interval, P wave amplitude, and QRS complex are

oftentimes indicative of myocardial disease [378]. Previous studies have shown that aged male

rats (20-months) had no difference in R-R interval, P wave, as well as QRS length; however, PR and QT interval were increased with age [132]. Our current findings support the existence of alterations in cardiac conductance but provide little information as to the underlying mechanism. The elevation in VAT and QRS interval suggest that aging might not only affect depolarization but that it may also be associated with changes in the ability of the heart to undergo repolarization. Correlation analysis demonstrated a high correlation between heart weight to MV A max velocity (0.752 cm/sec) and MV A max velocity to CSA (0.827) (Table S-4.1- S-4.4). Because the nature of correlation does not denote causation, it is important to note that further research is required to delineate the nature of these correlations and to better elucidate the causation of the age-associated changes listed in this study. Similarly, whether the changes in VAT and QRS interval we observed in the current study are due to differences in ion handling, ion channel density, alterations in how electrical signals may propagate through the myocardium or if they reflect age-associated increases in myocyte CSA or chamber dimensions (Figure 4.2, Table 4.4) is currently unclear and will require additional experimentation.

Heart rhythm propagation is dependent on cell to cell coupling between cardiomyocytes and this coupling is dependent, at least in part, on ion channels and gap junctions. Previous studies have shown that age-related changes in impulse propagation may be related to abnormalities in the pattern of ventricular activation [119]. Recent data has suggested that alterations in heart rhythm intervals during aging may be associated with alterations in Cx43 expression/activation/heterogeneity, fibrosis, and hypertrophy [119, 163-165, 379]. Other work examining Cx43 has demonstrated increases in atrial fibrillation in patients exhibiting increased heterogeneity of Cx43 distribution [368]. These possibilities appear to be consistent with our

data, where we observed qualitative alterations in Cx43 localization with aging in the female F344xBN heart (Figure 4.3). Future experiments to directly investigate if or how changes in Cx43 protein abundance and localization may affect cardiac rhythm in the aging female F344xBN rat model may be helpful in delineating whether Cx43 may play a role in the aging female heart.

In addition, we also examined if age-related changes in heart rhythm were associated with alterations in blood chemistry. It has been suggested that electrolyte disorders can affect the ion currents in the heart and that such changes might be related to the development of cardiac arrhythmias [367]. For example, previous studies have shown that decreased plasma sodium, potassium, and ionized calcium levels are associated with a higher risk of arrhythmias in hemodialysis patients [380, 381]. Although very little is known about the role of serum electrolytes in influencing cardiac function during aging, alterations in serum electrolytes have been associated with increased all-cause mortality among patients suffering from coronary heart disease [382]. For the most part, we found that age-related changes in blood chemistry appeared to be within the normal range. Recent work has suggested that decreases in plasma potassium may be related to the development of tachyarrhythmias [383]. Whether the age-associated reduction in potassium levels seen in this study, although within the normal physiological range, might play a role in the changes seen in the EKG data will require further investigation.

In conclusion, this study provides reference values for cardiac structure and function in the aging female F344xBN heart. Taken together, our data suggest that the female, unlike the male, F344xBN rat demonstrates subtle age-associated changes in cardiac structure, function, and conductance. The age-associated increase in heart wall thickness in the absence of fibrosis

and increase heterogeneity of Cx43 distribution may partially explain the age-associated alterations in heart rhythm intervals. The possibility of altered serum ion levels may also contribute to reduced conductance. Further study is needed to better understand the mechanistic basis of how aging may affect cardiac structure and function in the female F344xBN rat.

TABLE 4.1: TOTAL BODY WEIGHT (BW) AND HEART WEIGHT (HW) IN FEMALE F344XBN RATS AT 6-, 26-, AND 30-MONTHS OF AGE (MEANS ± SEM). 6-month animal; 26-month animal; 30-month animal; (*, $p < 0.05$) significant difference from 6-month animal; ($\dagger$, $p < 0.05$) significantly different from 26-month animal.

Groups	6-month	26-month	30-month
N	4	22	10
Heart Weight (g)	0.72 ± 0.02	0.95 ± 0.02*	1.0 ± 0.04*†
Body Weight (g)	235.3 ± 1.7	296.4 ± 6.5*	315.6 ± 8.6*
HW/BW Ratio (%)	0.317 ± 0.02	0.32 ± 0.01	0.33 ± 0.01

TABLE 4.2: ELECTROCARDIOGRAPHIC EVALUATION OF CARDIAC CONDUCTION PARAMETERS IN AGING FEMALE F344XBN RATS (MEAN ± SEM). 6-month animal; 26-month animal; 30-month animal; (*, $p < 0.05$) significant difference from 6-month animal; ($†$, $p < 0.05$) significantly different from 26-month animal.

EKG Measurements	6-months	26-months	30-months
Heart Rate	277.8 ± 4.67	277.6 ± 4.27	277.6 ± 6.45
VAT	0.036 ± 0.0013	0.044 ± 0.0010*	0.046 ± 0.0007*
ST Interval	0.055 ± 0.0035	0.080 ± 0.0018*	0.073 ± 0.0013*
T Amplitude	0.090 ± 0.0065	0.123 ± 0.0071*	0.098 ± 0.0080†
QS Interval	0.055 ± 0.0010	0.066 ± 0.0013*	0.070 ± 0.0005*†
QT Interval	0.110 ± 0.0035	0.146 ± 0.0023*	0.143 ± 0.0012*
PR Interval	0.035 ± 0.0027	0.033 ± 0.0015	0.032 ± 0.0010
T Duration	0.055 ± 0.0035	0.080 ± 0.0018*	0.073 ± 0.0013*
T-T Interval	0.217 ± 0.0034	0.217 ± 0.0032	0.218 ± 0.0050
R + S Amplitude	0.321 ± 0.0105	0.280 ± 0.0161	0.276 ± 0.0247
S Amplitude	-0.009 ± 0.0061	-0.007 ± 0.0049	-0.029 ± 0.0121
R Amplitude	0.035 ± 0.0027	0.033 ± 0.0015	0.032 ± 0.0010
Q Amplitude	-0.005 ± 0.0019	-0.014 ± 0.0024*	-0.018 ± 0.0017*
P Amplitude	0.006 ± 0.0052	0.037 ± 0.0018*	0.037 ± 0.0020*
P Duration	0.035 ± 0.0027	0.033 ± 0.0015	0.032 ± 0.0010
Mean Electrical Axis	34.41 ± 5.99	63.13 ± 4.86*	63.26 ± 3.72*

TABLE 4.3: ECHOCARDIOGRAPHIC EVALUATION OF CARDIAC FUNCTIONAL PARAMETERS IN AGING FEMALE F344XBN RATS (MEAN ± SEM). 6-month animal; 26-month animal; 30-month animal; ($*$, $p < 0.05$) significantly different from 6-month animal.

Groups	6-month	26-month	30-month
EF (%)	74 ± 0.9	82 ± 1.0*	78 ± 1.8
FS (%)	38 ± 0.7	46 ± 1.0	42 ± 1.7
ESV (mL)	0.143 ± 0.017	0.082 ± 0.005*	0.114 ± 0.10
EDV (mL)	0.535 ± 0.052	0.492 ± 0.20	0.523 ± 0.022
Heart Rate (bpm)	281 ± 16.5	259 ± 8.8	278 ± 10.1
E-E'	20.8 ± 1.02	14.7 ± 0.64	21.9 ± 2.63
LV IVRT (sec)	0.015 ± 0.002	0.036 ± 0.005*	0.030 ± 0.000
MV Dec Time (sec)	0.053 ± 0.005	0.057 ± 0.002	0.063 ± 0.003
MV Emax (cm/sec)	78 ± 3.3	62 ± 1.5*	55 ± 1.4*
MV Amax (cm/sec)	42 ± 1.3	36 ± 0.9	35 ± 1.6*
MV E/A	1.75 ± 0.03	1.60 ± 0.06	1.66 ± 0.10

TABLE 4.4: ECHOCARDIOGRAPHIC EVALUATION OF CARDIAC STRUCTURAL PARAMETERS IN

AGING FEMALE F344XBN RATS (MEAN ± SEM). 6-month animal; 26-month animal; 30-month

animal; (*, $p < 0.05$) significantly different from 6-month animal.

Groups	6-month	26-month	30-month
IVSs (cm)	0.193 ± 0.008	0.253 ± 0.003*	0.239 ± 0.013
IVSd (cm)	0.118 ± 0.012	0.151 ± 0.003	0.149 ± 0.004
LVIDs (cm)	0.378 ± 0.017	0.331 ± 0.009*	0.356 ± 0.011
LVIDd (cm)	0.610 ± 0.022	0.593 ± 0.009	0.606 ± 0.10
LVPWs (cm)	0.193 ± 0.002	0.267 ± 0.007	0.288 ± 0.009*
LVPWd (cm)	0.153 ± 0.010	0.166 ± 0.004	0.189 ± 0.008*
RVDd (cm)	0.105 ± 0.016	0.138 ± 0.009	0.111 ± 0.006
LVM (g)	0.487 ± 0.10	0.658 ± 0.09	0.646 ± 0.04

TABLE 4.5: BLOOD PARAMETERS FOR THE AGING FEMALE F344XBN RAT (MEAN ± SEM). 6-month animal; 26-month animal; 30-month animal; (*, $p < 0.05$) significantly different from 6-month animal; n = 4 - 6 group.

Parameters	6-month	26-month	30-month
ALB (g/dL)	4.4 ± 0.03	4.4 ± 0.1	4.2 ± 0.1
ALP (u/L)	217.9 ± 10.7	168.0 ± 9.6*	167.8 ± 7.4*
ALT (u/L)	45.1 ± 2.2	57.6 ± 3.7	49.8 ± 2.4
AMY (u/L)	551.1 ± 22.1	640.3 ± 29.6*	589.8 ± 18.0
TBIL (mg/dL)	0.2 ± 0.02	0.2 ± 0.02	0.3 ± 0.03
BUN (mg/dL)	17.5 ± 0.4	15.4 ± 0.6*	15.7 ± 0.5*
Ca+2 (mg/dL)	10.7 ± 0.09	11.2 ± 00.13*	11.0 ± 0.1
PHOS (mg/dL)	10.2 ± 0.4	8.1 ± 0.2*	7.8 ± 0.2*
CRE (mg/dL)	0.3 ± 0.02	0.4 ± 0.02	0.4 ± 0.03*
GLU (mg/dL)	372.8 ± 16.0	346.9 ± 10.3	323.7 ± 13.3*
Na$^+$ (mmol/L)	141.8 ± 0.9	142.0 ± 0.6	141.1 ± 0.5
K$^+$ (mmol/L)	7.12 ± 0.06	6.4 ± 0.14*	6.0 ± 0.11*
TP (g/dL)	5.8 ± 0.05	6.4 ± 0.08*	6.3 ± 0.11*
GLOB (g/dL)	1.56 ± 0.12	2.00 ± 0.10*	2.12 ± 0.11*
Ca/P (ratio)	1.03 ± 0.12	1.39 ± 0.12*	1.44 ± 0.14*
Na/K (ratio)	19.90 ± 0.66	22.40 ± 1.99*	23.58 ± 1.94*
BUN/CRE (ratio)	68.96 ± 16.1	46.77 ± 16.9*	49.64 ± 17.6*
A/G (ratio)	3.29 ± 0.68	3.32 ± 0.61*	2.14 ± 0.60*

FIGURE 4.1
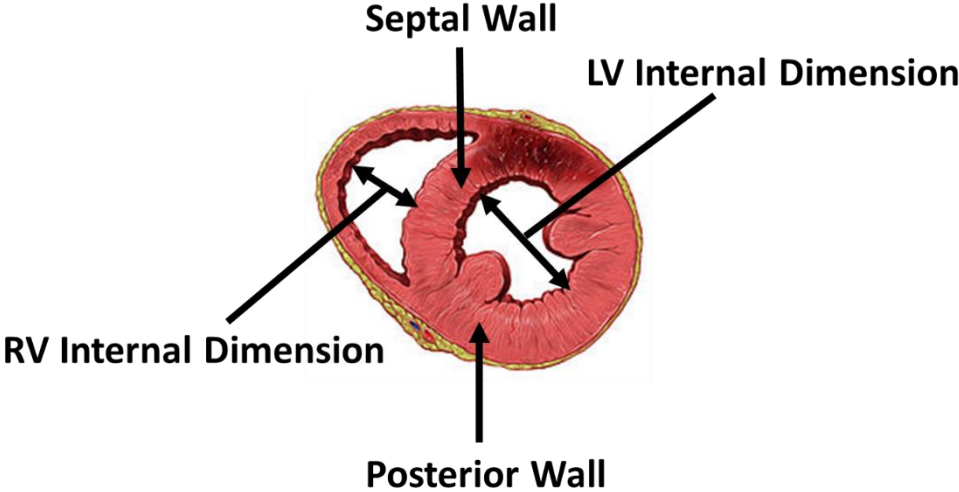
FIGURE 4.1: STRUCTURAL DIAGRAM OF THE FEMALE F344XBN HEART.

(Photo credit: Patrick J. Lynch, medical illustrator).

FIGURE 4.2
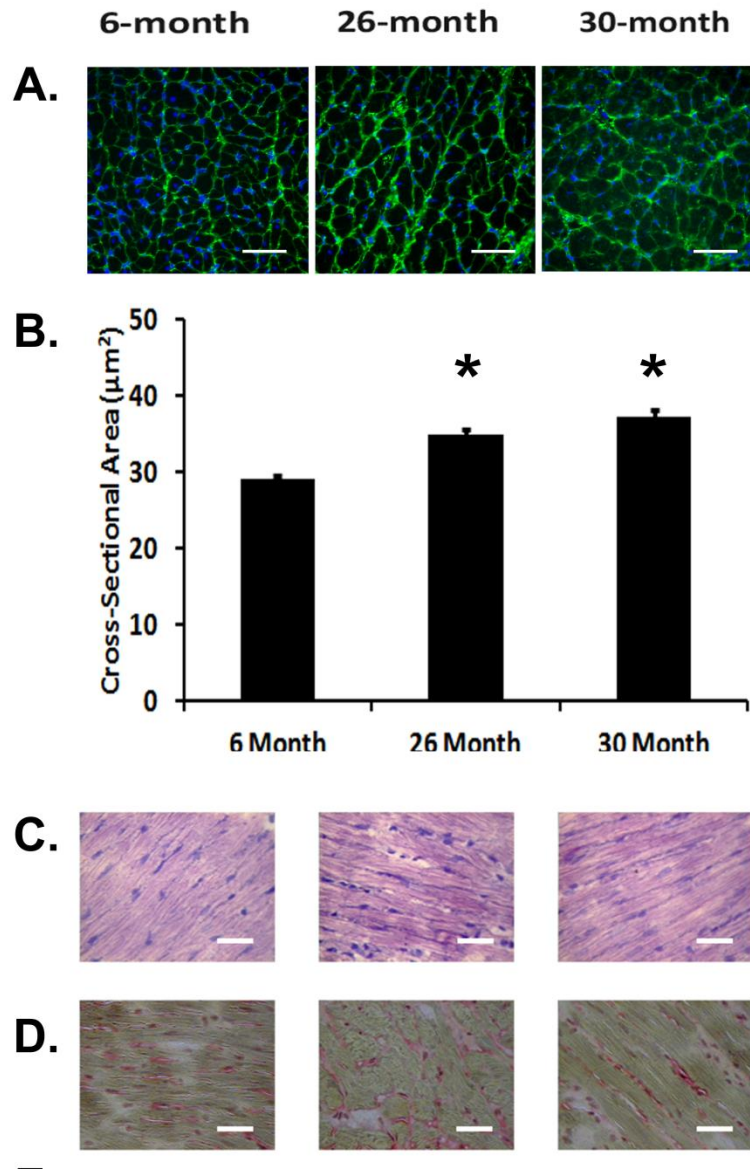
FIGURE 4.2: CSA, TISSUE MORPHOLOGY, AND FIBROSIS IN THE AGING FEMALE F344XBN HEART.

(**A**) Immunohistochemical staining of cardiac tissue stained with dystrophin. Bar = 100 μm. (**B**) Cross-sectional area of cardiac myocytes as determined by dystrophin staining, (**C**) Hematoxylin and Eosin, and (**D**) Picrosirius red staining of 6-, 26-, and 30-month female F344xBN hearts. (*, $p < 0.05$) significantly different from 6-month animal.

FIGURE 4.3

A.

B.

C.

6 Month

26 Month
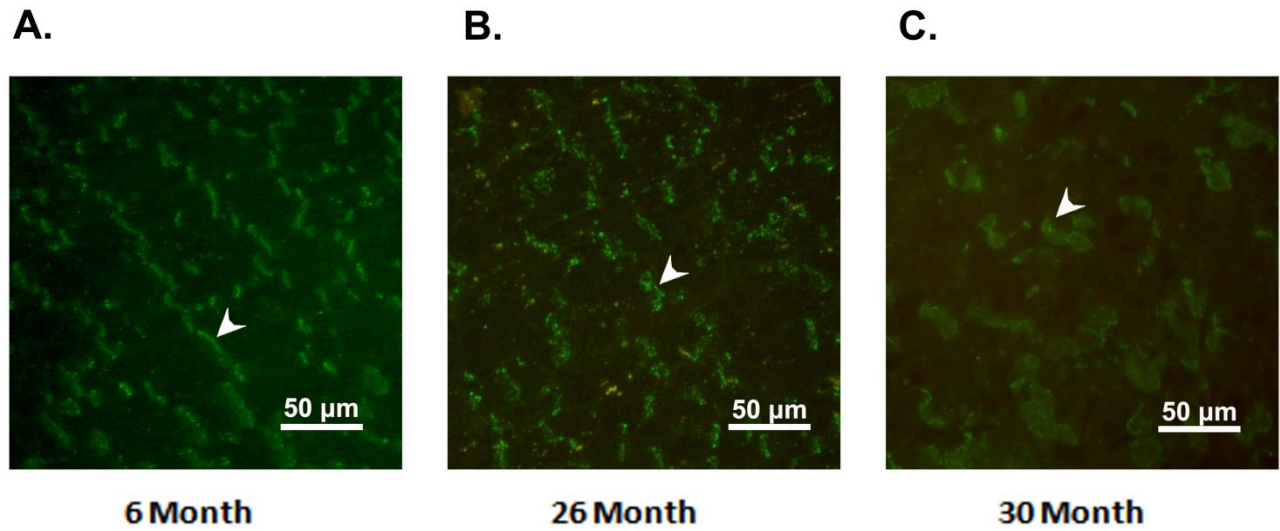
30 Month

FIGURE 4.3: AGE-ASSOCIATED CHANGES IN CONNEXIN 43 DISTRIBUTION IN THE AGING FEMALE F344XBN HEART.

Distribution of connexin 43 in (**A**) 6-, (**B**) 26-, and (**C**) 30-month female F344xBN hearts. Bar = 50 μm.
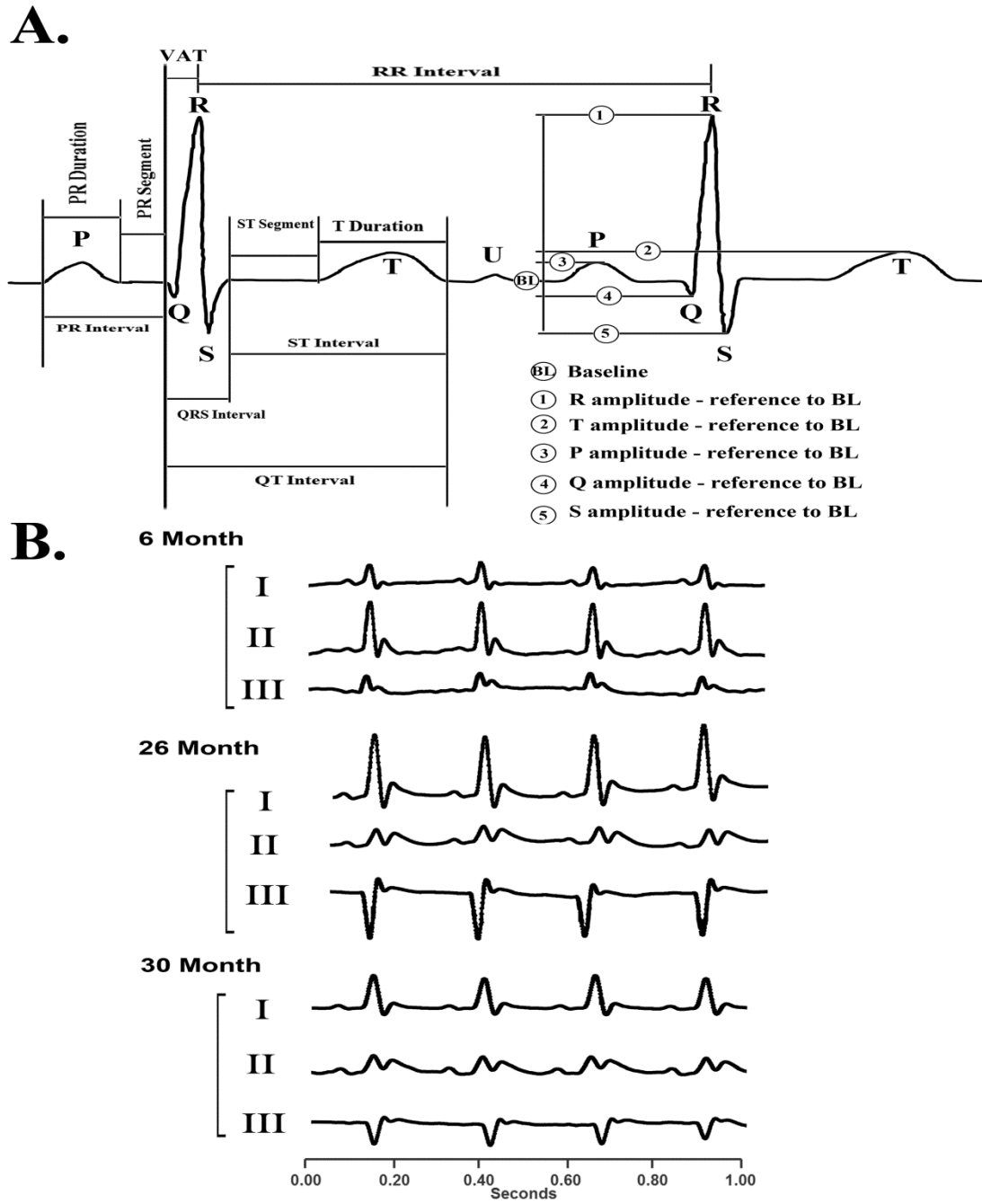
FIGURE 4.4

FIGURE 4.4: EKG IN THE AGING FEMALE F344XBN HEART.

(**A**) EKG interval diagram and (**B**) representative EKG tracing of leads I, II, and III obtained from 6- , 26, and 30-month females**.**

FIGURE 4.5
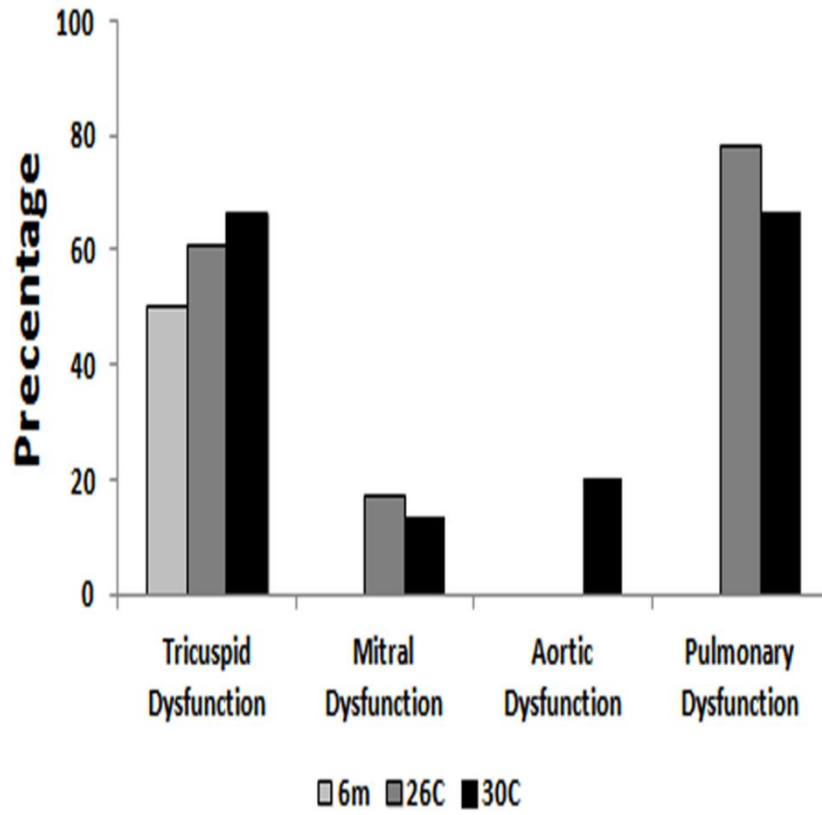
FIGURE 4.5: AGE-ASSOCIATED VALVE DYSFUNCTION IN THE FEMALE F344XBN HEART.

Percentage of female F344xBN rats with valve dysfunction at 6-, 26-, and 30-months.

TABLE S-4.1: REGRESSION ANALYSIS OF THE RELATIONSHIP BETWEEN HEART RHYTHM INTERVALS, AGE, BODY WEIGHT, HEART WEIGHT, CONNEXIN 43 EXPRESSION, CARDIOMYOCYTE CROSS SECTIONAL AREA, AND COLLAGEN STAINING INTENSITY OF 6-, 26-, AND 30-MONTH FEMALE F344XBN HEARTS. The following symbols indicate: (*) low correlation ($p < 0.05$); (†) moderate correlation ($p < 0.05$); (††) high correlation ($p < 0.05$); (†††) very high correlation ($p < 0.05$) between parameters. P values are located within parentheses. N.A. (not applicable) N.T. (not tested).

	Age (m)	ALB(g/dl)	ALP(u/l)	ALT(u/l)	AMY(u/l)	TBIL(mg/dl)	BUN(mg/dl)	Ca+2(mg/dl)	PHOS(mg/dl)	CRE(mg/dl)	GLU(mg/dl)	Na+(mmol/l)
Age(m)	N.T.	0.107	-0.073	0.127	0.389 *	0.216	-0.145	0.276	-0.551 †	0.209	-0.348 *	-0.112
ALB(g/dl)	0.107	N.T.	0.115	0.272	0.108	-0.539 †	-0.516 †	0.072	0.000	0.294	0.271	-0.214
ALP(u/l)	-0.073	0.115	N.T.	-0.184	0.193	0.039	-0.277	-0.462 *	-0.182	0.060	-0.098	-0.037
ALT(u/l)	0.127	0.272	-0.184	N.T.	0.449 *	-0.231	-0.043	-0.069	-0.127	-0.329 *	0.076	-0.439 *
AMY(u/l)	0.389 *	0.108	0.193	0.449 *	N.T.	-0.071	-0.184	-0.284	-0.537 †	0.027	0.284	-0.663 †
TBIL(mg/dl)	0.216	-0.539 †	0.039	-0.231	-0.071	N.T.	0.399 *	0.033	-0.006	0.029	-0.232	0.151
BUN(mg/dl)	-0.145	-0.516 †	-0.277	-0.043	-0.184	0.399 *	N.T.	-0.240	-0.217	0.109	-0.252	-0.103
Ca+2(mg/dl)	0.276	0.072	-0.462 *	-0.069	-0.284	0.033	-0.240	N.T.	0.477 *	0.146	-0.044	0.493 *
PHOS(mg/dl)	-0.551 †	0.000	-0.182	-0.127	-0.537 †	-0.006	-0.217	0.477 *	N.T.	-0.054	0.427 *	0.289
CRE(mg/dl)	0.209	0.294	0.060	-0.329 *	0.027	0.029	0.109	0.146	-0.054	N.T.	0.262	-0.278
GLU(mg/dl)	-0.348 *	0.271	-0.098	0.076	0.284	-0.232	-0.252	-0.044	0.427 *	0.262	N.T.	-0.559 †
Na+(mmol/l)	-0.112	-0.214	-0.037	-0.439 *	-0.663 †	0.151	-0.103	0.493 *	0.289	-0.278	-0.559 †	N.T.
K+(mmol/l)	-0.679 †	-0.169	-0.074	-0.062	-0.378 *	0.102	-0.181	0.211	0.778 ††	-0.184	0.258	0.342 *
TP(g/dl)	0.721 ††	0.551 †	0.109	0.143	0.339 *	0.045	-0.411 *	0.373 *	-0.266	0.216	-0.127	-0.027
GLOB(g/dl)	0.739 ††	-0.143	0.070	-0.087	0.308 *	0.491 *	-0.102	0.368	-0.289	0.052	-0.327 *	0.116
Ca/Phos	0.710 ††	0.036	0.034	0.111	0.518 †	0.055	0.113	-0.130	-0.915 †††	0.072	-0.411 *	-0.131
Na/K	0.660 †	0.111	0.079	-0.045	0.248	-0.067	0.192	-0.140	-0.741 ††	0.148	-0.337 *	-0.176
E/E'	0.049	0.143	0.441 *	-0.273	0.226	0.265	-0.269	-0.172	-0.249	-0.002	-0.077	0.195
RVDd	-0.022	0.129	-0.393 *	0.111	0.031	-0.031	0.100	0.217	0.068	-0.125	-0.173	0.048
IVSD	0.468 *	0.209	0.285	0.419 *	0.298	-0.027	0.037	-0.062	-0.351 *	-0.072	-0.489 *	-0.102
IVSs	0.473 *	0.172	-0.098	0.194	0.302 *	-0.251	-0.136	0.062	-0.070	-0.012	0.221	-0.444 *
LVIDd	0.265	0.121	-0.664 †	0.443 *	0.312 *	-0.252	-0.133	0.351 *	0.087	-0.231	0.260	-0.322 *
LVIDs	-0.135	-0.239	-0.473 *	0.478 *	0.043	0.306 *	0.317 *	0.120	0.338 *	-0.446 *	0.117	-0.199
LVPWd	0.345 *	-0.013	-0.068	0.373 *	-0.049	0.248	0.291	0.139	-0.310 *	-0.357 *	-0.518 †	0.296
LVPWs	0.747 ††	0.172	0.344 *	-0.261	0.155	0.225	-0.275	0.031	-0.569 †	0.164	-0.371 *	0.174
FS%	0.497 *	0.368 *	-0.204	0.194	0.284	-0.595 †	-0.481 *	0.226	-0.334 *	0.182	0.093	-0.117
EDV ml	0.270	0.151	-0.662 †	0.430 *	0.305 *	-0.271	-0.162	0.373 *	0.115	-0.175	0.294	-0.336 *
ESV ml	-0.203	-0.268	-0.496 *	0.439 *	-0.035	0.282	0.305 *	0.089	0.381 *	-0.469 *	0.131	-0.175
EF%	0.540 †	0.402 *	-0.135	0.008	0.360 *	-0.588 †	-0.502 †	0.240	-0.344 *	0.205	0.115	-0.152
Tricuspid Dysfunction	0.693 †	-0.064	0.343 *	0.047	0.197	0.592 †	0.061	-0.004	-0.545 †	-0.038	-0.607 †	0.180
Mitral Dysfunction	0.286	0.202	-0.517 †	0.083	0.213	-0.505 †	-0.240	0.316 *	0.069	0.284	0.375 *	-0.354 *
Aortic Dysfunction	0.693 †	-0.064	0.343 *	0.047	0.197	0.592 †	0.061	-0.004	-0.545 †	-0.038	-0.607 †	0.180
Pulmonary Dysfunction	0.874 ††	0.000	0.206	0.084	0.290	0.493 *	-0.017	0.110	-0.597 †	0.059	-0.557 †	0.078
MV E max vel	-0.842 ††	-0.295	0.169	-0.246	-0.430 *	-0.090	0.033	-0.231	0.442 *	-0.352 *	0.236	0.329 *
MV A max vel	-0.615 †	-0.351 *	-0.080	-0.357 *	-0.182	-0.185	-0.151	0.235	0.598 †	-0.061	0.366 *	0.250
MV E/A	-0.127	0.000	0.172	0.038	-0.350 *	0.194	0.373 *	-0.683 †	-0.555 †	-0.268	-0.292	-0.009
MV Dec time	0.214	-0.605 †	-0.310 *	-0.537 †	-0.008	0.477 *	0.121	0.270	0.103	0.168	-0.011	0.116
LV IVRT	0.830 ††	0.238	-0.341 *	-0.076	0.242	-0.038	-0.265	0.403 *	-0.328 *	0.213	-0.212	-0.025
Body Weight	0.832 ††	0.147	0.066	0.335 *	0.707 ††	-0.113	-0.450 *	0.055	-0.514 †	-0.007	-0.108	-0.346 *
Heart Weight	0.899 ††	0.188	0.159	0.047	0.271	0.150	-0.235	0.046	-0.618 †	0.023	-0.388 *	-0.057
BW/HW	0.155	0.090	0.055	-0.261	-0.488 *	0.272	0.292	-0.031	-0.209	0.005	-0.392 *	0.298
Electrical Axis	0.556 †	0.154	-0.582 †	0.242	0.212	0.292	0.213	0.423 *	-0.093	-0.050	-0.007	-0.231
Heart Rate	-0.004	0.111	-0.009	-0.117	-0.554 †	-0.033	0.260	-0.123	-0.079	0.290		0.037
VAT	0.720 ††	0.660 †	0.010	-0.108	0.279	-0.177	-0.260	0.389 *	-0.474 *	0.467 *	-0.314 *	0.055
ST interval	0.673 †	0.307 *	-0.303 *	0.071	0.232	-0.184	-0.274	0.371 *	-0.136	-0.201	-0.351 *	0.073
T amplitude	0.231	0.362 *	-0.442 *	0.058	0.206	0.096	-0.416 *	0.585 †	0.234	-0.254	0.066	0.195
QRS Interval	0.823 ††	0.630 †	-0.084	-0.151	0.164	-0.095	-0.174	0.447 *	-0.381 *	0.487 *	-0.260	0.042
QT Interval	0.823 ††	0.476 *	-0.256	-0.008	0.239	-0.173	-0.270	0.450 *	-0.252	0.047	-0.361 *	0.070
PR Interval	-0.223	-0.239	0.143	-0.224	-0.151	0.220	0.166	-0.123	0.303 *	0.397 *	0.521 †	-0.206
T duration	0.673 †	0.307 *	-0.303 *	0.071	0.232	-0.184	-0.274	0.371 *	-0.136	-0.201	-0.351 *	0.073
T-T Interval	0.025	-0.111	0.000	0.145	0.593 †	0.048	-0.228	0.110	0.033	-0.281	0.091	-0.070
R + S Amplitude	-0.235	-0.230	0.489 *	-0.162	0.114	-0.238	-0.327 *	-0.264	0.165	-0.055	0.016	0.102
S Amplitude	-0.148	-0.181	-0.564 †	0.122	-0.252	0.468 *	0.416 *	0.063	0.084	-0.386 *	0.028	0.001
R Amplitude	-0.223	-0.239	0.143	-0.224	-0.151	0.220	0.166	-0.123	0.303 *	0.397 *	0.521 †	-0.206
Q Amplitude	-0.634 †	-0.661 †	-0.215	-0.143	-0.529 †	0.260	0.532 †	-0.322 *	0.368 *	-0.165	0.259	-0.079
P Amplitude	0.677 †	0.655 †	0.017	0.199	0.400 *	-0.362 *	-0.173	0.418 *	-0.373 *	0.588 †	0.000	-0.194
P Duration	-0.223	-0.239	0.143	-0.224	-0.151	0.220	0.166	-0.123	0.303 *	0.397 *	0.521 †	-0.206
CSA Cardiac Myocytes	0.993 †††	0.084	-0.007	0.120	0.374 *	0.290	-0.118	0.243	-0.577 †	0.178	-0.408 *	-0.068
fibrosis	-0.338 *	-0.204	0.512 †	-0.089	-0.232	0.485 *	0.244	-0.325 *	-0.039	-0.290	-0.351 *	0.354 *
LVM (gm)	0.510 †	0.156	-0.313 *	0.704 ††	0.321 *	-0.099	0.081	0.189	-0.293	-0.329 *	-0.257	-0.185
E`	-0.635 †	-0.408 *	-0.238	0.001	-0.405 *	-0.242	0.373 *	-0.097	0.414 *	-0.181	0.254	-0.027

TABLE S-4.2 – S-4.5: REGRESSION ANALYSIS OF THE RELATIONSHIP BETWEEN STRUCTURAL AND FUNCTIONAL ECHOCARDIOGRAPHIC PARAMETERS AGE, BODY WEIGHT, HEART WEIGHT, CARDIOMYOCYTE CROSS SECTIONAL AREA, AND COLLAGEN STAINING INTENSITY OF 6-, 26-, AND 30-MONTH FEMALE F344XBN HEARTS. The following symbols indicate: (*) low correlation ($p < 0.05$); (†) moderate correlation ($p < 0.05$); (††) high correlation ($p < 0.05$); (†††) very high correlation ($p < 0.05$) between parameters. P values for correlations are located within parentheses.

	K+(mmol/l)	TP(g/dl)	GLOB(g/dl)	Ca/Phos	Na/K	E/E'	RVDd	IVSD	IVSs	LVIDd	LVIDs	LVPWd
Age(m)	-0.679 †	0.721 ††	0.739 ††	0.710 ††	0.660 †	0.049	-0.022	0.468 *	0.473 *	0.265	-0.135	0.345 *
ALB(g/dl)	-0.169	0.551 †	-0.143	0.036	0.111	0.143	0.129	0.209	0.172	0.121	-0.239	-0.013
ALP(u/l)	-0.074	0.109	0.070	0.034	0.079	0.441 *	-0.393 *	0.285	-0.098	-0.664 †	-0.473 *	-0.068
ALT(u/l)	-0.062	0.143	-0.087	0.111	-0.045	-0.273	0.111	0.419 *	0.194	0.443 *	0.478 *	0.373 *
AMY(u/l)	-0.378 *	0.339 *	0.308 *	0.518 †	0.248	0.226	0.031	0.298	0.302 *	0.312 *	0.043	-0.049
TBIL(mg/dl)	0.102	0.045	0.491 *	0.055	-0.067	0.265	-0.031	-0.027	-0.251	-0.252	0.306 *	0.248
BUN(mg/dl)	-0.181	-0.411 *	-0.102	0.113	0.192	-0.269	0.100	0.037	-0.136	-0.133	0.317	0.291
Ca+2(mg/dl)	0.211	0.373 *	0.368 *	-0.130	-0.140	-0.172	0.217	-0.062	0.062	0.351 *	0.120	0.139
PHOS(mg/dl)	0.778 ††	-0.266	-0.289	-0.915 †††	-0.741 ††	-0.249	0.068	-0.351	-0.070	0.087	0.338 *	-0.310 *
CRE(mg/dl)	-0.184	0.216	0.052	0.072	0.148	-0.002	-0.125	-0.072	-0.012	-0.231	-0.446 *	-0.357 *
GLU(mg/dl)	0.258	-0.127	-0.327 *	-0.411 *	-0.337 *	-0.077	-0.173	-0.489 *	0.221	0.260	0.117	-0.518 †
Na+(mmol/l)	0.342 *	-0.027	0.116	-0.131	-0.176	0.195	0.048	-0.102	-0.444 *	-0.322 *	-0.199	0.296
K+(mmol/l)	N.T.	-0.458 *	-0.366 *	-0.785 ††	-0.982 †††	-0.015	0.114	-0.485 *	-0.596 †	-0.250 *	0.172	-0.365 *
TP(g/dl)	-0.458 *	N.T.	0.742 ††	0.463 *	0.447 *	0.151	0.263	0.279	0.299	0.250	-0.057	0.308 *
GLOB(g/dl)	-0.366 *	0.742 ††	N.T.	0.483 *	0.393 *	0.076	0.239	0.115	0.192	0.173	0.109	0.293
Ca/Phos	-0.785 ††	0.463 *	0.483 *	N.T.	0.777 ††	0.336 *	-0.042	0.337 *	0.110	0.055	-0.315 *	0.455 *
Na/K	-0.982 †††	0.447 *	0.393 *	0.777 ††	N.T.	0.040	-0.154	0.452 *	0.554 *	0.190	-0.216	0.435 *
E/E'	-0.015	0.151	0.076	0.336 *	0.040	N.T.	-0.243	0.089	-0.394 *	-0.409 *	-0.395 *	0.087
RVDd	0.114	0.263	0.239	-0.042	-0.154	-0.243	N.T.	-0.132	-0.123	0.322 *	0.422 *	-0.072
IVSD	-0.485 *	0.279	0.115	0.337 *	0.452 *	0.089	-0.132	N.T.	0.340 *	0.037	0.015	0.491 *
IVSs	-0.596 †	0.299	0.192	0.110	0.554 †	-0.394 *	-0.123	0.340 *	N.T.	0.408 *	0.070	0.138
LVIDd	-0.250	0.250	0.173	0.055	0.190	-0.409 *	0.322 *	0.037	0.408 *	N.T.	0.622 †	-0.017
LVIDs	0.172	-0.057	0.109	-0.315 *	-0.216	-0.395 *	0.422 *	0.015	0.070	0.622 †	N.T.	0.166
LVPWd	-0.365 *	0.308 *	0.293	0.455 *	0.435 *	0.087	-0.072	0.491 *	0.138	-0.017	0.166	N.T.
LVPWs	-0.613 †	0.596 †	0.544 †	0.694 †	0.666 †	0.494 *	-0.348	0.355 *	0.307 *	-0.236	-0.553 †	0.387 *
FS%	-0.507 †	0.348 *	0.101	0.462 *	0.493 *	0.002	-0.109	0.058	0.398 *	0.436 *	-0.430 *	-0.160
EDV ml	-0.228	0.271	0.178	0.024	0.165	-0.449 *	0.332 *	0.002	0.419 *	0.996 †††	0.600 †	-0.062
ESV ml	0.240	-0.136	0.042	-0.388 *	-0.282	-0.429 *	0.422 *	-0.060	0.032	0.610 †	0.991 †††	0.088
EF%	-0.543 †	0.416 *	0.154	0.490 *	0.526 †	0.015	-0.142	0.115	0.455 *	0.413 *	-0.445 *	-0.106
Tricuspid Dysfunction	-0.421 *	0.604 †	0.745 ††	0.625 †	0.455 *	0.330 *	-0.032	0.439 *	0.106	-0.313 *	-0.148	0.638 †
Mitral Dysfunction	-0.232	0.047	-0.110	0.008	0.168	-0.378 *	0.018	-0.046	0.398 *	0.712 ††	0.040	-0.447 *
Aortic Dysfunction	-0.421 *	0.604 †	0.745 ††	0.625 †	0.455 *	0.330 *	-0.032	0.439 *	0.106	-0.313 *	-0.148	0.638 †
Pulmonary Dysfunction	-0.564 †	0.707 ††	0.811 ††	0.717 ††	0.580 †	0.247	-0.031	0.488 *	0.260	-0.110	-0.155	0.576 †
MV E max vel	0.582 †	-0.738 ††	-0.637 †	-0.519 †	-0.504 †	0.203	-0.370 *	-0.418 *	-0.501 †	-0.298	-0.008	-0.169
MV A max vel	0.687 †	-0.484 *	-0.241	-0.568 †	-0.649 †	-0.177	0.084	-0.695 †	-0.292	-0.087	-0.043	-0.580 †
MV E/A	-0.301 *	-0.190	-0.276	0.306 *	0.317 *	0.314 *	-0.284	0.133	-0.195	-0.350 *	-0.051	0.451 *
MV Dec time	0.156	-0.099	0.411 *	-0.029	-0.140	-0.081	0.218	-0.445 *	-0.002	0.088	0.053	-0.422 *
LV IVRT	-0.546 †	0.614 †	0.524 †	0.503 †	0.528 †	-0.028	0.217	0.258	0.569 †	0.382 *	-0.175	0.083
Body Weight	-0.527 †	0.509 †	0.474 *	0.600 †	0.450 *	0.132	-0.105	0.496 *	0.474 *	0.382 *	-0.142	0.056
Heart Weight	-0.770 ††	0.771 ††	0.736 ††	0.703 ††	0.785 ††	0.083	-0.043	0.422 *	0.486 *	0.192	-0.168	0.403 *
BW/HW	-0.385 *	0.377 *	0.350 *	0.198	0.483 *	-0.119	0.163	-0.022	0.064	-0.141		0.474 *
Electrical Axis	-0.488 *	0.509 †	0.607 †	0.301 *	0.487 *	-0.273	0.535 †	0.196	0.699 †	0.710 ††	0.468 *	0.456 *
Heart Rate	-0.142	0.109	0.068	-0.050	0.187	-0.423 *	-0.048	-0.344 *	-0.200	-0.063	-0.001	-0.005
VAT	-0.704 ††	0.784 ††	0.627 †	0.709 ††	0.724 ††	0.323 *	-0.012	0.346 *	0.252	0.167	-0.396 *	0.313 *
ST interval	-0.458 *	0.403 *	0.320 *	0.317 *	0.451 *	0.133	0.251	0.524 †	0.554 †	0.618 †	0.159	0.218
T amplitude	0.027	0.501 *	0.474 *	-0.005	-0.038	0.195	0.522 †	-0.085	-0.180	0.688 †	0.481 †	-0.141
QRS Interval	-0.708 ††	0.819 ††	0.706 ††	0.607 †	0.735 ††	0.088	0.114	0.286	0.490 *	0.162	-0.322 *	0.366 *
QT Interval	-0.618 †	0.622 †	0.516 †	0.474 *	0.624 †	0.133	0.230	0.499 *	0.604 †	0.517 †	-0.015	0.309 †
PR Interval	0.474 *	-0.195	-0.018	-0.460 *	-0.501 †	-0.307 *	0.213	-0.669 †	-0.480 *	-0.261	0.066	-0.614 †
T duration	-0.458 *	0.403 *	0.320 *	0.317 *	0.451 *	0.133	0.251	0.524 †	0.554 †	0.618 †	0.159	0.218
T-T Interval	0.110	-0.093	-0.048	0.103	-0.158	0.432 *	0.046	0.348	0.200	0.058	-0.004	0.046
R+S Amplitude	0.429 *	-0.505 †	-0.529 †	-0.295	-0.449 *	0.271	-0.375 *	-0.098		-0.538 †	-0.464 *	-0.398 *
S Amplitude	-0.066	0.109	0.274	-0.049	0.085	-0.080	0.337 *	-0.289	-0.339 *	0.557 †	0.647 †	-0.001
R Amplitude	0.474 *	-0.195	-0.018	-0.460 *	-0.501 †	-0.307 *	0.213	-0.669 †	-0.480 *	-0.261	0.066	-0.614 †
Q Amplitude	0.416 *	-0.632 †	-0.407 *	-0.609 †	-0.409 *	-0.615 †	0.144	-0.541 *	-0.087	-0.069	0.394 *	-0.312 *
P Amplitude	-0.562 †	0.628 †	0.390 *	0.596 †	0.551 †	0.129	-0.242	0.387 *	0.206	0.128	-0.370 *	0.332 *
P Duration	0.474 *	-0.195	-0.018	-0.460 *	-0.501 †	-0.307 *	0.213	-0.669 †	-0.480 *	-0.261	0.066	-0.614 †
CSA Cardiac Myocytes	-0.669 †	0.737 ††	0.777 ††	0.731 ††	0.659 †	0.099	-0.025	0.485 *	0.433 *	0.179	-0.144	0.411 *
fibrosis	0.264	-0.084	0.069	-0.046	-0.200	0.313 *	-0.016	0.020	-0.418 *	-0.716 ††	-0.033	0.422 *
LVM (gm)	-0.534 †	0.261	0.427 *	0.412 *	0.501 †	-0.613 †	0.651 †	0.433 *	0.652 †	0.479 *	0.641 †	0.128
E`	0.288	-0.111	0.126	-0.548 †	-0.257	-0.039	0.142	0.324 *	-0.202	-0.715 ††	-0.235	0.147

TABLE S-4.3:

	LVPWs		FS%		EDV ml		ESV ml		EF%		Tricuspid Dysfunction		Mitral Dysfunction		Aortic Dysfunction		Pulmonary Dysfunction		MV E max vel		MV A max vel		MV E/A	
Age(m)	0.747	††	0.497	*	0.270		-0.203		0.540	†	0.693	†	0.286		0.693	†	0.874	††	-0.842	††	-0.615	†	-0.127	
ALB(g/dl)	0.172		0.368	*	0.151		-0.268		0.402	*	-0.064		0.202		-0.064		0.000		-0.295		-0.351	*	0.000	
ALP(u/l)	0.344	*	-0.204		-0.662	†	-0.496	*	-0.135		0.343	*	-0.517	†	0.343	*	0.206		0.169		-0.080		0.172	
ALT(u/l)	-0.261		-0.031		0.430	*	0.439	*	0.008		0.047		0.083		0.047		0.084		-0.246		-0.357	*	0.038	
AMY(u/l)	0.155		0.284		0.305		-0.035		0.360	*	0.197		0.213		0.197		0.290		-0.430	*	-0.182		-0.350	*
TBIL(mg/dl)	0.225		-0.595	†	-0.271		0.282		-0.588	†	0.592	†	-0.505	†	0.592	†	0.493	*	-0.090		-0.185		0.194	
BUN(mg/dl)	-0.275		-0.481	*	-0.162		0.305	*	-0.502	†	0.061		-0.240		0.061		-0.017		0.033		-0.151		0.373	*
Ca+2(mg/dl)	0.031		0.226		0.373	*	0.089		0.240		-0.004		0.316	*	-0.004		0.110		-0.231		0.235		-0.683	†
PHOS(mg/dl)	-0.569	†	-0.334	*	0.115		0.381	*	-0.344	*	-0.545	†	0.069		-0.545	†	-0.597	†	0.442	*	0.598	†	-0.555	†
CRE(mg/dl)	0.164		0.182		-0.175		-0.469	*	0.205		-0.038		0.284		-0.038		0.059		-0.352	*	-0.061		-0.268	
GLU(mg/dl)	-0.371	*	0.093		0.294		0.131		0.115		-0.607	†	0.375	*	-0.607	†	-0.557	†	0.236		0.366	*	-0.292	
Na+(mmol/l)	0.174		-0.117		-0.336	*	-0.175		-0.152		0.180		-0.354	*	0.180		0.078		0.329	*	0.250		-0.009	
K+(mmol/l)	-0.613	†	-0.507	†	-0.228		0.240		-0.543	†	-0.421	*	-0.232		-0.421	*	-0.564	†	0.582	†	0.687	†	-0.301	*
TP(g/dl)	0.596	†	0.348	*	0.271		-0.136		0.416	*	0.604	†	0.047		0.604	†	0.707	††	-0.738	††	-0.484	*	-0.190	
GLOB(g/dl)	0.544	†	0.101		0.178		0.042		0.154		0.745	††	-0.110		0.745	††	0.811	††	-0.637	†	-0.241		-0.276	
Ca/Phos	0.694	†	0.462	*	0.024		-0.388	*	0.490	*	0.625	†	0.008		0.625	†	0.717	††	-0.519	†	-0.568	†	0.306	*
Na/K	0.666	†	0.493	*	0.165		-0.282		0.526	†	0.455	*	0.168		0.455	*	0.580	†	-0.504	†	-0.649	†	0.317	*
E/E'	0.494	*	0.002		-0.449	*	-0.429	*	0.015		0.330	*	-0.378	*	0.330	*	0.247		0.203		-0.177		0.314	*
RVDd	-0.348	*	-0.109		0.332	*	0.422	*	-0.142		-0.032		0.018		-0.032		-0.031		-0.370	*	0.084		-0.284	
IVSD	0.355	*	0.058		0.002		-0.060		0.115		0.439	*	-0.046		0.439	*	0.488	*	-0.418	*	-0.695	†	0.133	
IVSs	0.307	*	0.398	*	0.419	*	0.032		0.455	*	0.106		0.398	*	0.106		0.260		-0.501	†	-0.292		-0.195	
LVIDd	-0.236		0.436	*	0.996	†††	0.610	†	0.413	*	-0.313	*	0.712	††	-0.313	*	-0.110		-0.298		-0.087		-0.350	*
LVIDs	-0.553	†	-0.430	*	0.600	†	0.991	†††	-0.445	*	-0.148		0.040		-0.148		-0.155		-0.008		-0.043		-0.051	
LVPWd	0.387	*	-0.160		-0.062		0.088		-0.106		0.638	†	-0.447	*	0.638	†	0.576	†	-0.169		-0.580	†	0.451	*
LVPWs	N.T.		0.407	*	-0.245		-0.606	†	0.453	*	0.747	††	-0.135		0.747	††	0.811	††	-0.443	*	-0.560	†	0.253	
FS%	0.407	*	N.T.		0.451	*	-0.436	*	0.990	†††	-0.137		0.744	††	-0.137		0.103		-0.351	*	-0.095		-0.286	
EDV ml	-0.245		0.451	*	N.T.		0.591	†	0.430	*	-0.329	*	0.739	††	-0.329	*	-0.119		-0.325		-0.062		-0.396	*
ESV ml	-0.606	†	-0.436	*	0.591	†	N.T.		-0.465	*	-0.219		0.059		-0.219		-0.231		0.053		0.019		-0.036	
EF%	0.453	*	0.990	†††	0.430	*	-0.465	*	N.T.		-0.071		0.706	††	-0.071		0.165		-0.392	*	-0.123		-0.315	*
Tricuspid Dysfunction	0.747	††	-0.137		-0.329	*	-0.219		-0.071		N.T.		-0.492	*	1.000	†††	0.956	†††	-0.520	†	-0.608	†	0.316	*
Mitral Dysfunction	-0.135		0.744	††	0.739	††	0.059		0.706	††	-0.492	*	N.T.		-0.492	*	-0.215		-0.272		0.101		-0.529	†
Aortic Dysfunction	0.747	††	-0.137		-0.329	*	-0.219		-0.071		1.000	†††	-0.492	*	N.T.		0.956	†††	-0.520	†	-0.608	†	0.316	*
Pulmonary Dysfunction	0.811	††	0.103		-0.119		-0.231		0.165		0.956	†††	-0.215		0.956	†††	N.T.		-0.692	†	-0.663	†	0.174	
MV E max vel	-0.443	*	-0.351	*	-0.325	*	0.053		-0.392	*	-0.520	†	-0.272		-0.520	†	-0.692	†	N.T.		0.552	†	0.320	*
MV A max vel	-0.560	†	-0.095		-0.062		0.019		-0.123		-0.608	†	0.101		-0.608	†	-0.663	†	0.552	†	N.T.		-0.571	†
MV E/A	0.253		-0.286		-0.396	*	-0.036		-0.315	*	0.316	*	-0.529	†	0.316	*	0.174		0.320	*	-0.571	†	N.T.	
MV Dec time	0.030		0.041		0.106		0.084		-0.005		0.020		0.217		0.020		0.098		-0.193		0.397	*	-0.462	*
LV IVRT	0.605	†	0.665	†	0.397	*	-0.209		0.667	†	0.351	*	0.481	*	0.351	*	0.571	†	-0.805	††	-0.389	*	-0.312	*
Body Weight	0.551	†	0.680	†	0.381	*	-0.192		0.729	††	0.409	*	0.418	*	0.409	*	0.618	†	-0.673	†	-0.477	*	-0.250	
Heart Weight	0.808	††	0.501	†	0.193		-0.221		0.552	†	0.754	††	0.057		0.754	††	0.882	††	-0.715	††	-0.752	††	0.161	
BW/HW	0.317		-0.172		-0.140		0.017		-0.171		0.454	*	-0.400	*	0.454	*	0.374	*	-0.157		-0.443	*	0.517	†
Electrical Axis	0.272		0.229		0.704	††	0.397	*	0.262		0.323	*	0.258		0.323	*	0.447	*	-0.682	†	-0.470	*	-0.090	
Heart Rate	-0.114		-0.091		-0.025		0.044		-0.124		-0.002		-0.002		-0.002		-0.003		0.071		-0.087		0.321	*
VAT	0.768	††	0.738	††	0.172		-0.471	*	0.798	††	0.456	*	0.255		0.456	*	0.613	†	-0.589	†	-0.598	†	-0.067	
ST interval	0.406	*	0.611	†	0.588	†	0.116		0.611	†	0.194		0.516	†	0.194		0.415	*	-0.479	*	-0.491	*	-0.136	
T amplitude	-0.139		0.244		0.673	†	0.474	*	0.199		-0.127		0.410	*	-0.127		0.011		-0.059		-0.022		-0.326	*
QRS Interval	0.764	††	0.634	†	0.181		-0.393	*	0.701	††	0.560	†	0.244		0.560	†	0.727	††	-0.727	††	-0.595	†	-0.092	
QT Interval	0.608	†	0.705	††	0.503	†	-0.076		0.732	††	0.366	*	0.478	*	0.366	*	0.595	†	-0.646	†	-0.601	†	-0.138	
PR Interval	-0.572	†	-0.470	*	-0.206		0.119		-0.493	*	-0.193		-0.016		-0.193		-0.225		0.226		0.644	†	-0.279	
T duration	0.406	*	0.611	†	0.588	†	0.116		0.611	†	0.194		0.516	†	0.194		0.415	*	-0.479	*	-0.491	*	-0.136	
T-T Interval	0.133		0.092		0.018		-0.054		0.130		0.036		-0.015		0.036		0.035		-0.091		0.057		-0.297	
R + S Amplitude	-0.021		-0.089		-0.542	†	-0.434	*	-0.083		-0.132		-0.104		-0.132		-0.189		0.288		0.420	*	-0.229	
S Amplitude	-0.387	*	-0.129		0.536	†	0.665	†	-0.198		-0.257		0.143		-0.257		-0.237		0.218		-0.049		0.325	*
R Amplitude	-0.572	†	-0.470	*	-0.206		0.119		-0.493	*	-0.193		-0.016		-0.193		-0.225		0.226		0.644	†	-0.279	
Q Amplitude	-0.674	†	-0.611	†	-0.051		0.480	*	-0.692	†	-0.459	*	-0.155		-0.459	*	-0.579	†	0.372	*	0.471	*	0.148	
P Amplitude	0.507	†	0.624	†	0.144		-0.458	*	0.721	††	0.345	*	0.340	*	0.345	*	0.519	†	-0.484	*	-0.461	*	-0.225	
P Duration	-0.572	†	-0.470	*	-0.206		0.119		-0.493	*	-0.193		-0.016		-0.193		-0.225		0.226		0.644	†	-0.279	
CSA Cardiac Myocytes	0.782	††	0.413	*	0.181		-0.215		0.461	*	0.773	††	0.172		0.773	††	0.925	†††	-0.827	††	-0.643	†	-0.055	
fibrosis	0.092		-0.760	††	-0.743	††	-0.047		-0.724	††	0.444	*	-0.999	†††	0.444	*	0.161		0.313	*	-0.067		0.528	†
LVM (gm)	0.236		0.618	†	0.408	*	0.270		0.977	†††	0.243		0.255		0.378	*	0.378	*	-0.613	†	0.059		-0.370	*
E`	0.388	*	-0.274		-0.052		-0.667	†	0.156		-0.711	††	0.574	†	0.517	†	-0.711	††	-0.039		-0.579	†	0.597	†

TABLE S-4.4:

	MV Dec time	LV IVRT	Body Weight	Heart Weight	HW/BW	Electrical Axis	Heart Rate	VAT	ST interval	T amplitude	QRS Interval	QT Interval	PR Interval
Age(m)	0.214	0.830 ††	0.832 ††	0.899 ††	0.155	0.556 †	-0.004	0.720 ††	0.673 †	0.231	0.823 ††	0.823 ††	-0.223
ALB(g/dl)	-0.605 †	0.238	0.147	0.188	0.090	0.154	0.111	0.660 †	0.307 *	0.362 *	0.630 †	0.476 *	-0.239
ALP(u/l)	-0.310 *	-0.341 *	0.066	0.159	0.055	-0.582 †	-0.009	0.010	-0.303 *	-0.442 *	-0.084	-0.256	0.143
ALT(u/l)	-0.537 †	-0.076	0.335 *	0.047	-0.261	0.242	-0.117	-0.108	0.071	0.058	-0.151	-0.008	-0.224
AMY(u/l)	-0.008	0.242	0.707 ††	0.271	-0.488 *	0.212	-0.554 †	0.279	0.232	0.206	0.164	0.239	-0.151
TBIL(mg/dl)	0.477 *	-0.038	-0.113	0.150	0.272	0.292	-0.033	-0.177	-0.184	0.096	-0.095	-0.173	0.220
BUN(mg/dl)	0.121	-0.265	-0.450 *	-0.235	0.292	0.213	0.260	-0.260	-0.274	-0.416 *	-0.174	-0.270	0.166
Ca+2(mg/dl)	0.270	0.403 *	0.055	0.046	-0.031	0.423 *	-0.123	0.389 *	0.371 *	0.585 †	0.447 *	0.450 *	-0.123
PHOS(mg/dl)	0.103	-0.328 *	-0.514 †	-0.618 †	-0.209	-0.093	-0.079	-0.474 *	-0.136	0.234	-0.381 *	-0.252	0.303 *
CRE(mg/dl)	0.168	0.213	-0.007	0.023	0.005	-0.050	0.290	0.467 *	-0.201	-0.254	0.487 *	0.047	0.397 *
GLU(mg/dl)	-0.011	-0.212	-0.108	-0.388 *	-0.392 *	-0.007	-0.090	-0.314 *	-0.351 *	0.066	-0.260	-0.361 *	0.521 †
Na+(mmol/l)	0.116	-0.025	-0.346 *	-0.057	0.298	-0.231	0.037	0.055	0.073	0.195	0.042	0.070	-0.206
K+(mmol/l)	0.156	-0.546 †	-0.527 †	-0.770 ††	-0.385 *	-0.488 *	-0.142	-0.704 ††	-0.458 *	0.027	-0.708 ††	-0.618 †	0.474 *
TP(g/dl)	-0.099	0.614 †	0.509 †	0.771 ††	0.377 *	0.509 †	0.109	0.784 ††	0.403 *	0.501 †	0.819 ††	0.622 †	-0.195
GLOB(g/dl)	0.411 *	0.524 †	0.474 *	0.736 ††	0.350 *	0.607 †	0.068	0.627 †	0.320 *	0.474 *	0.706 ††	0.516 †	-0.018
Ca/Phos	-0.029	0.503 †	0.600 †	0.703 ††	0.198	0.301	-0.050	0.709 ††	0.317 *	-0.005	0.607 †	0.474 *	-0.460 *
Na/K	-0.140	0.528 †	0.450 *	0.785 ††	0.483 *	0.487 *	0.187	0.724 ††	0.451 *	-0.038	0.735 ††	0.624 †	-0.501 †
E/E'	-0.081	-0.028	0.132	0.083	-0.119	-0.273	-0.423 *	0.323 *	0.133	0.195	0.088	0.133	-0.307 *
RVDd	0.218	0.217	-0.105	-0.043	0.163	0.535 †	-0.048	-0.012	0.251	0.522 †	0.114	0.230	0.213
IVSD	-0.445 *	0.258	0.496 *	0.422 *	-0.022	0.196	-0.344 *	0.346 *	0.524 †	-0.085	0.286	0.499 *	-0.669 †
IVSs	-0.002	0.569 †	0.474 *	0.486 *	0.064	0.699 †	-0.200	0.252	0.554 †	-0.180	0.490 *	0.604 †	-0.480 *
LVIDd	0.088	0.382 *	0.382 *	0.192	-0.141	0.710 ††	-0.063	0.167	0.618 †	0.688 †	0.162	0.517 †	-0.261
LVIDs	0.053	-0.175	-0.142	-0.168	0.026	0.468 *	-0.001	-0.396 *	0.159	0.481 *	-0.322 *	-0.015	0.066
LVPWd	-0.422 *	0.083	0.056	0.403 *	0.474 *	0.456 *	-0.005	0.313 *	0.218	-0.141	0.366 *	0.309 *	-0.614 †
LVPWs	0.030	0.605 †	0.551 †	0.808 ††	0.317 *	0.272	-0.114	0.768 ††	0.406 *	-0.139	0.764 ††	0.608 †	-0.572 †
FS%	0.041	0.665 †	0.680 †	0.501 †	-0.172	0.229	-0.091	0.738 ††	0.611 †	0.244	0.634 †	0.705 ††	-0.470 *
EDV ml	0.106	0.397 *	0.381 *	0.193	-0.140	0.704 ††	-0.025	0.172	0.588 †	0.673 †	0.181	0.503 †	-0.206
ESV ml	0.084	-0.209	-0.192	-0.221	0.017	0.397 *	0.044	-0.471 *	0.116	0.474 *	-0.393 *	-0.076	0.119
EF%	-0.005	0.667 †	0.729 ††	0.552 †	-0.171	0.262	-0.124	0.798 ††	0.611 †	0.199	0.701 ††	0.732 ††	-0.493 *
Tricuspid Dysfunction	0.020	0.351 *	0.409 *	0.754 ††	0.454 *	0.323 *	-0.002	0.456 *	0.194	-0.127	0.560 †	0.366 *	-0.193
Mitral Dysfunction	0.217	0.481 *	0.418 *	0.057	-0.400 *	0.258	-0.002	0.255	0.516 †	0.410 *	0.244	0.478 *	-0.016
Aortic Dysfunction	0.020	0.351 *	0.409 *	0.754 ††	0.454 *	0.323 *	-0.002	0.456 *	0.194	-0.127	0.560 †	0.366 *	-0.193
Pulmonary Dysfunction	0.098	0.571 †	0.618 †	0.882 ††	0.374 *	0.447 *	-0.003	0.613 †	0.415 *	0.011	0.727 ††	0.595 †	-0.225
MV E max vel	-0.193	-0.805 ††	-0.673 †	-0.715 ††	-0.157	-0.682 †	0.071	-0.589 †	-0.479 *	-0.059	-0.727 ††	-0.646 †	0.226
MV A max vel	0.397 *	-0.389 *	-0.477 *	-0.752 ††	-0.443 *	-0.470 *	-0.087	-0.598 †	-0.491 *	-0.022	-0.595 †	-0.601 †	0.644 †
MV E/A	-0.462 *	-0.312 *	-0.250	0.161	0.517 †	-0.090	0.321 *	-0.067	-0.136	-0.326 *	-0.092	-0.138	-0.279
MV Dec time	N.T.	0.359 *	0.114	0.019	-0.148	0.219	-0.188	-0.118	0.081	0.149	0.001	0.059	0.329 *
LV IVRT	0.359 *	N.T.	0.682 †	0.683 †	0.071	0.677 †	-0.260	0.676 †	0.763 ††	0.204	0.783 ††	0.876 ††	-0.523 †
Body Weight	0.114	0.682 †	N.T.	0.684 †	-0.322 *	0.344 *	-0.434 *	0.565 †	0.635 †	0.178	0.464 *	0.653 †	-0.533 †
Heart Weight	0.019	0.683 †	0.684 †	N.T.	0.463 *	0.501 †	0.158	0.761 ††	0.507 †	0.108	0.806 ††	0.699 †	-0.444 *
BW/HW	-0.148	0.071	-0.322 *	0.463 *	N.T.	0.450 *	0.674 †	0.308 *	-0.033	-0.030	0.476 *	0.170	0.020
Electrical Axis	0.219	0.677 †	0.344 *	0.501 †	0.450 *	N.T.	-0.145	0.415 *	0.610 †	0.264	0.634 †	0.684 †	-0.387 *
Heart Rate	-0.188	-0.260	-0.434 *	0.158	0.674 †	-0.145	N.T.	0.016	-0.375 *	0.004	0.117	-0.230	0.554 †
VAT	-0.118	0.676 †	0.565 †	0.761 ††	0.308 *	0.415 *	0.016	N.T.	0.486 *	0.222	0.910 †††	0.720 ††	-0.415 *
ST interval	0.081	0.763 ††	0.635 †	0.507 †	-0.033	0.610 †	-0.375 *	0.486 *	N.T.	0.589 †	0.509 †	0.939 †††	-0.531 †
T amplitude	0.149	0.204	0.178	0.108	-0.030	0.264	0.004	0.222	0.589 †	N.T.	0.141	0.490 *	0.072
QRS Interval	0.001	0.783 ††	0.464 *	0.806 ††	0.476 *	0.634 †	0.117	0.910 †††	0.509 †	0.141	N.T.	0.773 ††	-0.297
QT Interval	0.059	0.876 ††	0.653 †	0.699 †	0.170	0.684 †	-0.230	0.720 ††	0.939 †††	0.490 *	0.773 ††	N.T.	-0.510 †
PR Interval	0.329 *	-0.523 †	-0.533 †	-0.444 *	0.020	-0.387 *	0.554 †	-0.415 *	-0.531 †	0.072	-0.297	-0.510 †	N.T.
T duration	0.081	0.763 ††	0.635 †	0.507 †	-0.033	0.610 †	-0.375 *	0.486 *	1.000 †††	0.589 †	0.509 †	0.939 †††	-0.531 †
T-T Interval	0.173	0.263	0.447 *	-0.140	-0.664 †	0.165	-0.998 †††	0.005	0.362 *	-0.024	-0.097	0.228	-0.561 †
R + S Amplitude	0.085	-0.171	0.094	-0.420 *	-0.668 †	-0.605 †	-0.540 †	-0.387 *	-0.129	-0.380 *	-0.443 *	-0.271	0.015
S Amplitude	0.003	-0.245	-0.261	-0.022	0.304 *	0.150	0.436 *	-0.034	0.104	0.707 ††	-0.122	0.028	0.208
R Amplitude	0.329 *	-0.523 †	-0.533 †	-0.444 *	0.020	-0.387 *	0.554 †	-0.415 *	-0.531 †	0.208	-0.297	-0.510 †	1.000 †††
Q Amplitude	0.322 *	-0.472 *	-0.712 ††	-0.513 †	0.166	-0.127	0.379 *	-0.776 ††	-0.539 †	0.456 *	-0.594 †	-0.634 †	0.456 *
P Amplitude	-0.357 *	0.399 *	0.512 †	0.501 †	0.049	0.199	0.109	0.805 ††	0.259	-0.746 ††	0.730 ††	0.482 *	-0.148
P Duration	0.329 *	-0.523 †	-0.533 †	-0.444 *	0.020	-0.387 *	0.554 †	-0.415 *	-0.531 †	-0.148	-0.297	-0.510 †	1.000 †††
CSA Cardiac Myocytes	0.191	0.788 ††	0.802 ††	0.919 †††	0.212	0.543 †	-0.004	0.715 ††	0.630 †	-0.645 †	0.823 ††	0.792 ††	-0.230
fibrosis	-0.225	-0.518 †	-0.455 *	-0.104	0.385 *	-0.285	0.002	-0.287	-0.541 †	-0.225	-0.282	-0.511 †	0.028
LVM (gm)	0.332 *	0.140	0.465 *	0.093	0.672 †	-0.105	0.343 *	0.593 †	0.288	-0.266	0.564 †	-0.626 †	0.593 †
E`	-0.100	-0.604 †	-0.254	0.427 *	-0.675 †	-0.465 *	-0.216	-0.604 †	-0.586 †	0.098	-0.465 *	-0.445 *	-0.454 *

TABLE S-4.5:

	T duration	T-T Interval	R + S Amplitude	S Amplitude	R Amplitude	Q Amplitude	P Amplitude	P Duration	CSA Cardiac Myocytes	fibrosis	LVM (gm)	E`
Age(m)	0.673 †	0.025	-0.235	-0.148	-0.223	-0.634 †	0.677 †	-0.223	0.993 †††	-0.338 *	0.510 †	-0.635 †
ALB(g/dl)	0.307 *	-0.111	-0.230	-0.181	-0.239	-0.661 †	0.655 †	-0.239	0.084	-0.204	0.156	-0.408 *
ALP(u/l)	-0.303 *	0.000	0.489	-0.564 †	0.143	-0.215	0.017	0.143	-0.007	0.512 †	-0.313 *	-0.238
ALT(u/l)	0.071	0.145	-0.162	0.122	-0.224	-0.143	0.199	-0.224	0.120	-0.089	0.704 ††	0.001
AMY(u/l)	0.232	0.593 †	0.114	-0.252	-0.151	-0.529 †	0.400 *	-0.151	0.374 *	-0.232	0.321 *	-0.405 *
TBIL(mg/dl)	-0.184	0.048	-0.238	0.468 *	0.220	0.260	-0.362 *	0.220	0.290	0.485 *	-0.099	-0.242
BUN(mg/dl)	-0.274	-0.228	-0.327 *	0.416 *	0.166	0.532 †	-0.173	0.166	-0.118	0.244	0.081	0.373 *
Ca+2(mg/dl)	0.371 *	0.110	-0.264	0.063	-0.123	-0.322 *	0.418 *	-0.123	0.243	-0.325 *	0.189	-0.097
PHOS(mg/dl)	-0.136	0.033	0.165	0.084	0.303 *	0.368 *	-0.373 *	0.303 *	-0.577 †	-0.039	-0.293	0.414 *
CRE(mg/dl)	-0.201	-0.281	-0.055	-0.386 *	0.397 *	-0.165	0.588 †	0.397 *	0.178	-0.290	-0.329 *	-0.181
GLU(mg/dl)	-0.351 *	0.091	0.016	0.028	0.521 †	0.259	0.000	0.521 †	-0.408 *	-0.351 *	-0.257	0.254
Na+(mmol/l)	0.073	-0.070	0.102	0.001	-0.206	-0.079	-0.194	-0.206	-0.068	0.354 *	-0.185	-0.027
K+(mmol/l)	-0.458 *	0.110	0.429 *	-0.066	0.474 *	0.416 *	-0.562 †	0.474 *	-0.669 †	0.264	-0.534 †	0.288
TP(g/dl)	0.403 *	-0.093	-0.505 †	0.109	-0.195	-0.632 †	0.628 †	-0.195	0.737 ††	-0.084	0.261	-0.111
GLOB(g/dl)	0.320 *	-0.048	-0.529 †	0.274	-0.018	-0.407 *	0.390 *	-0.018	0.777 ††	0.069	0.427 *	0.126
Ca/Phos	0.317 *	0.103	-0.295	-0.049	-0.460 *	-0.609 †	0.596 †	-0.460 *	0.731 ††	-0.046	0.412 *	-0.548 †
Na/K	0.451 *	-0.158	-0.449 *	0.085	-0.501 †	-0.409 *	0.551 †	-0.501 †	0.659 †	-0.200	0.501 †	-0.257
E/E'	0.133	0.432 *	0.271	-0.080	-0.307 *	-0.615 †	0.129	-0.307 *	0.099	0.313 *	-0.613 †	-0.039
RVDd	0.251	0.046	-0.375 *	0.337 *	0.213	0.144	-0.242	0.213	-0.025	-0.016	0.651 †	0.142
IVSD	0.524 †	0.348 *	0.159	-0.289	-0.669 †	-0.541 †	0.387 *	-0.669 †	0.485 *	0.020	0.433 *	0.324 *
IVSs	0.554 †	0.200	-0.098	-0.339 *	-0.480 *	-0.087	0.206	-0.480 *	0.433 *	-0.418 *	0.652 †	-0.202
LVIDd	0.618 †	0.058	-0.538 †	0.557 †	-0.261	-0.069	0.128	-0.261	0.179	-0.716 ††	0.479 *	-0.715 ††
LVIDs	0.159	-0.004	-0.464 *	0.647 †	0.066	0.394 *	-0.370 *	0.066	-0.144	-0.033	0.641 †	-0.235
LVPWd	0.218	0.046	-0.398 *	-0.001	-0.614 †	-0.312 *	0.332 *	-0.614 †	0.411 *	0.422 *	0.128	0.147
LVPWs	0.406 *	0.133	-0.021	-0.387 *	-0.572 †	-0.674 †	0.507 †	-0.572 †	0.782 ††	0.092	0.236	0.388 *
FS%	0.611 †	0.092	-0.089	-0.129	-0.470 *	-0.611 †	0.624 †	-0.470 *	0.413 *	-0.760 ††	0.618 †	-0.274
EDV ml	0.588 †	0.018	-0.542 †	0.536 †	-0.206	-0.051	0.144	-0.206	0.181	-0.743 ††	0.408 *	-0.052
ESV ml	0.116	-0.054	-0.434 *	0.665 †	0.119	0.480 *	-0.458 *	0.119	-0.215	-0.047	0.270	-0.667 †
EF%	0.611 †	0.130	-0.083	-0.198	-0.493 *	-0.692 †	0.721 ††	-0.493 *	0.461 *	-0.724 ††	0.977 †††	0.156
Tricuspid Dysfunction	0.194	0.036	-0.132	-0.257	-0.193	-0.459 *	0.345 *	-0.193	0.773 ††	0.444 *	0.243	-0.711 ††
Mitral Dysfunction	0.516 †	-0.015	-0.104	0.143	-0.016	-0.155	0.340 *	-0.016	0.172	-0.999 †††	0.255	0.574 †
Aortic Dysfunction	0.194	0.036	-0.132	-0.257	-0.193	-0.459 *	0.345 *	-0.193	0.773 ††	0.444 *	0.378 *	0.517 *
Pulmonary Dysfunction	0.415 *	0.035	-0.189	-0.237	-0.225	-0.579 †	0.519 †	-0.225	0.925 †††	0.161	0.378 *	-0.711 ††
MV E max vel	-0.479 *	-0.091	0.288	0.218	0.226	0.372 *	-0.484 *	0.226	-0.827 ††	0.313 *	-0.613 †	-0.039
MV A max vel	-0.491 *	0.057	0.420 *	-0.049	0.644 †	0.471 *	-0.461 *	0.644 †	-0.643 †	-0.067	0.059	-0.579 †
MV E/A	-0.136	-0.297	-0.229	0.325 *	-0.279	0.148	-0.225	-0.279	-0.055	0.528 †	-0.370 *	0.597 †
MV Dec time	0.081	0.173	0.085	0.003	0.329 *	0.322 *	-0.357 *	0.329 *	0.191	-0.225	0.332 *	-0.100
LV IVRT	0.763 ††	0.263	-0.171	-0.245	-0.523 †	-0.472 *	0.399 *	-0.523 †	0.788 ††	-0.518 †	0.140	-0.604 †
Body Weight	0.635 †	0.447 *	0.094	-0.261	-0.533 †	-0.712 ††	0.512 †	-0.533 †	0.802 ††	-0.455 *	0.465 *	-0.254
Heart Weight	0.507 †	-0.140	-0.420 *	-0.022	-0.444 *	-0.513 †	0.501 †	-0.444 *	0.919 †††	-0.104	0.093	0.427 *
BW/HW	-0.033	-0.664 †	-0.668 †	0.304 *	0.020	0.166	0.049	0.020	0.212	0.385 *	0.672 †	-0.675 †
Electrical Axis	0.610 †	-0.605 †	0.150		-0.387 *	-0.127	0.199	-0.387 *	0.543 †	-0.285	-0.105	-0.465 *
Heart Rate	-0.375 *	-0.998 †††	-0.540 †	0.436 *	0.554 †	0.379 *	0.109	0.554 †	-0.004	0.002	0.343 *	-0.216
VAT	0.486 *	0.005	-0.387 *	-0.034	-0.415 *	-0.776 ††	0.805 ††	-0.415 *	0.715 ††	-0.287	0.593 †	-0.604 †
ST interval	1.000 †††	0.362 *	-0.129	0.104	-0.531 †	-0.539 †	0.259	-0.531 †	0.630 †	-0.541 †	0.288	-0.586 †
T amplitude	0.589 †	-0.024	-0.380 *	0.707 ††	0.208	0.456 *	-0.746 ††	-0.148	-0.645 †	-0.225	-0.266	0.098
QRS Interval	0.509 †	-0.097	-0.443 *	-0.122	-0.297	-0.594 †	0.730 ††	-0.297	0.823 ††	-0.282	0.564 †	-0.465 *
QT Interval	0.939 †††	-0.271	0.028		-0.510 †	-0.634 †	0.482 †	-0.510 †	0.792 ††	-0.511 †	-0.626 †	-0.445 *
PR Interval	-0.531 †	-0.561 †	0.015	0.208	1.000 †††	0.456 *	-0.148	1.000 †††	-0.230	0.028	0.593 †	-0.454 *
T duration	N.T.	0.362 *	-0.129	0.104	-0.531 †	-0.539 †	0.259	-0.531 †	0.630 †	-0.541 †	0.126	-0.062
T-T Interval	0.362 *	N.T.	0.516 †	-0.440 *	-0.561 †	-0.395 *	-0.075	-0.561 †	0.028	0.013	0.139	0.297
R + S Amplitude	-0.129	0.516 †	N.T.	-0.698 †	0.015	-0.061	-0.254	0.015	-0.231	0.114	0.251	0.807 ††
S Amplitude	0.104	-0.440 *	-0.698 †	N.T.	0.208	0.207	-0.141	0.208	-0.173	-0.133	-0.626 †	-0.428 *
R Amplitude	-0.531 †	-0.561 †	0.015	0.208	N.T.	0.456 *	-0.148	1.000 †††	-0.230	0.028	-0.361 *	0.428 *
Q Amplitude	-0.539 †	-0.395 *	-0.061	0.207	0.456 *	N.T.	-0.746 ††	0.456 *	-0.639 †	0.185	0.400 *	0.613 †
P Amplitude	0.259	-0.075	-0.254	-0.141	-0.148	-0.746 ††	N.T.	-0.148	0.659 †	-0.369 *	-0.626 †	-0.671 †
P Duration	-0.531 †	-0.561 †	0.015	0.208	1.000 †††	0.456 *	-0.148	N.T.	-0.230	0.028	-0.172	-0.119
CSA Cardiac Myocytes	0.630 †	0.028	-0.231	-0.173	-0.230	-0.639 †	0.659 †	-0.230	N.T.	-0.225	-0.266	0.098
fibrosis	-0.541 †	0.013	0.114	-0.133	0.028	0.185	-0.369 *	0.028	-0.225	N.T.	-0.266	-0.119
LVM (gm)	0.126	0.139	0.251	-0.626 †	-0.361 *	0.400 *	-0.626 †	-0.172	-0.266	-0.266	N.T.	-0.106
E`	-0.062	0.297	0.807 ††	-0.428 *	0.428 *	0.613 †	-0.671 †	-0.119	0.098	-0.119	-0.106	N.T.

CHAPTER 5

AGE-ASSOCIATED ALTERATIONS OF MORPHOLOGY AND PROTEIN SIGNALING IN THE FEMALE F344XBN RAT AORTA

Although the age-associated alterations in cardiac structure and function were found concurrently with increased oxidative-nitrosative stress, the direct relationship between the two remains unclear. Similar to the heart, aging has been shown to alter aortic structure and function in men in addition to the aging male F344xBN rat [346]. This chapter details the findings in regards to alterations in aortic structure and signaling in the aging female F344xBN aorta as outlined in Specific Aim III.

ABSTRACT

The F344xBN male rat has been shown to undergo many of the same age-associated vascular changes seen in humans [346]. However, limited research has been done to determine if the female F344xBN rat is a good aging female rodent model to study age-associated changes in the vasculature. Aortae from 6-, 26-, and 30-month female F344xBN rats were stained with hematoxylin and eosin, and a trichrome stain to determine intima-medial thickness and fibrosis, respectively. Age-associated changes in expression and phosphorylation of proteins were measured by immunoblotting. Aging in the female F344xBN rat was associated with an increase in aortic intima-medial thickness, activation of p44/42 MAPK and Hsp27 expression, in addition

to decreased activation of NF-κβ p50. Hsp90 expression decreased with age in the female F344xBN aorta. There were no age-associated changes in activation of eNOS or Akt or expression of the apoptotic regulators Bax and Bcl-2. Taken together, these data are consistent with the possibility that the female F344xBN rat may be an appropriate animal model to study age-associated changes in the cardiovascular system.

INTRODUCTION

Cardiovascular disease remains the leading cause of death despite new discoveries in medical technology and increased awareness/education [337-339]. Aging in the human vasculature is associated with increased dilation of the lumen, thickening of the media and intima, increased stiffness, and endothelial dysfunction [339]. Sex may also play a role in age-associated alterations in vascular structure. Lower incidences of CVD-associated morbidity and mortality in premenopausal women compared to age-matched men have been reported [384]. Currently, the NIA recommends the F344xBN rat as an aging model for various age associated pathologies including CVD. This model has been shown to be excellent to study age-associated changes in the vasculature of male rats; however, no investigations have been performed to determine if age-associated changes are present in the female F344xBN rat [10, 11, 385] .

In addition to structural and functional changes, there is also evidence that aging may also affect the regulation of several signaling pathways including the MAPK, NF-κβ, eNOS, Hsp, and apoptotic signaling in the male rat aorta [332, 343-346]. The MAPKs are serine/threonine protein kinases that play a role in the regulation of cellular proliferation, differentiation, development, cell cycle, and cell death [191]. The major MAPK signaling pathways include the

extracellular signal-regulated protein kinase cascade (p44/42 cascade), c-Jun amino-terminal kinase/stress-activated protein kinase cascade (JNK/SAPK), and the p38-MAPK cascade. Signaling through the MAPK pathways is activated by growth factors, cytokines, physical, and chemical stress which causes the activation of the upstream activator of MAPK kinase kinase [166] and the MAPK kinase (MKK) [166, 191]. The MKK then phosphorylates the downstream MAPK on serine and threonine residues leading to MAPK activation [191]. In the aorta, the MAPKs have been shown to participate in several different processes including VSMC proliferation, contraction, migration, differentiation, and cell survival following activation by oxidative-nitrosative stress [326-330]. Whether aging may affect the regulation of these pathways in the aging female rat aorta is currently unclear.

The production of NO is stimulated by growth factors, mechanical forces, estrogen, hydrogen peroxide, and angiotensin II [282-285]. Endothelial nitric oxide synthase, like most enzymes, is regulated by phosphorylation as it is thought that eNOS phosphorylation by Akt and AMPK is associated with increased activity. In addition to phosphorylation, eNOS is also indirectly regulated by calmodulin and Hsp90 which function to stabilize eNOS levels [386, 387]. It is thought that aging is associated with increased endothelial dysfunction that is characterized by decreased NO levels [387-390]. Whether the decreases in NO with aging are due to decreased NOS levels, NO production or increased NO scavenging is not entirely understood [293, 304, 305]. The purpose, therefore, of this study was to examine if age-associated changes in structure and protein signaling are present in the aging female F344xBN aorta. We hypothesized that aging female F344xBN, similar to that seen in humans, would be associated with increased intima-medial thickness and alterations in the regulation of intracellular signaling pathways.

MATERIALS AND METHODS

Animals

All procedures were performed in accordance with the Guide for the Care and Use of Laboratory Animals as approved by the Council of the American Physiological Society, the Animal Use Review Board of Marshall University, as well as the Public Health Service Animal Welfare Policy. Adult (6-month), aged (26-month), and very aged (30-month) female F344xBN rats were obtained from the NIA and housed two per cage in an AAALAC approved vivarium. Animals were housed under the following conditions: 12 h-12 h light-dark cycle and temperature of 22 ± 2°C; food and water were provided *ad libitum*. Rats were allowed to recover from shipment for at least two weeks before experimentation, during which time the animals were carefully observed and weighed weekly. Rats were removed from the study if they had signs of failure to thrive such as precipitous weight loss, disinterest in environment, or unexpected gait alterations.

Materials

Antibodies against p38 [#9212], p-p38 MAPK (T180/Y182) [#4631], p44/42 MAPK [#9102], p-p44/42 MAPK (Erk1/2) (Thr202/Tyr204) [#4377], SAPK/JNK [#9252], p-JNK [#9251], AMPKα [#2532], p-AMPKα (Thr172) [#2535], eNOS [#9572], p-eNOS (Ser1177) [#9571], NF-κβ p65 [#3987], p-NF-κβ p65 (Ser536) (93H1) [#3033], Hsp27 (rodent preferred) [#2442], Bcl-2 (50E3) [#2870], Akt [#9272], phospho-Akt(Ser473) [#9271], phospho-Akt(Thr308) [#9275], HSP90 (C45G5) Rabbit mAB [#4877], GAPDH (14C10) Rabbit mAB [#2118], 3T3 Control Cell Extracts [#9203], biotinylated protein ladder [#7727], mouse and rabbit IgG antibodies [#7076, #7074]

were purchased from Cell Signaling Technology (Beverly, MA). Antibodies against NF-κβ p50 [#sc-8414], p-NF-κβ p50 [#sc-33022], HSP70 (K-20) [#sc-1060], HeLa Whole Cell Lysate [sc-2200], L6 +IGF Cell Lysate [sc-24127], and Bax (N-20) [#sc-493] were purchased from Santa Cruz Biotechnology, Inc. (Santa Cruz, CA). The following materials were acquired and used for immunoblotting procedures: Precision Plus Protein Dual Color Standards (Bio-Rad, Hercules, CA, [#161-0374]); precast 10% and 15% PAGE r Gold Precast Gels (Lonza, Rockland, ME); Amersham Hybond-enhanced chemiluminescence (ECL) membranes (Amersham Biosciences, Piscataway, NJ, [RPN2020D]); ECL western blot detection reagent (Amersham Biosciences, Piscataway, NJ); Restore western blot stripping buffer (Pierce, (Rockford, IL); and albumin from bovine serum (minimum 98% electrophoresis, Sigma, St. Louis, MO). All other chemicals were purchased from Sigma (St. Louis, MO).

Aorta Collection

Anesthetization of female F344xBN rats was achieved with an intraperitoneal injection of ketamine (40 mg/kg) and xylazine (10 mg/kg), supplemented as necessary for reflexive responses. A midline laparotomy was performed in order to remove the aorta from the left ventricle to the branching of the renal arteries. The aortae were stored in a Krebs-Ringer bicarbonate buffer (118 mM NaCl, 4.7 mM KCl, 2.5 mM $CaCl_2$, 1.2 mM KH_2PO_4, 1.2 mM $MgSO_4$, 24.2 mM $NaHCO_3$, 10 mM α-D-glucose; pH 7.4) equilibrated with 5% CO_2/95% O_2 and maintained at 37°C as previously described by Rice and colleagues for the removal of blood and connective tissue. Aortae were weighed before they were snap frozen in liquid nitrogen [166].

Histological Analysis

Frozen aortae (n = 4) were sectioned (8 μm) onto poly-lysine coated slides using an IEC Minotome Cryostat. Aortic sections were stained using hematoxylin and eosin stain to determine morphology.

Immunoblot Analysis

Aortic tissues were pulverized in liquid nitrogen and washed in ice cold PBS as previously published [345]. The samples were centrifuged at 4000 x g at 4°C for 20 minutes. The pellet was resuspended in TPER buffer supplemented with 0.5 M EDTA, 0.1 M EGTA, 1.0 M MgCl2, 0.1 M NaVO$_3$, 0.5 M PMSF, phosphatase inhibitor cocktail 3 (P0044, Sigma), and proteinase inhibitor cocktail (P8340, Sigma). Samples were incubated on ice for 30 minutes and vortexed every five minutes during the incubation. The samples were centrifuged at 4000 x g at 4°C for 20 minutes, after which the supernatants were then transferred into new tubes and stored at -80°C. Protein concentration was measured using the Pierce 660 nm Protein Assay (Rockford, IL), following manufacturer's instructions. Briefly, concentrations of triplicates of each sample and BSA as a standard were measured using a SpectraMax Plus 384 kinetic microplate reader (Molecular Devices, Sunnyvale, CA). Each sample was diluted to 5 μg/μl using SDS-loading buffer and boiled for 5 minutes at 95°C. Proteins were separated on 10% and 15% SDS-PAGE gels and transferred to nitrocellulose membrane in order to probe with primary and secondary antibodies as described previously [345]. Chemoluminescent images were captured using the FlourChemE system, and band intensity was determined using Alphaview software (Cell Biosciences, CA). GAPDH band intensity was used to normalize the band intensity of the signaling protein.

Statistical Methods

Results are given as mean ± SEM. The statistical software Sigma Stat 11.0 was used to perform statistical analyses. Age comparisons between morphologic indices and protein expression were evaluated by One Way ANOVA, or Kruskal-Wallis One Way Analysis of Variance on Ranks with the Student-Newman-Keuls, or Dunn's methods as the post hoc test, respectively. Regression analysis was performed with dependent variables against the independent variables age and intima-medial thickness.   The level of significance accepted *a priori* was $\leqslant 0.05$.

RESULTS

Aortic intima-medial thickness increases with age in the female F344xBN

As reported previously, body weight was increased at 26- (274.0 ± 4.9 g) and 30-months (321.3 ± 7.2 g) compared to that observed in the 6-month female F344xBN rats (Chapter 3, Table 3.2). Aortic intima-medial thickness was higher at 26- (97.3 + 4.0 μm) and at 30-months (140.2 + 2.0 μm) compared to that observed in the 6-month old animals (86.2 + 6.3 μm, Figure 5.1). No apparent changes in structure were observed with trichrome staining.

Phosphorylation of p44/42 MAPK is altered with aging but not AMPKα, p38 MAPK, or JNK MAPK

No age-associated changes in expression or phosphorylation of AMPKα or total MAPK protein levels were observed with aging (Table 5.1, Figure 5.2). Compared to that found in the 6-month aortae, the phosphorylation (activation) of p44/42 MAPK at Thr^{202} and Tyr^{204} was increased 125% at 26-months and 187% at 30-months (Table 5.1, Figure 5.3).   The

phosphorylation of p38 and JNK MAPK activation did not change with age.

No change in eNOS, Akt, or apoptosis in the aging female F344xBN aorta

Immunoblotting was used in order to determine age-associated alterations in expression and/or activity of eNOS. Aging was not associated with a significant change in the regulation of eNOS and Akt (Figures 5.4A - B; Table 5.1). No significant difference was found in the expression of Bax, Bcl-2, or the Bax/Bcl-2 ratio with aging (Table 5.1, Figure 5.5).

Differential regulation of heat shock proteins in the aging female aorta

Hsp27 expression increased 32% at 30-months when compared to that observed in 6-month aortae (Figure 5.6, Table 5.1). Conversely, Hsp90 protein levels were decreased 59% and 52% at 26- and 30-months (Figure 5.6, Table 5.1). The expression of Hsp70 was unaltered with aging (Figure 5.6, Table 5.1).

Activation of NF-κβ p50 is decreased with age

The protein levels of NF-κβ p50 and NF- κβ p65 did not change with age. The ratio of total to phosphorylated NF-κβ p50 was decreased 50% and 55% at 26- and 30-months, respectively, compared to that found in the 6-month old animals (Figure 5.7, Table 5.1).

DISCUSSION

An increase in aortic intima-medial thickness has been shown to be correlated with the development of CVD [268]. Consistent with previous work from our laboratory using the male

F344xBN model, we found that aging in the female F344xBN aorta is also characterized by increases in intima-media thickness [346]. To investigate the potential mechanism(s) responsible for this finding, we next examined the regulation of MAPK signaling. The MAPK proteins play a role in several different signaling pathways and are involved in the control of cell growth, proliferation, survival, motility, and differentiation [274]. It is thought that the MAPKs participate in the pathogenesis of aortic dysfunction in several diseases [391]. In the male F344xBN aorta, the phosphorylation (activation) of p44/42, p38, and JNK MAPKs was reduced, increased, or slightly increased with age [332]. Conversely, in the female F334xBN aorta, the activation of p44/42 MAPK was significantly increased with age. Previous studies have found that this age-associated increase of p44/42 MAPK activation was associated with increases in VSMC proliferation and migration [260, 273, 274, 392]. Consistent with these findings, we also noted that elevations in p44/p42 MAPK phosphorylation appeared to be highly correlated with increases in intima-medial thickness (Figure 5.1, Table 5.2A). Whether this increase in p44/p42 MAPK phosphorylation is solely responsible for the aortic remodeling we observed in the current study is currently unclear and will require further investigation.

Age-associated endothelial dysfunction has been linked to changes in expression and activity of eNOS [298]. It is currently unclear how aging may affect eNOS expression and activity. In the current study, we found no significant change in total eNOS expression or phosphorylation (activation) with increasing age. Consistent with this finding, we also found that expression and phosphorylation of Akt, which functions as an upstream regulator of eNOS, is also unchanged with aging. Like Akt, Hsp90 also plays an important role in the regulation of eNOS and NO production. It is thought that association of Hsp90 with eNOS increases NO generation [393]. We

found a decrease in Hsp90 expression with increasing age (Figure 5.6). This decreased expression may be associated with a reduction in NO production. Whether this finding is associated with diminished aortic relaxation or alterations in animal blood pressure with aging will require additional study.

Heat shock proteins are induced by cell stress and function to stabilize protein structure or to protect the cell from injury [394, 395]. Supporting this notion, with aging we found that Hsp27 expression was increased in the female F344xBN aorta (Figure 5.6). Similar to our findings for p44/p42 MAPK, this increase in Hsp27 was also found to be highly correlated to increases in intima-medial thickness (Table 5.2B). Previous data has suggested that decreased levels of Hsp27 are associated with the pathogenesis of atherosclerosis [396]. Whether this increase in Hsp27 levels is a compensatory response to aging or diminished estrogen levels to maintain aortic function with aging is currently unclear.

NF-κβ is an important proinflammatory transcription factor that induces transcription of chemokines, cytokines, adhesion molecules, secondary inflammatory enzymes, and anti-apoptotic factors [223, 224]. Previous work in our laboratory demonstrated that aging was not associated with alterations in NF-κβ expression in the male F344xBN [187]. Conversely, in the present study we found that the phosphorylation (activation) of NF-κβ p50 was increased with age. Why aging might increase NF-κβ p50 activity levels is not yet clear, however, previous studies have demonstrated that increases in NF-κβ expression are regulated, at least in part, by ROS levels and that it may function in the control of VSMC proliferation [327-329, 397, 398]. Whether NF-κβ p50 might functions in a similar manner in the aging F344xBN aorta will require further investigation.

In conclusion, our data suggest that aging in the female F344xBN aorta is characterized by increases in intima-medial thickness, increased p44/42 MAPK activation, decreased Hsp90, increased Hsp27 protein levels, and increased activation of NF-κβ p50. This combination of age-associated signaling alterations may be a compensatory response by the aorta to mitigate the age-related loss in circulating estrogen. Whether similar findings are also seen in aging women is currently unclear. Additional work is needed to more fully understand the underlying mechanisms of the age-associated changes in the aging female F344xBN aorta.

ACKNOWLEDGEMENTS

TABLE 5.1: AORTIC TISSUE EXPRESSION FOR TOTAL AND PHOSPHORYLATED PROTEINS IN AORTA FROM 6-MONTH, 26-MONTH, AND 30-MONTH FEMALE F344XBN RATS. Data are presented as changes of 6-month adult value ± SE. Values for proteins were obtained from n = 5 aortae per age group. An asterisk (*) indicates significant difference from 6-month age group ($p < 0.05$).

	6-month	26-month	30-month
Metabolic			
AMPKα	100.0 ± 6.4	+ 4.1 ± 11.2	-16.1 ± 3.5
p-AMPKα	100.0 ± 10.8	+93.3 ± 33.1	+39.0 ± 30.8
Signaling			
JNK	100.0 ± 13.3	+1.0 ± 6.6	+16.3 ± 5.1
p-JNK	100.0 ± 9.9	-9.8 ± 4.2	+2.8 ± 24.4
p38	100.0 ± 22.1	-38.2 ± 8.8	-22.7 ± 13.7
p-p38	100.0 ± 9.7	+34.5 ± 17.0	+54.6 ± 22.0
p44/42	100.0 ± 14.7	+8.9 ± 4.0	+14.9 ± 16.5
p-p44/42	100.0 ± 6.4	+124.5 ± 28.4*	+187.3 ± 47.6*
eNOS	100.0 ± 7.3	+76.5 ± 15.9	+110.5 ± 39.9*
p-eNOS (Ser1177)	100.0 ± 30.2	+125.3 ± 52.7	+23.8 ± 43.0
Akt	100.0 ± 29.1	+34.4 ± 31.9	-1.5 ± 35.7
p-Akt (Ser473)	100.0 ± 12.8	+27.5 ± 12.1	-7.5 ± 7.7
p-Akt (Thr308)	100.0 ± 21.2	+69.2 ± 48.3	+35.6 ± 12.4
Apoptotic Regulators			
Bax	100.0 ± 11.8	-34.7 ± 16.7	-41.9 ± 16.1
Bcl-2	100.0 ± 29.1	-6.8 ± 13.3	-30.1 ± 14.3
Heat shock proteins			
Hsp27	100.0 ± 6.8	+2.2 ± 3.5*	+31.8 ± 6.2*
Hsp70	100.0 ± 8.1	+55.5 ± 23.6	+19.7 ± 11.4
Hsp90	100.0 ± 20.3	-59.4 ± 5.2*	-52.0 ± 9.3*
Transcription Factors			
NF-κβ p50	100.0 ± 13.1	+65.8 ± 40.9	+49.3 ± 17.7
pNF-κβ p50	100.0 ± 8.6	-20.3 ± 5.6	-31.0 ± 4.4*
NF-κβ p65	100.0 ± 10.3	+3.0 ± 19.9	-11.9 ± 28.8
pNF-κβ p65	100.0 ± 11.9	+5.1 ± 9.4	-2.9 ± 7.8

TABLE 5.2A: REGRESSION ANALYSIS OF THE RELATIONSHIP BETWEEN SIGNALING PROTEINS TO AGE AND INTIMA-MEDIAL THICKNESS IN THE AORTAE OF 6-, 26-, AND 30-MONTH OLD FEMALE F344XBN RATS. Values for proteins and thickness were obtained from n = 5 aortae for each age group. The following symbols indicate: (*) low correlation (p < 0.05) and (**) moderate correlation (p < 0.05) between parameters. P values are located within parentheses. N.T. (not tested).

	Age	Intima-medial Thickness
Independent Variable		
Age	N.T.	0.741*
		(0.022)
Intima-medial thickness	0.741*	N.T.
	(0.022)	
Metabolic		
AMPKα	0.326	0.690*
	(0.391)	(0.04)
p-AMPKα	0.555	0.067
	(0.121)	(0.864)
Signaling		
JNK	0.389	0.498
	(0.301)	(0.172)
p-JNK	0.044	0.024
	(0.91)	(0.952)
p38	0.547	0.082
	(0.128)	(0.834)
p-p38	0.740*	0.692*
	(0.023)	(0.039)
p44/42	0.364	0.204
	(0.336)	(0.589)
p-p44/42	0.888**	0.732*
	(0.001)	(0.025)
eNOS	0.837**	0.709*
	(0.005)	(0.032)
p-eNOS (Ser1177)	0.384	0.189
	(0.307)	(0.627)
Akt	0.132	0.214
	(0.736)	(0.581)
p-Akt(Ser473)	0.123	0.354
	(0.753)	(0.35)
p-Akt(Thr308)	0.486	0.075
	(0.185)	(0.849)

TABLE 5.2B: REGRESSION ANALYSIS OF THE RELATIONSHIP BETWEEN SIGNALING PROTEINS TO AGE AND INTIMA-MEDIAL THICKNESS IN THE AORTAE OF 6-, 26-, AND 30-MONTH OLD FEMALE F344XBN RATS. Values for proteins and thickness were obtained from n = 5 aortae for each age group. The following symbols indicate: (*) low correlation ($p < 0.05$), (†) moderate correlation ($p < 0.05$), (††) high correlation ($p < 0.05$), and (†††) very high correlation ($p < 0.05$) between parameters. P values are located within parentheses. N.T. (not tested).

	Age	Intima-medial Thickness
Independent Variable		
Apoptotic Regulators		
Bax	0.725*	0.483
	(0.027)	(0.188)
Bcl-2	0.377	0.579
	(0.317)	(0.102)
Heat Shock Proteins		
Hsp27	0.615	0.903†††
	(0.078)	(<0.001)
Hsp70	0.519	0.004
	(0.152)	(0.993)
Hsp90	0.834††	0.388
	(0.005)	(0.302)
Transcription Factors		
NF-κβ p50	0.851	0.701
	(0.004)	(0.035)
p-NF-κβ p50	0.617	0.329
	(0.077)	(0.387)
NF-κβ p65	0.120	0.159
	(0.758)	(0.682)
p-NF-κβ p65	0.001	0.032
	(0.999)	(0.934)

FIGURE 5.1

FIGURE 5.1: AGING INCREASES INTIMA-MEDIAL THICKNESS IN THE FEMALE F344XBN AORTA.

Hematoxylin and eosin staining of 6-, 26-, and 30-month female F344xBN aortae. Bar indicates 100 μm. n = 4 aortae per age group.

FIGURE 5.2

FIGURE 5.2: AGING DOES NOT ALTER THE EXPRESSIONS OF MAPKS AND AMPK-ALPHA IN THE F344XBN AORTA.

Total levels of aortic AMPK-α as well as p38, p44/42, and JNK MAPKs were determined by immunoblotting in 6-, 26-, and 30-month female rats. Results were normalized to GAPDH expression and expressed as fold change of the 6-month value. n = 5 aortae per group.

FIGURE 5.3

FIGURE 5.3: PHOSPHORYLATION STATUS OF P44/42 MAPK IS INCREASED WITH AGE IN THE FEMALE RAT AORTA BUT NOT P38 MAPK, JNK MAPK, OR AMPK-ALPHA.
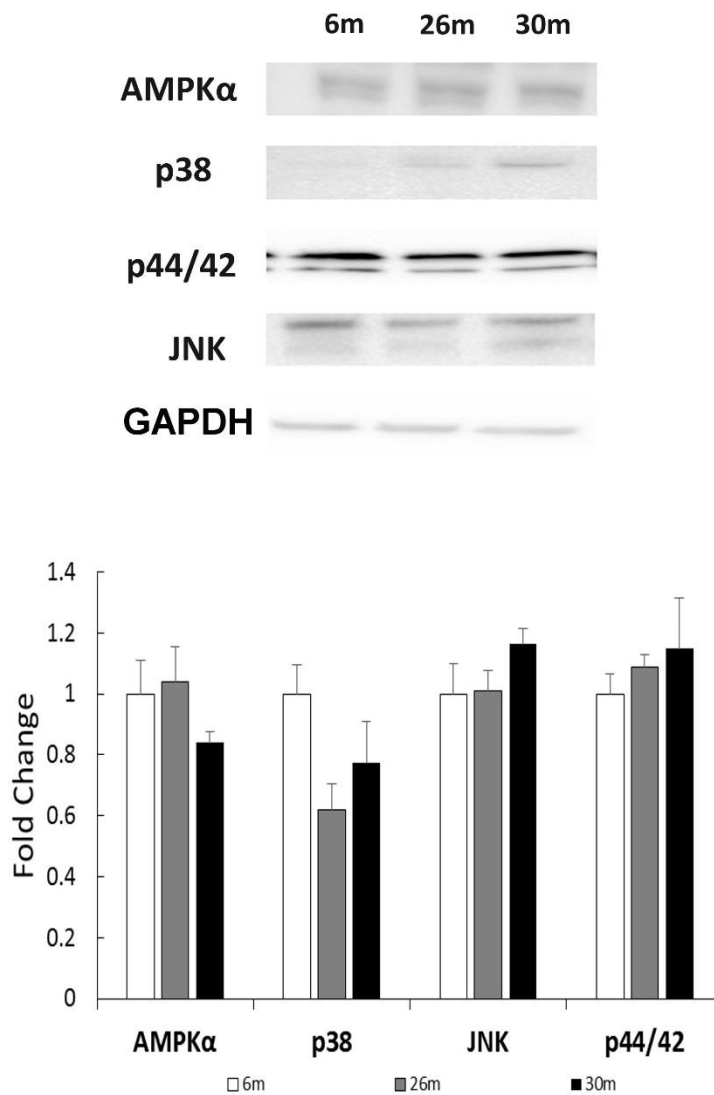
Age-related changes in phosphorylated AMPKα in addition to p38, p44/42, and JNK MAPK expression were analyzed by immunoblotting in 6-, 26-, and 30-month female rat aortae. Results were normalized to GAPDH expression and expressed as fold change of the 6-month value. An asterisk (*) indicates significance difference from the 6-month value, ($p < 0.05$) or less, n = 5 aortae per group.

FIGURE 5.4
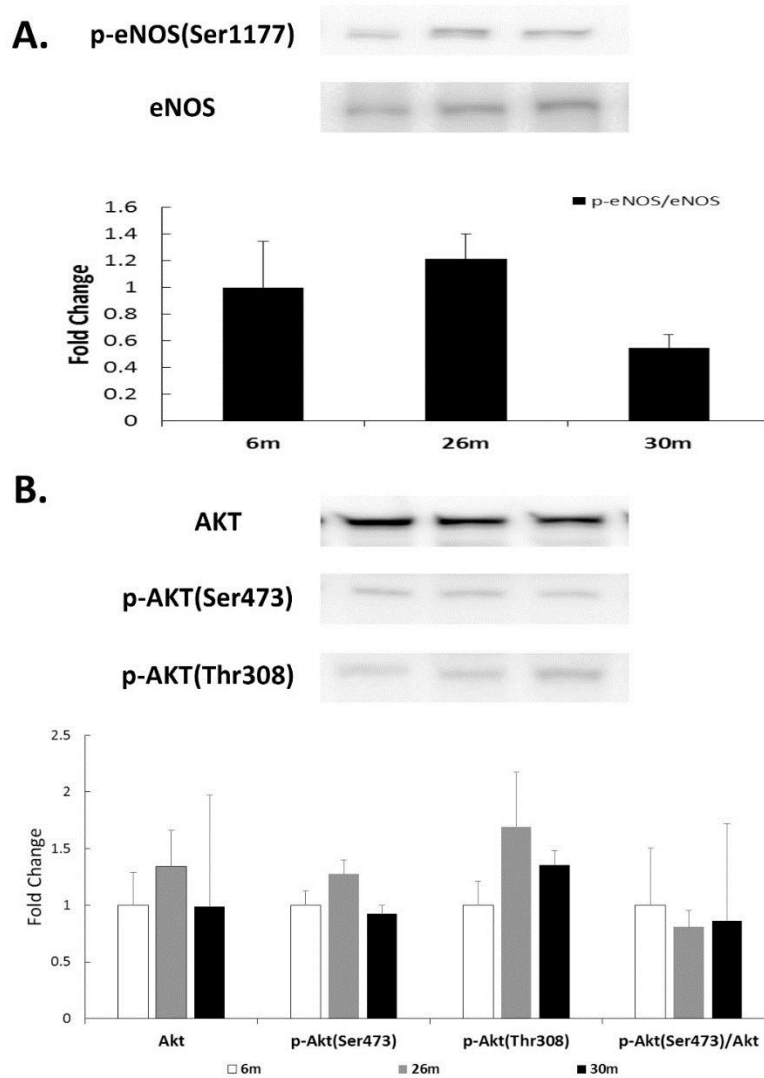
FIGURE 5.4: ENOS AND AKT ACTIVATION ARE NOT ALTERED WITH AGING IN THE FEMALE F344XBN AORTA.

Immunoblotting was used to detect (**A**) the ratio p-eNOS(Ser1177) / total eNOS expression. (**B**) Akt, p-Akt (Ser473), and p-Akt (Thr308) in 6-, 26-, and 30-month female rat aortae. Results were normalized to GAPDH expression and expressed as fold change of the 6-month value, n = 5 aortae per group.

FIGURE 5.5
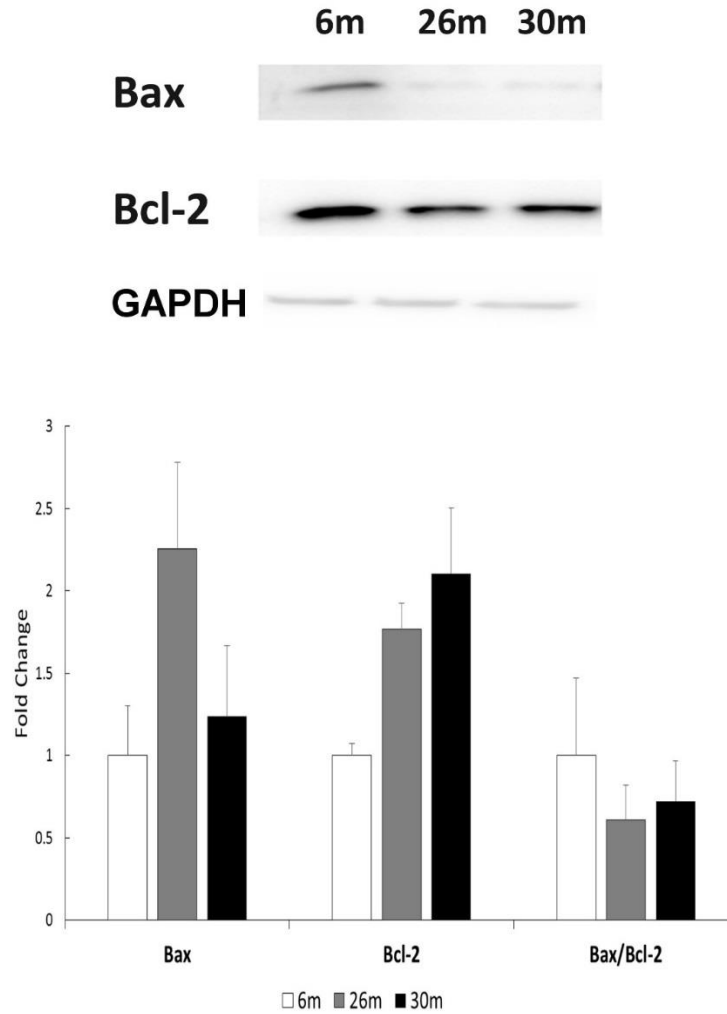
FIGURE 5.5: NO AGE-ASSOCIATED INCREASE IN APOPTOSIS WITH AGE IN THE FEMALE RAT AORTA.

Protein expression of Bax and Bcl-2 were detected by immunoblotting in 6-, 26-, and 30-month female rat aortae. Results were normalized to GAPDH expression and expressed as fold change of the 6-month value. n = 5 aortae per group.
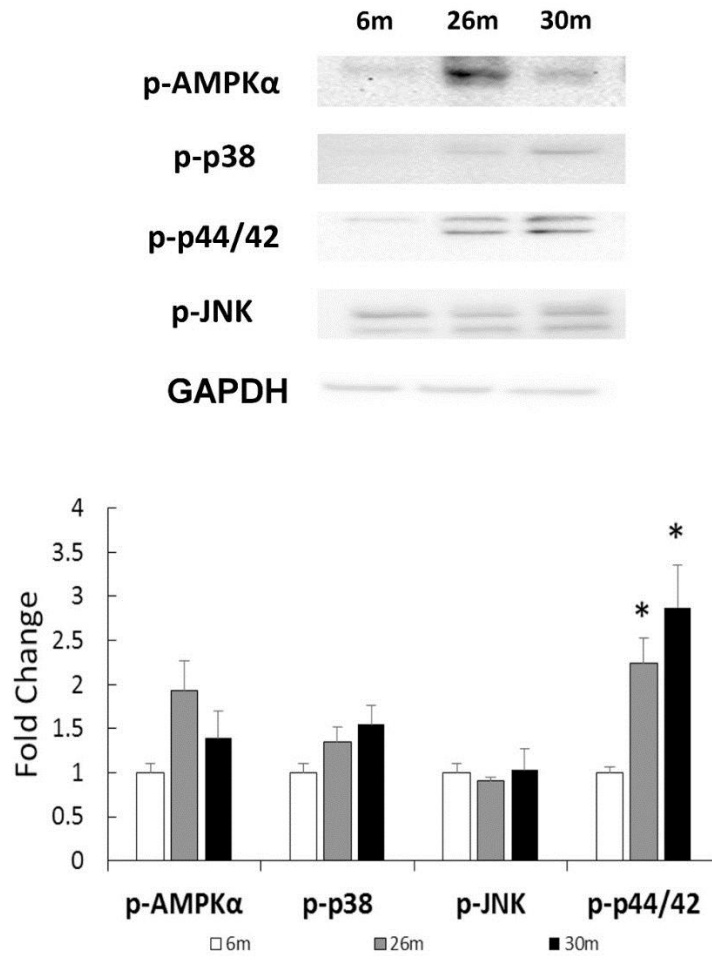
FIGURE 5.6
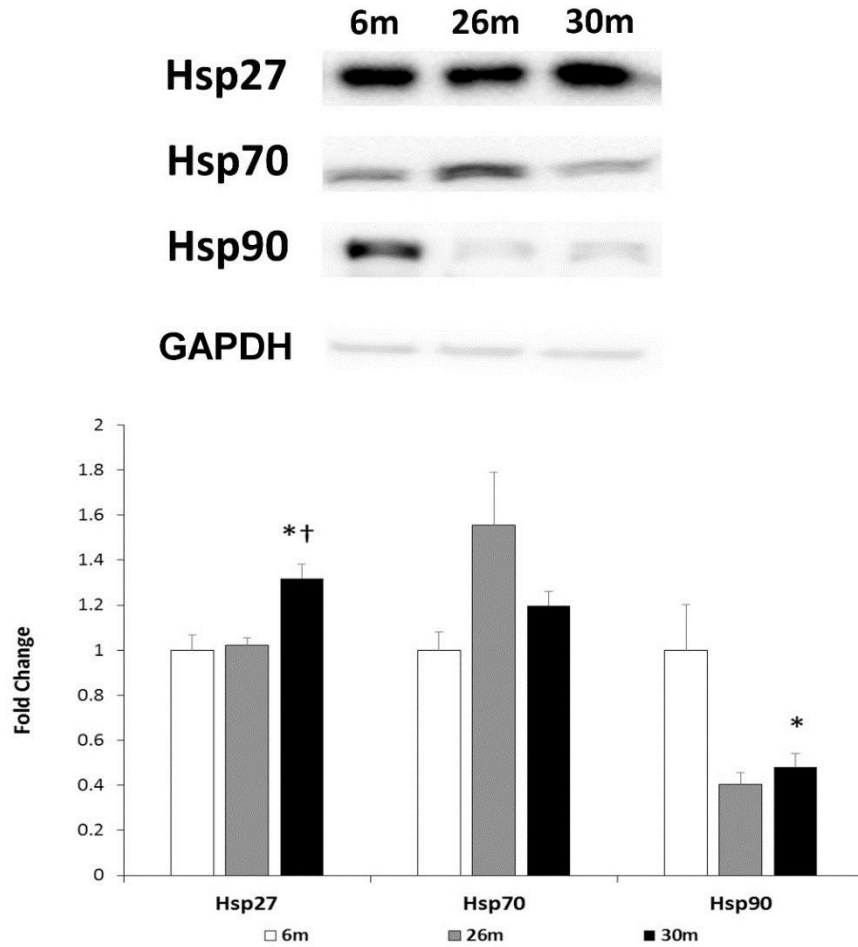
FIGURE 5.6: DIFFERENTIAL REGULATION OF HSPS IN THE AGING FEMALE RAT AORTA.

Age-related changes in Hsp27, Hsp70, and Hsp90 expression were analyzed by

immunoblotting in 6-, 26-, and 30-month female rat aortae. Results were normalized to GAPDH

expression and expressed as fold change of the 6-month value. An asterisk (*) indicates

significant difference from the 6-month value ($p < 0.05$) or less. (†) indicates significant

difference from 26-month value ($p < 0.05$), n = 5 aortae per group.

FIGURE 5.7
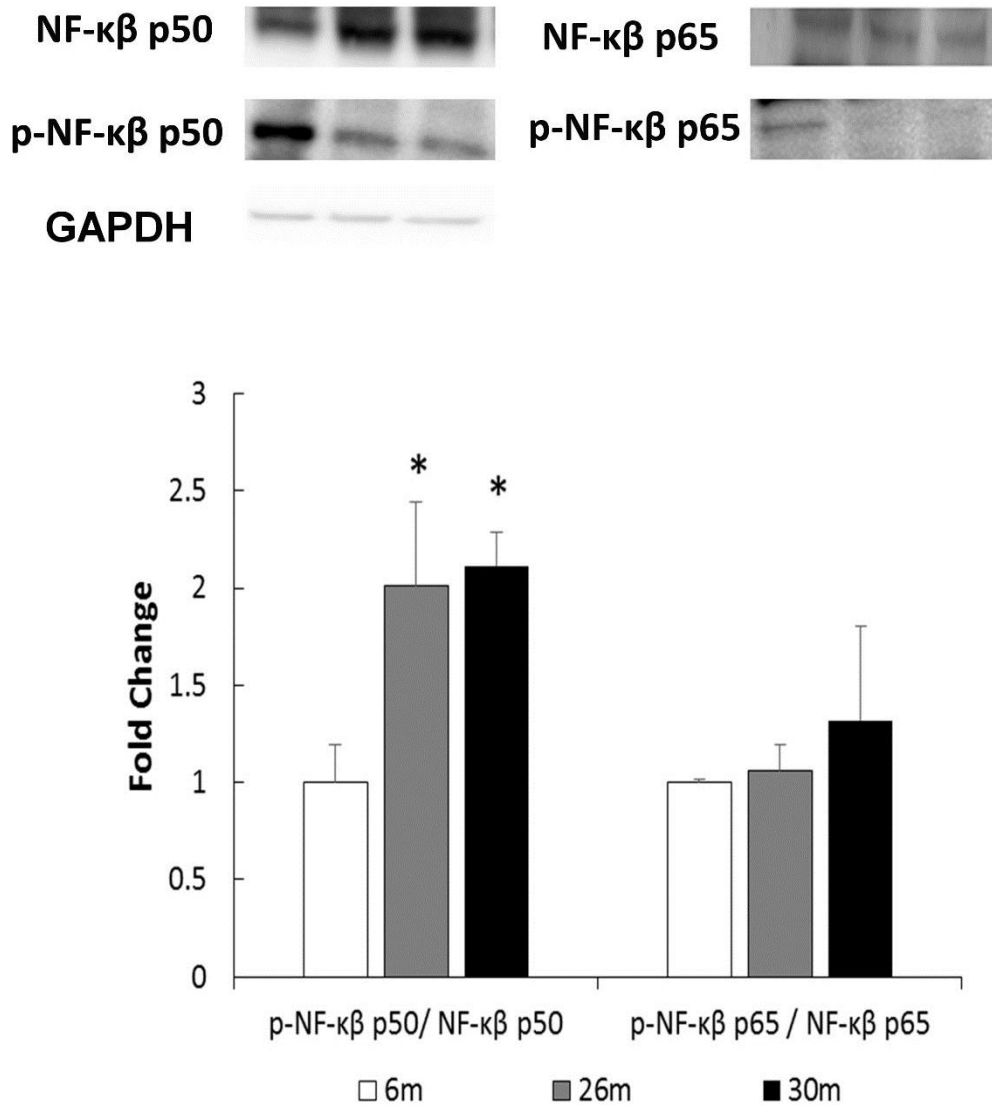
FIGURE 5.7: ACTIVATION OF NF-KB P50 IS DECREASED WITH AGE.

Transcriptional regulation in the 6-, 26-, and 30-month female F344xBN aorta was determined by analyzing the expression of NF-κβ p50, p-NF-κβ p50, NF-κβ p65, and p-NF-κβ p65. Results were normalized to GAPDH expression and expressed as percent of the 6-month value. An asterisk (*) indicates significance difference from the 6-month value ($p < 0.05$) or less, n = 5 aortae per group.

CHAPTER 6

DISCUSSION AND CONCLUSIONS

The number of elderly persons in the United States is projected to increase by more than 20% by the year 2030. This growth in the elderly population is expected to significantly test our already overloaded health care system due to the fact that aging is a primary risk factor for the development of CVD. The effect of sex on cardiovascular risk has not been fully elucidated; however, recent data suggests that premenopausal women have a decreased risk of CVD compared to men of comparable age [24, 69]. This cardio-protective benefit appears to be lost over time as the risk of CVD in postmenopausal women is similar to that seen in aged men [25]. Whether aging in animal models induces many of the cardiovascular changes seen in humans is not well understood. The primary purpose of this study was to investigate how aging affects cardiovascular structure and function in the female F344xBN rat.

CARDIAC AGING IS ASSOCIATED WITH INCREASES IN OXIDATIVE STRESS AND APOPTOSIS IN THE FEMALE F344XBN RAT

Recent work has suggested that aging in the female Wistar, Fisher 344, and Sprague-Dawley rats as well as B6 mice is associated with increased ROS levels [5, 6, 188-190]. How aging may affect the levels of oxidative-nitrosative stress in the aging female F344xBN rodent model has not been elucidated. Similar to that observed in other aging models, the findings of this study suggest there is an increase in oxidative-nitrosative stress and apoptosis in the female F344xBN

heart. Specifically, aging was found to be associated with increased levels of superoxide, 4-HNE, and nitrotyrosine. It is thought that oxidative stress is typically caused by increases in ROS production, a decline in antioxidant buffering capacity, or some combination of both. In this study, the mRNA expression of SOD1, SOD2, Cat, and Gpx were not altered with aging. This suggests that the increase in oxidative-nitrosative stress is probably not due to a decrease in antioxidant buffering capacity.
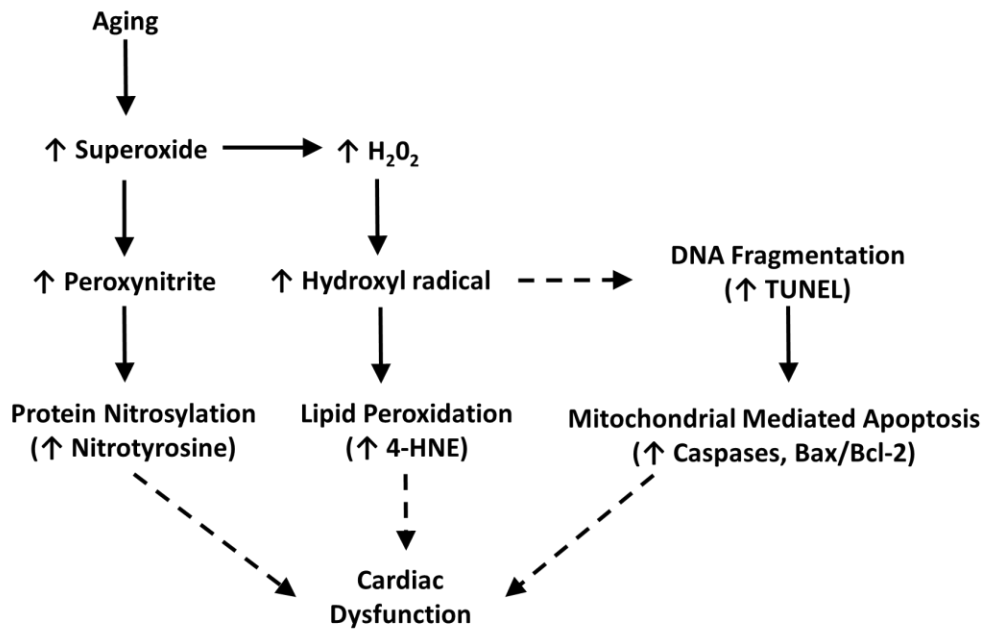
FIGURE 6.1

FIGURE 6.1: POTENTIAL MECHANISM OF AGE-ASSOCIATED OXIDATIVE-NITROSATIVE DAMAGE IN THE FEMALE F344XBN HEART.

Solid arrows indicated findings from study. Dotted arrows represent potential mechanism of oxidative-nitrosative damage.

OXIDATIVE-NITROSATIVE STRESS AND APOPTOSIS IN THE AGING MALE AND FEMALE F344XBN

RAT HEART

Cardiac aging is typically characterized by increases in oxidative-nitrosative stress in male rodent models [184, 187, 399]. Compared to that observed in females, the hearts of aging male rats exhibited increases in protein carbonylation, advanced oxidation protein products, nitrotyrosine, non-protein thiol, reduced glutathione, and iron levels [5]. Although aging is associated with increases in oxidative stress in both male and female hearts, female rat hearts exhibited lower mitochondrial hydrogen peroxide production and oxidative damage, as well as a greater mitochondria differentiation [6]. It is thought that females have a higher mitochondrial differentiation which is a metabolic adaptation to increase energy efficiency, as it is associated with their lower mitochondrial free radical production and oxidative damage [6]. Previous studies have shown that female Sprague Dawley, Wistar, and F344 rats have lower ROS production in addition to oxidative levels compared to males, which may explain the greater mean life-span [188-190].

Similar to humans and other rodent models, aging in the male and female F344xBN rat was associated with increased superoxide production as well as oxidative-nitrosative stress as indicated by increased levels of lipid peroxidation and protein nitrosylation (Table 6.1). Although antioxidant activity was not determined in this study, we did not observe differences in the antioxidant mRNA expression with aging in the female F344xBN heart. Whether age is associated with alterations in antioxidant levels and activity in the male F344xBN heart is unknown.

While indices of oxidative-nitrosative stress were increased in both male and female F344xBN rats, male animals appeared to exhibit greater levels of oxidative-nitrosative cardiac

111

damage [197]. One possible explanation could be sex-associated differences in ROS/RNS production as well as antioxidant expression/activity. Indeed, previous research has suggested that ROS production is lower in aged female compared to male Wistar rats [189]. Similarly, other data has demonstrated that the aging female Fisher 344 rat exhibits lower ROS production and increased SOD2 and Gpx levels when compared to its male counterpart [189, 190, 400]. It is thought that hormones may be responsible, at least in part, for sex related differences as estrogen has been shown to increase the expression of antioxidant genes/activity [189, 401]. Conversely, other work has shown that estrogen levels are not predictive of antioxidant activity suggesting that estrogen levels alone may not be the sole determinant of ROS levels with aging [190, 402, 403].

APOPTOSIS IN THE AGING MALE AND FEMALE F344XBN HEART

Aged cardiomyocytes exhibit increased susceptibility to mitochondrial permeability transition pore opening which may be a cause of increased ROS production and apoptosis [404, 405]. In addition to changes in oxidative stress, aging in the female F344xBN heart was also associated with an increase in the number of TUNEL positive nuclei and evidence of mitochondrial–mediated apoptosis. Although mitochondrial-mediated apoptosis signaling was increased in both aging male and female F344xBN hearts, the magnitude of age-related change appeared to be less in the female animals [197] (Figure 3.5-7). Consistent with this finding, Bax was increased with age in the male but unchanged in the female hearts. In addition to Bax, we also observed differences in the regulation of Akt. Akt signaling is thought to be largely anti-apoptotic given its proclivity to inactivate Bad and procaspase-9 by phosphorylation [406-409].

Akt exhibited decreased expression and activation with age in the male F344xBN hearts while the

p-Akt/Akt ratio was increased in the aging female hearts (data not shown). Whether these

changes in signaling can fully explain the apparent differences in age-related cardiac apoptosis

observed between male and female hearts is currently unclear and will require further

investigation.

TABLE 6.1: AGE-ASSOCIATED ALTERATIONS IN OXIDATIVE-NITROSATIVE STRESS AND APOPTOTIC SIGNALING THE MALE AND FEMALE F344XBN HEART. Age-associated comparisons of oxidative-nitrosative stress and protein signaling in female and male F344xBN rats. Arrows indicate significant increase (↑) and decrease (↓) in parameters ($p < 0.05$) compared to 6-month age groups within gender. N.A. – not applicable. N.C. - no change. N.D. - not determined. Parentheses indicate size of protein fragment in kilodaltons (kDa).

	Female 26m	Female 30m	Male 30m	Male 36m
Oxidative-Nitrosative Stress				
HE	↑	↑	↑	↑
Nitro-Tyrosine	↑	↑	↑	↑
4-HNE	↑	↑	↑	↑
Apoptotic Signaling				
TUNEL	↑	↑	↑	↑
Bax	N.C.	N.C.	N.C.	↑
Bcl-2	↓	↑	↑	↑
Bax/Bcl-2	N.C.	↑	N.D.	N.D.
Casp-9	N.C.	N.C.	N.C.	↑
Casp-9 (40kDa)	N.C.	N.C.	N.C.	↑
Casp-9 (38kDa)	↑	↑	N.C.	N.C.
Casp-9 (17kDa)	↑	↑	N.D.	N.D.
Casp-3	↓	↓	↑	↓
Casp-3 (19kDa)	N.C.	↑	↓	↑
Casp-3 (17kDa)	N.C.	↑	N.D.	N.D.
Akt	N.C.	N.C.	↓	N.C.
p-Akt (Ser473)	N.C.	N.C.	↓	N.C.
p-Akt (Thr308)	N.D.	N.D.	↓	N.D.
p-Akt(473)/Akt	↑	↑	N.D.	N.D.
Heat Shock Proteins				
Hsp27	N.C.	N.C.	↑	↑
Hsp70	N.C.	N.C.	↑	↑

CARDIAC STRUCTURE AND FUNCTION IS LARGELY PRESERVED IN THE AGING FEMALE F344XBN RAT

Aging in mammals is typically characterized by increased cardiomyocyte death, impaired contractility, and ventricular remodeling [221, 90]. Previous studies from our laboratory and others have demonstrated that aging in the male F344xBN is associated with left ventricle chamber dilatation, mild left ventricular hypertrophy, decrements in systolic function, and increased diastolic dysfunction [94]. Data from the current study suggest that aging in the female F344xBN heart is associated with cardiac hypertrophy (increase in posterior wall thickness and cardiomyocyte CSA), diastolic dysfunction (increase in LV IVRT), increased valvular dysfunction, and alterations in heart rhythm intervals. These data are consistent with the previous work by Boluyt and colleagues using the aging female F344 rodent [2]. In their study, diastolic dysfunction in the female F344 was attributed to changes in the amount of collagen, increased collagen crosslinking, and a shift from alpha to beta myosin heavy chain [2, 4, 122, 123, 411]. Although we did not determine if aging in the F344xBN was associated with changes in myosin heavy chain isoform expression, we did find that collagen deposition did not appear to change appreciably. Whether this discrepancy between studies is due to differences in animal strain, age investigated, or other factors is currently unclear.

Our data suggest that aging in the female F344xBN is characterized by changes in cardiac rhythm including an increased VAT, ST interval, T amplitude, QRS interval, QT interval, T duration, Q amplitude, P amplitude, and a shift in the mean electrical axis. Previous studies have found that cardiac conduction is slowed during aging in humans and rats [130, 412-415]. To our knowledge, this is the first study to investigate alterations in heart rhythm intervals in the female

F344xBN rat model. Potential explanations for the slowing of cardiac conduction could include differences in cardiomyocyte excitability, cardiomyocyte structure, or alterations in cardiomyocyte orientation [41, 412, 416-419]. Specific to this study, the prolonged conduction in the aging female F344xBN heart might be related to cardiomyocyte hypertrophy as previous work has demonstrated that cardiomyocyte enlargement appears to be associated with slowed cardiac conduction [412]. The prolonged heart intervals in the aging female F344xBN rat heart may also be related to the alterations in the spatial distribution of Cx43 (Figure 4.3). Additional study, perhaps examining Cx43 phosphorylation with aging, may be useful to determine what role, if any, Cx43 may play in the delayed cardiac conduction we observed.

TABLE 6.2: SUMMARY OF FINDINGS OF CARDIAC STRUCTURE AND FUNCTION IN THE AGING FEMALE F344XBN HEART. ↑ and ↓ indicates increase and decrease respectively.

Structure	Function
↑ Cardiomyocyte hypertrophy	Diastolic dysfunction (↑ Emax)
↑ Posterior wall thickness	Valve dysfunction
No fibrosis	No arrhythmias
↑ Cx43 heterogeneity and redistribution	Prolonged conduction (↑ QRS and QT intervals)

COMPARISON OF AGING CARDIAC STRUCTURE AND FUNCTION IN THE MALE AND FEMALE F344XBN RAT

Hypertrophy

Recent studies have demonstrated that the aging heart exhibits an accumulation of

damaged, high-ROS producing mitochondria that may result in the activation of MAPK signaling which is important in the induction of cardiac hypertrophy [420-423]. Previous data has suggested that aging in the male F344xBN rat is associated with cardiac hypertrophy (increased heart weight to body weight ratio, LVM, and posterior wall thickening), increased ROS levels, and the activation of MAPK signaling [187]. In the aging female F344xBN heart, we did not find evidence of significant hypertrophy although cardiomyocyte CSA and posterior wall thickness was increased. Whether this lack of hypertrophy in the aging female F344xBN is due to lower levels of oxidative-nitrosative stress is currently unclear and will require additional experimentation.

Systolic Function

Systolic dysfunction is defined as impaired ventricular contraction which can be caused by alterations in cardiac signaling, increased blood pressure, as well as cardiac valve regurgitation. Previous data has demonstrated that aging in the male F344xBN is associated with increased end systolic volume suggesting decreased ventricular ejection [94]. Conversely, systolic function in the aging female F344xBN heart appeared to be largely conserved. This absence of systolic dysfunction seems to fit well to that observed in other aging studies that employed healthy women and with our finding that aging in the female animals appeared to occur without the development of cardiac hypertrophy [466].

Diastolic Function

Diastolic dysfunction, or impaired filling of the ventricles, has been shown to increase in aging women [424, 425]. While aging in both male and female F344xBN rats was associated with

evidence of diastolic dysfunction, the degree and mechanism of impairment appeared to differ.

For example, aging in the male F344xBN rats was associated with a significant increase in the E/A

ratio and evidence of increased cardiac fibrosis [94]. Conversely, in the female rats, we noted

significant and progressive decreases in Emax and increasing trends in LV IVRT as well as MV decel

time but no evidence of age-associated fibrosis. It is thought that diastolic dysfunction can be

caused by alterations in the re-uptake of calcium, decreased sarco/endoplasmic reticulum Ca^{2+}

(SERCA)-2 protein expression, valvular dysfunction, as well as increases in the deposition of

extracellular matrix (fibrosis) [426-428]. Similarly, increases in oxidative-nitrosative stress have

also been shown to contribute to diastolic dysfunction by impairing SERCA2 function, increasing

the phosphorylation of phospholamban, and altering ryanodine receptor channel function [429].

In addition to increases in ROS levels, we also noted that aging in the female F344xBN heart was

associated with increased incidence of mitral regurgitation. Although not observed here, the

accumulation of extracellular matrix can lead to increased fibrosis causing increased cardiac

stiffness, decreased compliance, and alterations in myocardial excitation-contraction coupling

[426, 427]. Whether further studies in addition to immunoblotting to assess calcium signaling

would yield meaningful data is not yet clear.

GENDER COMPARISON OF ARRHYTHMIAS IN THE F344XBN RAT

Although previous data has demonstrated that aging in the male F344xBN is associated

with increases in the number of premature ventricular contractions, we failed to find evidence of

similar phenomena in the aging female rats. Why the incidence of cardiac arrhythmia may differ

between male and female animals is not clear but may be explained, at least in part, by

differences in the cardiac gap junction protein Cx43. Kakarla and colleagues found that Cx43 levels were decreased in the aging male F344xBN heart (unpublished data). Paralleling this decrease in Cx43, they also observed that aging was associated with increased cardiac fibrosis [197]. In the aging female, neither Cx43 levels nor the degree of ventricular fibrosis appeared to change with aging. Whether these two differences, alone, are responsible for the absence of arrhythmias we see in the aging female heart will require further investigation.

Although we did not find evidence of arrhythmias, aging in the female F344xBN heart did appear to be associated with prolonged cardiac conduction. Whether similar alterations in cardiac conduction also occur in the male F344xBN heart is, to our knowledge, unknown. Why aging may slow cardiac conduction is not clear; however, we did note that the presence of conduction abnormalities appeared to be associated with alterations in the subcellular distribution of Cx43. Other work has shown that the expression of Cx43 is significantly higher in female compared to male rats [167]. Whether this increased expression of Cx43 in the female F344xBN functions to attenuate the development of cardiac conduction abnormalities with aging is unclear.

In summary, our data suggest that aging in the F344xBN rat, similar to that seen in humans, is associated with sex related differences in cardiac structure and function. The male F344xBN exhibited progressive diastolic and systolic left ventricular chamber dilatation; mild diastolic and systolic left ventricular hypertrophy; progressive age-associated decrements in resting left ventricular systolic function; and mild diastolic dysfunction [94]. Aging in the female F344xBN was characterized by increased cardiomyocyte CSA, posterior wall thickening, left ventricle chamber dilatation, slight diastolic dysfunction, and alterations in heart rhythm intervals

that were associated with alterations in the spatial distribution of Cx43. Whether additional changes or if the magnitude of existing alterations increases further with aging progression in female rat is unclear.

TABLE 6.3: COMPARISON OF CARDIAC STRUCTURE IN MALE AND FEMALE F344XBN RATS.
Age-associated comparisons of cardiac morphology and structure in female and male F344xBN rats. Arrows indicate significant ($p < 0.05$) increase (↑) or decrease (↓) in parameters compared to 6-month age groups within gender. N.A. – not applicable. N.C. -- no change. N.D. – not determined. PVC- premature ventricular contractions. (d) – diastole. (s) – systole.

	Female 26m	Female 30m	Male 30m	Male 36m
Tissue Weights				
BW	↑	↑	↑	↑
HW	↑	↑	↑	↑
HW/BW	N.C.	N.C.	↑	↑
LVM	N.C.	N.C.	↑	N.C.
Cardiac structure				
IVS(d)	N.C.	N.C.	N.C.	N.C.
IVS(s)	↑	N.C.	↑	↑
LVID(d)	N.C.	N.C.	↑	↑
LVID(s)	↓	N.C.	↑	↑
LVPW(d)	N.C.	↑	↑	N.C.
LVPW(s)	N.C.	↑	↑	N.C.
RVDd	N.C.	N.C.	N.C.	N.C.
Histology				
Fibrosis	N.C.	N.C.	N.C.	↑
Loss of cardiomyocytes	N.D.	N.D.	N.C.	↑
Cross striations	N.D.	N.D.	N.C.	↑

TABLE 6.4: COMPARISON OF CARDIAC FUNCTION IN MALE AND FEMALE F344XBN RATS. Age-associated comparisons of cardiac function in female and male F344xBN rats. Arrows indicate significant ($p < 0.05$) increase (↑) or decrease (↓) in parameters compared to 6-month age groups within gender. N.A. – not applicable. N.C. -- no change. N.D. – not determined. PVC-premature ventricular contractions.

	Female 26m	Female 30m	Male 30m	Male 36m
Systolic Function				
EF	↑	N.C.	N.C.	N.C.
FS	N.C.	N.C.	N.C.	N.C.
ESV	↓	N.C.	↑	↑
Diastolic Function				
MV Decel time	N.C.	N.C.	N.C.	N.C.
Emax	↓	↓	↑	↑
Amax	N.C.	↓	N.C.	N.C.
E/A	N.C.	N.C.	N.C.	↑
Heart Rhythms				
Arrhythmias	None	None	PVC (1/10)	PVC (13/18)
Conduction	↑	↑	N.D.	N.D.
Cx43	Redistributed	Redistributed	↓	↓
Valve Function				
Valve dysfunction	↑	↑	N.D.	N.D.

AORTIC AGING IN THE FEMALE F344XBN RAT IS ASSOCIATED WITH INCREASES IN MEDIAL THICKNESS

Alterations in vascular structure and function increase the risk for CVD [42, 258, 268]. Age-associated alterations in aorta structure and function include intima-medial thickening, deposition of extracellular matrix, infiltration of leukocytes, endothelial dysfunction, impaired distensibility, and increased stiffness [13, 263, 264, 266, 268, 430]. In the male F344xBN aorta, previous data has suggested that aging is associated with increases in oxidative stress, apoptosis, and intima-medial thickness [271]. The data of the current study indicate that aging in the female F344xBN rat aorta is associated with an increase in intima-medial thickness and alterations in the p44/42 MAPK, NF-κβ p50, and Hsp27 expression. Whether these alterations are due to increased levels of oxidative stress, as has been posited for the aging male F344xBN aorta cannot be determined as indices of oxidative-nitrosative stress were not measured in this study [345].

The MAPKs regulate many cellular processes including VSCM proliferation, contraction, migration, differentiation, and cell survival [14-18]. Although not investigated here, the increased phosphorylation (activation) of p44/42 MAPK observed in the present study may be due to the de-differentiation of the VSMCs to a more proliferative phenotype as noted by others [274]. Similarly, although not measured, age-related decreases in estrogen levels might also have contributed to the increased intima-medial thickness as estrogen is thought to inhibit VSMC proliferation [319].

Consistent with previous studies, we found no change in eNOS expression with age [8, 300, 431]. Two important signaling molecules, Akt and Hsp90, which are involved in the activation of eNOS by estrogen, were also investigated in this study. Recent work has suggested

that eNOS activation is dependent, at least in part, on Akt phosphorylation and that reduced expression of Akt might be a potential mechanism underlying endothelial dysfunction and the decreased NO bioavailability observed in aging endothelial cells [283, 292, 432]. The disassociation of Hsp90 and eNOS has also been shown to cause reduced NO bioactivity and endothelial dysfunction [393, 433-439]. In the current study, we did not find any changes in Akt expression; however, aging did appear to diminish Hsp90 expression. More work is needed in order to determine how these age-associated changes in aortic structure and protein signaling are related to each other as well as their potential impact on aortic function.

DIFFERENCES IN AORTIC AND CARDIAC AGING IN THE FEMALE F344XBN RAT

It is thought that aging is associated with increased intima-medial thickness of the aorta [88, 89, 344, 346]. The thickness of the arterial wall, as indexed by the thickness of the intimal and medial layers, increases in a linear fashion nearly threefold between the ages of 20 and 90 years, even in the absence of atherosclerotic plaques [440]. Similar to that seen in humans, we found that aging in the female F344xBN aorta is characterized by increases in the intima-medial thickness. The factor(s) responsible for the increased wall thickness are currently unclear but may be related to VSMC proliferation. Indeed, unlike cardiac muscle, VSMC appear to adopt more of a proliferative phenotype with increased aging [274, 441-443]. It has been hypothesized that the p44/42 MAPK signaling pathway contributes to the proliferative phenotype and aging has been shown to be associated with increased p44/42 MAPK activation in the aorta [260, 273, 274, 392, 444, 445, 446]. Consistent with these data, we also found that aging significantly increased p44/42 MAPK phosphorylation.

The differential regulation of Hsp expression in the aging female F344xBN heart and aorta also indicate a tissue-specific response to stress. Heat shock protein expression is normally induced with increased cellular stress [201]. No alterations in Hsp expression were observed in the aging female F344xBN heart although we did observe an age-associated increase in oxidative-nitrosative stress. Conversely, we found an increased expression of Hsp27 as well as a decreased expression of Hsp90 with aging in the aorta. Decreases in Hsp27 expression appeared to be highly correlated to increases in intima-medial thickness, and have also been found in the progression of atherosclerosis [396]. Rayner and colleagues also found that Hsp27 is regulated by estrogen and is atheroprotective [239, 240, 447]. Although Hsp90 functions to help in the degradation of damaged proteins, it also plays an important role in NO production. The association of Hsp90 with eNOS increases NO generation. Conversely, the disassociation of Hsp90 from eNOS leads to the increased production of superoxide in aortic endothelial cells [393]. We found that aging was characterized by decreased Hsp90 expression in the female F344xBN aorta. This decreased expression may be associated with a reduction in NO production and eNOS stability. Although correlation analysis suggested a high correlation between eNOS and Hsp90 expression and age, additional study is needed to determine cause and effect as well as physiological significance.

FIGURE 6.2
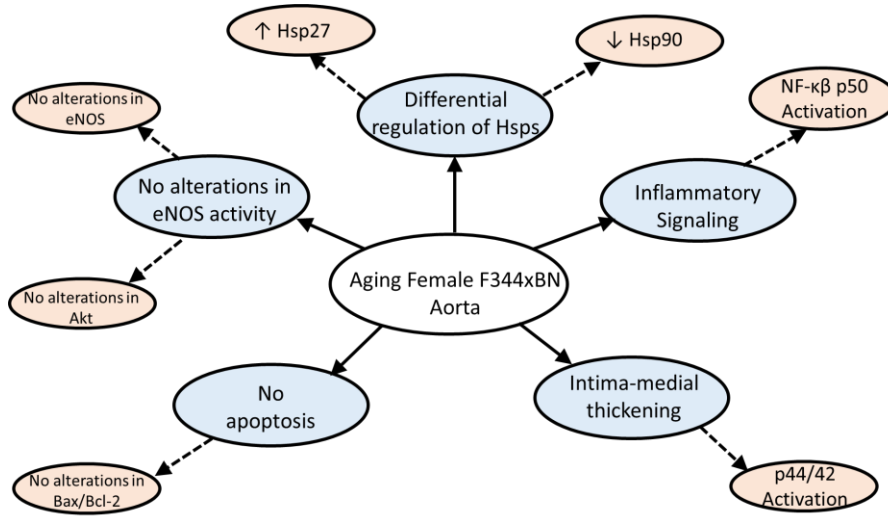
FIGURE 6.2: AGE-ASSOCIATED ALTERATIONS IN AORTIC STRUCTURE, FUNCTION, AND SIGNALING IN THE FEMALE F344XBN.

With age the following was observed in the female F344xBN aorta: differential regulation of Hsps, activation of inflammatory signaling, intima-medial thickening, as well as no alterations in eNOS activity or apoptosis. Solid lines indicate age-altered aortic cellular processes. Dotted lines indicate laboratory results. ↓ and ↑ indicate decrease and increase respectively.

TABLE 6.5: COMPARISON OF AGE-ASSOCIATED ALTERATIONS IN THE FEMALE F344XBN HEART AND AORTA. Age-associated comparisons of cardiac and aortic in morphology and signaling of female and male F344xBN rats.   Arrows indicate significant increase (↑) or decrease (↓) in parameters compared to 6-month values within gender. N.A. -- not applicable. N.C. – no change. N.D. – not determined.

	26m Heart	30m Heart	26m Aorta	30m Aorta
Proliferation/Hypertrophy				
Intima-medial thickness	N.A.	N.A.	N.C.	↑
HW/BW	N.C.	N.C.	N.A.	N.A.
Akt Signaling				
Akt	N.C.	N.C.	N.C.	N.C.
p-Akt(473)	N.C.	N.C.	N.C.	N.C.
p-Akt(308)	N.C.	N.D.	N.C.	N.C.
p-Akt(473)/Akt	↑	↑	N.C.	N.C.
Apoptosis Signaling				
Bax	N.C.	↑	N.C.	N.C.
Bcl-2	↓	N.C.	N.C.	N.C.
Bax/Bcl-2	N.C.	↑	N.C.	N.C.
Heat Shock Proteins				
Hsp27	N.C.	N.C.	↑	↑
Hsp70	N.C.	N.C.	N.C.	N.C.
Hsp90	N.C.	N.C.	↓	↓

CONCLUSION

In conclusion, this study observed three aspects of cardiovascular aging in the female F344xBN rat: 1) age-associated increases in oxidative-nitrosative stress and evidence of mitochondrial-mediated apoptosis in the female F344xBN heart; 2) alterations in cardiac structure as well as Cx43 heterogeneity and spatial distribution that may contribute to age-associated heart rhythm interval changes; and 3) that aortic aging in the female F344xBN is associated with increased activation of p44/42 MAPK and intima-medial thickness.

Taken together, the data of the present study suggest that cardiovascular structure and function is, for the most part, remarkably conserved in the 30-month old female F344xBN rat. This finding is consistent with the notion that the female F344xBN rat model may be applicable for investigating the effects of increasing age in the absence of underlying pathology on the cardiovascular system. Future research examining the potential effects of alterations in hormonal levels on cardiovascular structure and function may be warranted.

SUMMARY

1. Aging in the female F344xBN heart is associated with increases in posterior wall thickness and cardiomyocyte fiber CSA.

2. Aging in the female F344xBN heart is characterized by increases in superoxide production, lipid peroxidation, and nitration of tyrosine residues. This age-associated increase of oxidative-nitrosative stress did not appear to be related to changes in antioxidant mRNA expression.

3. Aging in the female F344xBN heart is characterized by increases in the number of TUNEL positive nuclei and activation of the mitochondrial-mediated pathway of apoptosis.

4. Aging in the female F344xBN rat heart is associated with cardiac hypertrophy, diastolic dysfunction, and evidence of increased valvular dysfunction.

5. Aging in the female F344xBN rat heart is associated with changes in the localization of Cx43 and alterations in heart rhythm intervals.

6. Aortic intima-medial thickness was increased with age in the female F344xBN rat.

7. Aging increased the activation of p44/42 MAPK in the female F344xBN aorta.

8. Aging in the female F344xBN aorta did not appear to alter the expression or phosphorylation of eNOS and Akt.

FUTURE DIRECTIONS

The present study determined the age-associated alterations in cardiovascular structure, function, and signaling in the female F344xBN rat. Future studies will investigate in detail the mechanisms of these findings with respect to the specific aims below.

SPECIFIC AIMS 1 AND 2: NATURAL AGING VS. OVAARIECTOMIZED AGING IN FEMALE F344XBN RATS

Findings from the present study suggest that aging in the female F344xBN rat is associated with cardiac hypertrophy, diastolic dysfunction, and alterations in heart rhythm intervals. The present study also suggests that aging is associated with increases in oxidative-nitrosative stress and apoptosis. Future studies could investigate if the age-associated alterations occur in young, aged, and very aged ovariectomized female F344xBN rats to see whether the absence of estrogen has a role in the development of age-associated CVD in the female F344xBN rat. It is anticipated that the results of such studies will provide insight as to how aging and the presence of hormones may play a role in cardiac dysfunction, oxidative stress, and apoptosis.

SPECIFIC AIM 3: AORTA AND OXIDATIVE STRESS

This investigation has shown that there is an increase in intima-medial thickness and p44/42 MAPK activation in the aging female F344xBN aorta. Future studies will determine if these age-associated aortic alterations in young, aged, and very aged female F344xBN are due to increased oxidative stress. These results will provide valuable information regarding how aging and oxidative stress play a role in the regulation of VSMC proliferation and protein signaling.

LIMITATIONS

1. Although the F344xBN rats are genetically identical to one another, they still have alleles from each of the parental strain. Due to the presence of different strain alleles as well as regulation of the X chromosome allele expression, it is difficult to control which allele is expressed in each individual using this model.

2. Echocardiogram and electrocardiogram parameters were measured under anesthetization with ketamine/xylazine for restraint in aging female rodents.

3. Age-associated alterations in some indices of cardiovascular structure and function can only be measured upon the death of the animal which prevents pre- and post-aging measurements from the same animal.

4. Rat ventricles are assumed to have the shape of a normal ventricle or with a non-uniform wall contraction. Volumes determined by ECHO are estimates from changes in dimensions.

5. Only the EKG leads I, II, and III were used due to the small size of the rat.

6. The cumulative effects of aging on the rat when comparing young to old age groups.

References

1. Johannes, J. and C.N. Bairey Merz, *Is cardiovascular disease in women inevitable?: preparing for menopause and beyond.* Cardiol Rev, 2011. **19**(2): p. 76-80.

2. Boluyt, M.O., et al., *Echocardiographic assessment of age-associated changes in systolic and diastolic function of the female F344 rat heart.* J Appl Physiol, 2004. **96**(2): p. 822-8.

3. Wyke, A.W. and H.R. Perkins, *The specificity of enzymes adding amino acids in the synthesis of the peptidoglycan precursors of Corynebacterium poinsettiae and Corynebacterium insidiosum.* J Gen Microbiol, 1975. **88**(1): p. 159-68.

4. Thomas, D.P., et al., *Aging- and training-induced alterations in collagen characteristics of rat left ventricle and papillary muscle.* Am J Physiol, 1992. **263**(3 Pt 2): p. H778-83.

5. Kayali, R., et al., *Gender difference as regards myocardial protein oxidation in aged rats: male rats have increased oxidative protein damage.* Biogerontology, 2007. **8**(6): p. 653-61.

6. Colom, B., et al., *Caloric restriction and gender modulate cardiac muscle mitochondrial H2O2 production and oxidative damage.* Cardiovasc Res, 2007. **74**(3): p. 456-65.

7. Liu, M., et al., *Aging might increase myocardial ischemia / reperfusion-induced apoptosis in humans and rats.* Age (Dordr), 2012. **34**(3): p. 621-32.

8. Stice, J.P., J.P. Eiserich, and A.A. Knowlton, *Role of aging versus the loss of estrogens in the reduction in vascular function in female rats.* Endocrinology, 2009. **150**(1): p. 212-9.

9. Badreck-Amoudi, A., et al., *The effect of age on residual strain in the rat aorta.* J Biomech Eng, 1996. **118**(4): p. 440-4.

10. Lipman, R.D., et al., *Pathologic characterization of brown Norway, brown Norway x Fischer 344, and Fischer 344 x brown Norway rats with relation to age.* J Gerontol A Biol Sci Med Sci, 1996. **51**(1): p. B54-9.

11. Turturro, A., et al., *Growth curves and survival characteristics of the animals used in the Biomarkers of Aging Program.* J Gerontol A Biol Sci Med Sci, 1999. **54**(11): p. B492-501.

12. Go, A.S., et al., *Heart disease and stroke statistics--2013 update: a report from the American Heart Association.* Circulation, 2013. **127**(1): p. e6-e245.

13. Lakatta, E.G., *Arterial and cardiac aging: major shareholders in*

cardiovascular disease enterprises: Part III: cellular and molecular clues to heart and arterial aging. Circulation, 2003. **107**(3): p. 490-7.

14. Lloyd-Jones, D., et al., *Heart disease and stroke statistics--2009 update: a report from the American Heart Association Statistics Committee and Stroke Statistics Subcommittee.* Circulation, 2009. **119**(3): p. e21-181.

15. National Heart, L., and Blood Institute, *Incidence and Prevalence: 2006 Chart Book on Cardiovascular and Lung Diseases*, 2006, National Heart, Lung, and Blood Institute; : Bethesda, MD.

16. Adams, K.F., Jr., et al., *Gender differences in survival in advanced heart failure. Insights from the FIRST study.* Circulation, 1999. **99**(14): p. 1816-21.

17. Tunstall-Pedoe, H., et al., *Sex differences in myocardial infarction and coronary deaths in the Scottish MONICA population of Glasgow 1985 to 1991. Presentation, diagnosis, treatment, and 28-day case fatality of 3991 events in men and 1551 events in women.* Circulation, 1996. **93**(11): p. 1981-92.

18. Tunstall-Pedoe, H., et al., *Myocardial infarction and coronary deaths in the World Health Organization MONICA Project. Registration procedures, event rates, and case-fatality rates in 38 populations from 21 countries in four continents.* Circulation, 1994. **90**(1): p. 583-612.

19. Marrugat, J., et al., *Influence of gender in acute and long-term cardiac mortality after a first myocardial infarction. REGICOR Investigators.* J Clin Epidemiol, 1994. **47**(2): p. 111-8.

20. Greenland, P., et al., *In-hospital and 1-year mortality in 1,524 women after myocardial infarction. Comparison with 4,315 men.* Circulation, 1991. **83**(2): p. 484-91.

21. Dai, D.F. and P.S. Rabinovitch, *Cardiac aging in mice and humans: the role of mitochondrial oxidative stress.* Trends Cardiovasc Med, 2009. **19**(7): p. 213-20.

22. Jackson, C.F. and N.K. Wenger, *Cardiovascular disease in the elderly.* Rev Esp Cardiol, 2011. **64**(8): p. 697-712.

23. Steinwachs, D.M., et al., *The future of cardiology: utilization and costs of care.* J Am Coll Cardiol, 2000. **35**(5 Suppl B): p. 91B-98B.

24. Jousilahti, P., et al., *Sex, age, cardiovascular risk factors, and coronary heart disease: a prospective follow-up study of 14 786 middle-aged men and women in Finland.* Circulation, 1999. **99**(9): p. 1165-72.

25. Kafonek, S.D., *Postmenopausal hormone replacement therapy and cardiovascular risk reduction. A review.* Drugs, 1994. **47 Suppl 2**: p. 16-24.

26. Hayward, C.S., R.P. Kelly, and P. Collins, *The roles of gender, the menopause and hormone replacement on cardiovascular function.* Cardiovasc Res, 2000. **46**(1): p. 28-49.

27. Shub, C., et al., *Determination of left ventricular mass by echocardiography in a normal population: effect of age and sex in addition to body size.* Mayo Clin Proc, 1994. **69**(3): p. 205-11.

28. Dannenberg, A.L., D. Levy, and R.J. Garrison, *Impact of age on echocardiographic left ventricular mass in a healthy population (the Framingham Study).* Am J Cardiol, 1989. **64**(16): p. 1066-8.

29. Marcus, R., et al., *Sex-specific determinants of increased left ventricular mass in the Tecumseh Blood Pressure Study.* Circulation, 1994. **90**(2): p. 928-36.

30. Simon, T., et al., *Sex differences in the prognosis of congestive heart failure: results from the Cardiac Insufficiency Bisoprolol Study (CIBIS II).* Circulation, 2001. **103**(3): p. 375-80.

31. Dart, A.M., X.J. Du, and B.A. Kingwell, *Gender, sex hormones and autonomic nervous control of the cardiovascular system.* Cardiovasc Res, 2002. **53**(3): p. 678-87.

32. Sastre, J., et al., *Mitochondria, oxidative stress and aging.* Free Radic Res, 2000. **32**(3): p. 189-98.

33. Tosato, M., et al., *The aging process and potential interventions to extend life expectancy.* Clin Interv Aging, 2007. **2**(3): p. 401-12.

34. Valko, M., et al., *Free radicals, metals and antioxidants in oxidative stress-induced cancer.* Chem Biol Interact, 2006. **160**(1): p. 1-40.

35. Elahi, M.M., Y.X. Kong, and B.M. Matata, *Oxidative stress as a mediator of cardiovascular disease.* Oxid Med Cell Longev, 2009. **2**(5): p. 259-69.

36. Yazdanyar, A. and A.B. Newman, *The burden of cardiovascular disease in the elderly: morbidity, mortality, and costs.* Clin Geriatr Med, 2009. **25**(4): p. 563-77, vii.

37. Sheydina, A., D.R. Riordon, and K.R. Boheler, *Molecular mechanisms of cardiomyocyte aging.* Clin Sci (Lond), 2011. **121**(8): p. 315-29.

38. Karavidas, A., et al., *Aging and the cardiovascular system.* Hellenic J Cardiol, 2010. **51**(5): p. 421-7.

39. DP, S.J.a.Z., *Cardiovascular disease in the elderly*. 8th ed, ed. Z.D. Braunwald E, Libby P. 2007, Philadelphia: WB Saunders.

40. Hatch, F., M.K. Lancaster, and S.A. Jones, *Aging is a primary risk factor for cardiac arrhythmias: disruption of intracellular Ca2+ regulation as a key*

suspect. Expert Rev Cardiovasc Ther, 2011. **9**(8): p. 1059-67.

41.   Lakatta, E.G., *Cardiovascular regulatory mechanisms in advanced age.* Physiol Rev, 1993. **73**(2): p. 413-67.

42.   Najjar, S.S., A. Scuteri, and E.G. Lakatta, *Arterial aging: is it an immutable cardiovascular risk factor?* Hypertension, 2005. **46**(3): p. 454-62.

43.   Rosamond, W., et al., *Heart disease and stroke statistics--2008 update: a report from the American Heart Association Statistics Committee and Stroke Statistics Subcommittee.* Circulation, 2008. **117**(4): p. e25-146.

44.   Okura, H., et al., *Age- and gender-specific changes in the left ventricular relaxation: a Doppler echocardiographic study in healthy individuals.* Circ Cardiovasc Imaging, 2009. **2**(1): p. 41-6.

45.   Mosca, L., et al., *Cardiovascular disease in women: a statement for healthcare professionals from the American Heart Association. Writing Group.* Circulation, 1997. **96**(7): p. 2468-82.

46.   Narkiewicz, K., et al., *Gender-selective interaction between aging, blood pressure, and sympathetic nerve activity.* Hypertension, 2005. **45**(4): p. 522-5.

47.   N.K., W., *Women's heart research: it's about time.* J Women Health 1995. **4**: p. 459–460.

48.   Burt, V.L., et al., *Prevalence of hypertension in the US adult population. Results from the Third National Health and Nutrition Examination Survey, 1988-1991.* Hypertension, 1995. **25**(3): p. 305-13.

49.   Bella, J.N., et al., *Gender difference in diastolic function in hypertension (the HyperGEN study).* Am J Cardiol, 2002. **89**(9): p. 1052-6.

50.   Frazier, C.G., et al., *Associations of gender and etiology with outcomes in heart failure with systolic dysfunction: a pooled analysis of 5 randomized control trials.* J Am Coll Cardiol, 2007. **49**(13): p. 1450-8.

51.   Klapholz, M., et al., *Hospitalization for heart failure in the presence of a normal left ventricular ejection fraction: results of the New York Heart Failure Registry.* J Am Coll Cardiol, 2004. **43**(8): p. 1432-8.

52.   Yancy, C.W., et al., *Clinical presentation, management, and in-hospital outcomes of patients admitted with acute decompensated heart failure with preserved systolic function: a report from the Acute Decompensated Heart Failure National Registry (ADHERE) Database.* J Am Coll Cardiol, 2006. **47**(1): p. 76-84.

53.   Masoudi, F.A., et al., *Gender, age, and heart failure with preserved left ventricular systolic function.* J Am Coll Cardiol, 2003. **41**(2): p. 217-23.

54. Kimmelstiel, C.D. and M.A. Konstam, *Heart failure in women.* Cardiology, 1995. **86**(4): p. 304-9.
55. Shapira, I., et al., *Cardiac rupture in patients with acute myocardial infarction.* Chest, 1987. **92**(2): p. 219-23.
56. Batts, K.P., D.M. Ackermann, and W.D. Edwards, *Postinfarction rupture of the left ventricular free wall: clinicopathologic correlates in 100 consecutive autopsy cases.* Hum Pathol, 1990. **21**(5): p. 530-5.
57. Becker, L.C., et al., *Left ventricular, peripheral vascular, and neurohumoral responses to mental stress in normal middle-aged men and women. Reference Group for the Psychophysiological Investigations of Myocardial Ischemia (PIMI) Study.* Circulation, 1996. **94**(11): p. 2768-77.
58. Krumholz, H.M., M. Larson, and D. Levy, *Sex differences in cardiac adaptation to isolated systolic hypertension.* Am J Cardiol, 1993. **72**(3): p. 310-3.
59. Carroll, J.D., et al., *Sex-associated differences in left ventricular function in aortic stenosis of the elderly.* Circulation, 1992. **86**(4): p. 1099-107.
60. Dittrich, H., et al., *Acute myocardial infarction in women: influence of gender on mortality and prognostic variables.* Am J Cardiol, 1988. **62**(1): p. 1-7.
61. Kostis, J.B., et al., *Sex differences in the management and long-term outcome of acute myocardial infarction. A statewide study. MIDAS Study Group. Myocardial Infarction Data Acquisition System.* Circulation, 1994. **90**(4): p. 1715-30.
62. Bueno, H., et al., *Influence of sex on the short-term outcome of elderly patients with a first acute myocardial infarction.* Circulation, 1995. **92**(5): p. 1133-40.
63. Vaccarino, V., et al., *Prevalence of coronary heart disease risk factors in northern-Italian male and female employees.* Eur Heart J, 1995. **16**(6): p. 761-9.
64. Greenberg, M.A. and H.S. Mueller, *Why the excess mortality in women after PTCA?* Circulation, 1993. **87**(3): p. 1030-2.
65. Bell, M.R., et al., *The changing in-hospital mortality of women undergoing percutaneous transluminal coronary angioplasty.* JAMA, 1993. **269**(16): p. 2091-5.
66. Kelsey, S.F., et al., *Results of percutaneous transluminal coronary angioplasty in women. 1985-1986 National Heart, Lung, and Blood Institute's Coronary Angioplasty Registry.* Circulation, 1993. **87**(3): p. 720-7.

67.   Acinapura, A.J., et al., *Internal mammary artery bypass: thirteen years of experience. Influence of angina and survival in 5125 patients.* J Cardiovasc Surg (Torino), 1992. **33**(5): p. 554-9.

68.   Khan, S.S., et al., *Increased mortality of women in coronary artery bypass surgery: evidence for referral bias.* Ann Intern Med, 1990. **112**(8): p. 561-7.

69.   Klein, M., et al., *Equilibrium and kinetic aspects of the interaction of isolated variable and constant domains of light chain with the Fd' fragment of immunoglobulin G.* Biochemistry, 1979. **18**(8): p. 1473-81.

70.   Reckelhoff, J.F. and C. Maric, *Sex and gender differences in cardiovascular-renal physiology and pathophysiology.* Steroids, 2010. **75**(11): p. 745-6.

71.   Burrus, O., *[Social treatment of AIDS].* Rev Infirm, 1992. **42**(16): p. 21-3.

72.   Lu, K.H., et al., *Chronological changes in sex steroid, gonadotropin and prolactin secretions in aging female rats displaying different reproductive states.* Biol Reprod, 1979. **21**(1): p. 193-203.

73.   Acosta, J.I., et al., *Transitional versus surgical menopause in a rodent model: etiology of ovarian hormone loss impacts memory and the acetylcholine system.* Endocrinology, 2009. **150**(9): p. 4248-59.

74.   Timaras P, Q.W., Vernadakis A, *Hormones and aging*. 1995, New York: CRC Press.

75.   Meites J, L.J., *Reproductive aging and neuroendocrine function*. Oxford review of reproductive biology. 1994, New York: Oxford Press.

76.   Lobo, R.A., *Surgical menopause and cardiovascular risks.* Menopause, 2007. **14**(3 Pt 2): p. 562-6.

77.   Shuster, L.T., et al., *Prophylactic oophorectomy in premenopausal women and long-term health.* Menopause Int, 2008. **14**(3): p. 111-6.

78.   Morrison, J.H., et al., *Estrogen, menopause, and the aging brain: how basic neuroscience can inform hormone therapy in women.* J Neurosci, 2006. **26**(41): p. 10332-48.

79.   Rocca, W.A., B.R. Grossardt, and L.T. Shuster, *Oophorectomy, menopause, estrogen, and cognitive aging: the timing hypothesis.* Neurodegener Dis, 2010. **7**(1-3): p. 163-6.

80.   Sluijmer, A.V., et al., *Endocrine activity of the postmenopausal ovary: the effects of pituitary down-regulation and oophorectomy.* J Clin Endocrinol Metab, 1995. **80**(7): p. 2163-7.

81.   Laughlin, G.A., et al., *Hysterectomy, oophorectomy, and endogenous sex hormone levels in older women: the Rancho Bernardo Study.* J Clin Endocrinol Metab, 2000. **85**(2): p. 645-51.

82. Kharchilava, O.M. and L.A. Valeeva, *[Effects of surgical ovariectomy on dopamine receptors of the heart and brain].* Patol Fiziol Eksp Ter, 2008(4): p. 21-3.

83. Lee, S.D., et al., *Cardiac Fas-dependent and mitochondria-dependent apoptosis in ovariectomized rats.* Maturitas, 2008. **61**(3): p. 268-77.

84. Stice, J.P., et al., *17beta-Estradiol, aging, inflammation, and the stress response in the female heart.* Endocrinology, 2011. **152**(4): p. 1589-98.

85. Baeza, I., et al., *Effects of growth hormone, melatonin, oestrogens and phytoestrogens on the oxidized glutathione (GSSG)/reduced glutathione (GSH) ratio and lipid peroxidation in aged ovariectomized rats.* Biogerontology, 2010. **11**(6): p. 687-701.

86. Fabris, B., et al., *Stimulation of cardiac apoptosis in ovariectomized hypertensive rats: potential role of the renin-angiotensin system.* J Hypertens, 2011. **29**(2): p. 273-81.

87. Liou, C.M., et al., *Effects of 17beta-estradiol on cardiac apoptosis in ovariectomized rats.* Cell Biochem Funct, 2010. **28**(6): p. 521-8.

88. Lakatta, E.G. and S.J. Sollott, *Perspectives on mammalian cardiovascular aging: humans to molecules.* Comp Biochem Physiol A Mol Integr Physiol, 2002. **132**(4): p. 699-721.

89. Olivetti, G., et al., *Gender differences and aging: effects on the human heart.* J Am Coll Cardiol, 1995. **26**(4): p. 1068-79.

90. Brenner, D.A., C.S. Apstein, and K.W. Saupe, *Exercise training attenuates age-associated diastolic dysfunction in rats.* Circulation, 2001. **104**(2): p. 221-6.

91. Benjamin, E.J., et al., *Determinants of Doppler indexes of left ventricular diastolic function in normal subjects (the Framingham Heart Study).* Am J Cardiol, 1992. **70**(4): p. 508-15.

92. Grossman, W., *Diastolic dysfunction in congestive heart failure.* N Engl J Med, 1991. **325**(22): p. 1557-64.

93. Lakatta, E.G. and F.C. Yin, *Myocardial aging: functional alterations and related cellular mechanisms.* Am J Physiol, 1982. **242**(6): p. H927-41.

94. Walker, E.M., Jr., et al., *Age-associated changes in hearts of male Fischer 344/Brown Norway F1 rats.* Ann Clin Lab Sci, 2006. **36**(4): p. 427-38.

95. Myreng, Y. and S. Nitter-Hauge, *Age-dependency of left ventricular filling dynamics and relaxation as assessed by pulsed Doppler echocardiography.* Clin Physiol, 1989. **9**(2): p. 99-106.

96. Spirito, P. and B.J. Maron, *Influence of aging on Doppler echocardiographic*

indices of left ventricular diastolic function. Br Heart J, 1988. **59**(6): p. 672-9.

97.   Pugh, K.G. and J.Y. Wei, *Clinical implications of physiological changes in the aging heart.* Drugs Aging, 2001. **18**(4): p. 263-76.

98.   Schulman, S.P., et al., *Age-related decline in left ventricular filling at rest and exercise.* Am J Physiol, 1992. **263**(6 Pt 2): p. H1932-8.

99.   Wong, L.S., et al., *Aging, telomeres and heart failure.* Heart Fail Rev, 2010. **15**(5): p. 479-86.

100.   Gupta, A.K., et al., *Cardiac arrhythmias in the elderly.* Card Electrophysiol Rev, 2002. **6**(1-2): p. 120-8.

101.   Olivetti, G., et al., *Cardiomyopathy of the aging human heart. Myocyte loss and reactive cellular hypertrophy.* Circ Res, 1991. **68**(6): p. 1560-8.

102.   Muscari, C., et al., *Age-dependent differences of ATP breakdown and ATP-catabolite release in ischemic and reperfused hearts.* Mech Ageing Dev, 1993. **67**(1-2): p. 1-11.

103.   Bernhard, D. and G. Laufer, *The aging cardiomyocyte: a mini-review.* Gerontology, 2008. **54**(1): p. 24-31.

104.   Raizada, V., et al., *Alterations in cardiac myosin isozymes associated with aging and chronic hypertension: their modulation with nifedipine.* Cardiovasc Res, 1993. **27**(10): p. 1869-72.

105.   Dhahbi, J.M., et al., *Gene expression and physiologic responses of the heart to the initiation and withdrawal of caloric restriction.* J Gerontol A Biol Sci Med Sci, 2006. **61**(3): p. 218-31.

106.   Burgess, M.L., J.C. McCrea, and H.L. Hedrick, *Age-associated changes in cardiac matrix and integrins.* Mech Ageing Dev, 2001. **122**(15): p. 1739-56.

107.   Lie, J.T. and P.I. Hammond, *Pathology of the senescent heart: anatomic observations on 237 autopsy studies of patients 90 to 105 years old.* Mayo Clin Proc, 1988. **63**(6): p. 552-64.

108.   Pandya, K., H.S. Kim, and O. Smithies, *Fibrosis, not cell size, delineates beta-myosin heavy chain reexpression during cardiac hypertrophy and normal aging in vivo.* Proc Natl Acad Sci U S A, 2006. **103**(45): p. 16864-9.

109.   Stratton, J.R., et al., *Beta-adrenergic effects on left ventricular filling: influence of aging and exercise training.* J Appl Physiol, 1994. **77**(6): p. 2522-9.

110.   Lakatta, E.G., et al., *Diminished inotropic response of aged myocardium to catecholamines.* Circ Res, 1975. **36**(2): p. 262-9.

111.   McLean, M.R., P.B. Goldberg, and J. Roberts, *An ultrastructural study of the effects of age on sympathetic innervation and atrial tissue in the rat.* J Mol

Cell Cardiol, 1983. **15**(2): p. 75-92.

112. Berg, B.N., *The electrocardiogram in aging rats.* J Gerontol, 1955. **10**(4): p. 420-3.

113. Berg, B.N. and C.R. Harmison, *Blood pressure and heart size in aging rats.* J Gerontol, 1955. **10**(4): p. 416-9.

114. Hacker, T.A., et al., *Age-related changes in cardiac structure and function in Fischer 344 x Brown Norway hybrid rats.* Am J Physiol Heart Circ Physiol, 2006. **290**(1): p. H304-11.

115. Slotwiner, D.J., et al., *Relation of age to left ventricular function in clinically normal adults.* Am J Cardiol, 1998. **82**(5): p. 621-6.

116. Anversa, P., et al., *Myocyte cell loss and myocyte cellular hyperplasia in the hypertrophied aging rat heart.* Circ Res, 1990. **67**(4): p. 871-85.

117. Betsuyaku, T., et al., *Cardiac structure and function in young and senescent mice heterozygous for a connexin43 null mutation.* J Mol Cell Cardiol, 2002. **34**(2): p. 175-84.

118. Forman, D.E., et al., *Cardiac morphology and function in senescent rats: gender-related differences.* J Am Coll Cardiol, 1997. **30**(7): p. 1872-7.

119. Rossi, S., et al., *Ventricular activation is impaired in aged rat hearts.* Am J Physiol Heart Circ Physiol, 2008. **295**(6): p. H2336-47.

120. Morita, N., et al., *Increased susceptibility of aged hearts to ventricular fibrillation during oxidative stress.* Am J Physiol Heart Circ Physiol, 2009. **297**(5): p. H1594-605.

121. Zhang, X.P., et al., *Increased apoptosis and myocyte enlargement with decreased cardiac mass; distinctive features of the aging male, but not female, monkey heart.* J Mol Cell Cardiol, 2007. **43**(4): p. 487-91.

122. Thomas, D.P., et al., *Exercise training attenuates aging-associated increases in collagen and collagen crosslinking of the left but not the right ventricle in the rat.* Eur J Appl Physiol, 2001. **85**(1-2): p. 164-9.

123. Boluyt, M.O., et al., *Regional variation in cardiac myosin isoforms of female F344 rats during aging.* J Gerontol A Biol Sci Med Sci, 1999. **54**(8): p. B313-7.

124. Boluyt, M.O., et al., *Cardiac adaptations to aortic constriction in adult and aged rats.* Am J Physiol, 1989. **257**(2 Pt 2): p. H643-8.

125. Perk, M., *Prognostic value of the ECG.* CMAJ, 2012. **184**(13): p. 1499.

126. Peters, A., et al., *Air pollution and incidence of cardiac arrhythmia.* Epidemiology, 2000. **11**(1): p. 11-7.

127. Wellenius, G.A., et al., *Electrocardiographic changes during exposure to residual oil fly ash (ROFA) particles in a rat model of myocardial infarction.*

Toxicol Sci, 2002. **66**(2): p. 327-35.

128. McCauley, L.A., et al., *Work characteristics and pesticide exposures among migrant agricultural families: a community-based research approach.* Environ Health Perspect, 2001. **109**(5): p. 533-8.

129. Hazari, M.S., et al., *Continuous electrocardiogram reveals differences in the short-term cardiotoxic response of Wistar-Kyoto and spontaneously hypertensive rats to doxorubicin.* Toxicol Sci, 2009. **110**(1): p. 224-34.

130. Xing, S., et al., *Genetic influence on electrocardiogram time intervals and heart rate in aging mice.* Am J Physiol Heart Circ Physiol, 2009. **296**(6): p. H1907-13.

131. Go, A.S., *The epidemiology of atrial fibrillation in elderly persons: the tip of the iceberg.* Am J Geriatr Cardiol, 2005. **14**(2): p. 56-61.

132. Dias da Silva, V.J., et al., *Chronic converting enzyme inhibition normalizes QT interval in aging rats.* Braz J Med Biol Res, 2002. **35**(9): p. 1025-31.

133. Molander, U., et al., *ECG abnormalities in the elderly: prevalence, time and generation trends and association with mortality.* Aging Clin Exp Res, 2003. **15**(6): p. 488-93.

134. James, A.F., S.C. Choisy, and J.C. Hancox, *Recent advances in understanding sex differences in cardiac repolarization.* Prog Biophys Mol Biol, 2007. **94**(3): p. 265-319.

135. Wasserstrom, J.A., et al., *Characteristics of intracellular Ca2+ cycling in intact rat heart: a comparison of sex differences.* Am J Physiol Heart Circ Physiol, 2008. **295**(5): p. H1895-904.

136. Macfarlane, P.W., et al., *Effects of age, sex, and race on ECG interval measurements.* J Electrocardiol, 1994. **27 Suppl**: p. 14-9.

137. Taneja, T., et al., *Effects of sex and age on electrocardiographic and cardiac electrophysiological properties in adults.* Pacing Clin Electrophysiol, 2001. **24**(1): p. 16-21.

138. Schneiderman, J., et al., *Increased type 1 plasminogen activator inhibitor gene expression in atherosclerotic human arteries.* Proc Natl Acad Sci U S A, 1992. **89**(15): p. 6998-7002.

139. Levy, D., et al., *Electrocardiographic changes with advancing age. A cross-sectional study of the association of age with QRS axis, duration and voltage.* J Electrocardiol, 1987. **20 Suppl**: p. 44-7.

140. Rautaharju, P.M., et al., *Sex differences in the evolution of the electrocardiographic QT interval with age.* Can J Cardiol, 1992. **8**(7): p. 690-5.

141.   Sugerman, H.J., *Obesity and intracranial hypertension.* Int J Obes Relat Metab Disord, 1995. **19**(10): p. 762-3.

142.   Pocchiari, R.J., R.L. Hamlin, and S.A. McCune, *Electrocardiographic findings in rats with cardiomyopathy.* Am J Vet Res, 1993. **54**(4): p. 607-11.

143.   Netuka, I., et al., *Late effect of early hypoxic disturbance in the rat heart: gender differences.* Physiol Res, 2010. **59**(1): p. 127-31.

144.   Xiao, L., et al., *Sex-based transmural differences in cardiac repolarization and ionic-current properties in canine left ventricles.* Am J Physiol Heart Circ Physiol, 2006. **291**(2): p. H570-80.

145.   Liu, X.K., et al., *In vivo androgen treatment shortens the QT interval and increases the densities of inward and delayed rectifier potassium currents in orchiectomized male rabbits.* Cardiovasc Res, 2003. **57**(1): p. 28-36.

146.   Pham, T.V. and M.R. Rosen, *Sex, hormones, and repolarization.* Cardiovasc Res, 2002. **53**(3): p. 740-51.

147.   James, A.F., L.A. Arberry, and J.C. Hancox, *Gender-related differences in ventricular myocyte repolarization in the guinea pig.* Basic Res Cardiol, 2004. **99**(3): p. 183-92.

148.   Leblanc, N., et al., *Age and gender differences in excitation-contraction coupling of the rat ventricle.* J Physiol, 1998. **511 (Pt 2)**: p. 533-48.

149.   Philp, K.L., et al., *Greater antiarrhythmic activity of acute 17beta-estradiol in female than male anaesthetized rats: correlation with Ca2+ channel blockade.* Br J Pharmacol, 2006. **149**(3): p. 233-42.

150.   Jiang, C., et al., *Effect of 17 beta-oestradiol on contraction, Ca2+ current and intracellular free Ca2+ in guinea-pig isolated cardiac myocytes.* Br J Pharmacol, 1992. **106**(3): p. 739-45.

151.   Spach, M.S., et al., *Changes in anisotropic conduction caused by remodeling cell size and the cellular distribution of gap junctions and Na(+) channels.* J Electrocardiol, 2001. **34 Suppl**: p. 69-76.

152.   Dhein, S. and S.B. Hammerath, *Aspects of the intercellular communication in aged hearts: effects of the gap junction uncoupler palmitoleic acid.* Naunyn Schmiedebergs Arch Pharmacol, 2001. **364**(5): p. 397-408.

153.   Spach, M.S. and P.C. Dolber, *Relating extracellular potentials and their derivatives to anisotropic propagation at a microscopic level in human cardiac muscle. Evidence for electrical uncoupling of side-to-side fiber connections with increasing age.* Circ Res, 1986. **58**(3): p. 356-71.

154.   Spach, M.S., et al., *Mechanism of origin of conduction disturbances in aging human atrial bundles: experimental and model study.* Heart Rhythm, 2007.

4(2): p. 175-85.

155.   Yamada, K.A., et al., *Up-regulation of connexin45 in heart failure.* J Cardiovasc Electrophysiol, 2003. **14**(11): p. 1205-12.

156.   Stein, M., et al., *Dominant arrhythmia vulnerability of the right ventricle in senescent mice.* Heart Rhythm, 2008. **5**(3): p. 438-48.

157.   Knezl, V., et al., *Distinct lethal arrhythmias susceptibility is associated with sex-related difference in myocardial connexin-43 expression.* Neuro Endocrinol Lett, 2008. **29**(5): p. 798-801.

158.   Jansen, J.A., et al., *Reduced Cx43 expression triggers increased fibrosis due to enhanced fibroblast activity.* Circ Arrhythm Electrophysiol, 2012. **5**(2): p. 380-90.

159.   Wu, W. and Z. Lu, *Loss of anti-arrhythmic effect of vagal nerve stimulation on ischemia-induced ventricular tachyarrhythmia in aged rats.* Tohoku J Exp Med, 2011. **223**(1): p. 27-33.

160.   Yoshida, M., et al., *Alterations in adhesion junction precede gap junction remodelling during the development of heart failure in cardiomyopathic hamsters.* Cardiovasc Res, 2011. **92**(1): p. 95-105.

161.   Burstein, B., et al., *Changes in connexin expression and the atrial fibrillation substrate in congestive heart failure.* Circ Res, 2009. **105**(12): p. 1213-22.

162.   Kato, T., Y.K. Iwasaki, and S. Nattel, *Connexins and atrial fibrillation: filling in the gaps.* Circulation, 2012. **125**(2): p. 203-6.

163.   Howarth, F.C., et al., *Effects of streptozotocin-induced diabetes on connexin43 mRNA and protein expression in ventricular muscle.* Mol Cell Biochem, 2008. **319**(1-2): p. 105-14.

164.   Xiao, J., et al., *[Resveratrol restored the structural and functional association between M3 receptor and connexin 43 gap junction proteins in ischemia-reperfusion injury of isolated rat heart].* Yao Xue Xue Bao, 2007. **42**(1): p. 19-25.

165.   Jansen, J.A., et al., *Reduced heterogeneous expression of Cx43 results in decreased Nav1.5 expression and reduced sodium current that accounts for arrhythmia vulnerability in conditional Cx43 knockout mice.* Heart Rhythm, 2012. **9**(4): p. 600-7.

166.   Rosenkranz-Weiss, P., et al., *Gender-specific differences in expression of mRNAs for functional and structural proteins in rat ventricular myocardium.* J Mol Cell Cardiol, 1994. **26**(2): p. 261-70.

167.   Tribulova, N., et al., *Sex differences in connexin-43 expression in left ventricles of aging rats.* Physiol Res, 2005. **54**(6): p. 705-8.

168. Yu, W., G. Dahl, and R. Werner, *The connexin43 gene is responsive to oestrogen.* Proc Biol Sci, 1994. **255**(1343): p. 125-32.

169. Pluciennik, F., et al., *Reversible interruption of gap junctional communication by testosterone propionate in cultured Sertoli cells and cardiac myocytes.* J Membr Biol, 1996. **149**(3): p. 169-77.

170. Grohe, C., et al., *Cardiac myocytes and fibroblasts contain functional estrogen receptors.* FEBS Lett, 1997. **416**(1): p. 107-12.

171. Chung, T.H., et al., *The interaction of estrogen receptor alpha and caveolin-3 regulates connexin43 phosphorylation in metabolic inhibition-treated rat cardiomyocytes.* Int J Biochem Cell Biol, 2009. **41**(11): p. 2323-33.

172. Lancaster, T.S., S.J. Jefferson, and D.H. Korzick, *Local delivery of a PKCepsilon-activating peptide limits ischemia reperfusion injury in the aged female rat heart.* Am J Physiol Regul Integr Comp Physiol, 2011. **301**(5): p. R1242-9.

173. Quigley, S. and I. Reed, *Magnetic resonance image of the pelvis.* BMJ, 2011. **343**: p. d5312.

174. Boengler, K., et al., *Loss of ischemic preconditioning's cardioprotection in aged mouse hearts is associated with reduced gap junctional and mitochondrial levels of connexin 43.* Am J Physiol Heart Circ Physiol, 2007. **292**(4): p. H1764-9.

175. Jones, S.A., M.K. Lancaster, and M.R. Boyett, *Ageing-related changes of connexins and conduction within the sinoatrial node.* J Physiol, 2004. **560**(Pt 2): p. 429-37.

176. Halliwell, B., *Oxidative stress and cancer: have we moved forward?* Biochem J, 2007. **401**(1): p. 1-11.

177. Valko, M., et al., *Free radicals and antioxidants in normal physiological functions and human disease.* Int J Biochem Cell Biol, 2007. **39**(1): p. 44-84.

178. Ramond, A., et al., *Oxidative stress mediates cardiac infarction aggravation induced by intermittent hypoxia.* Fundam Clin Pharmacol, 2013. **27**(3): p. 252-61.

179. Dean, O.M., et al., *N-acetyl cysteine restores brain glutathione loss in combined 2-cyclohexene-1-one and d-amphetamine-treated rats: relevance to schizophrenia and bipolar disorder.* Neurosci Lett, 2011. **499**(3): p. 149-53.

180. Singh, N., et al., *Oxidative stress and heart failure.* Mol Cell Biochem, 1995. **147**(1-2): p. 77-81.

181. Coimbra, N.C., C. Tomaz, and M.L. Brandao, *Evidence for the involvement of

serotonin in the antinociception induced by electrical or chemical stimulation of the mesencephalic tectum. Behav Brain Res, 1992. **50**(1-2): p. 77-83.

182. Brieger, K., et al., *Reactive oxygen species: from health to disease.* Swiss Med Wkly, 2012. **142**: p. w13659.

183. Leanderson, P., et al., *Formation of DNA adduct 8-hydroxy-2'-deoxyguanosine induced by man-made mineral fibres.* IARC Sci Publ, 1988: p. 422 - 424.

184. Tatarkova, Z., et al., *Effects of aging on activities of mitochondrial electron transport chain complexes and oxidative damage in rat heart.* Physiol Res, 2011. **60**(2): p. 281-9.

185. Huang, H. and K.G. Manton, *The role of oxidative damage in mitochondria during aging: a review.* Front Biosci, 2004. **9**: p. 1100-17.

186. de la Asuncion, J.G., et al., *AZT treatment induces molecular and ultrastructural oxidative damage to muscle mitochondria. Prevention by antioxidant vitamins.* J Clin Invest, 1998. **102**(1): p. 4-9.

187. Asano, S., et al., *Aging influences multiple indices of oxidative stress in the heart of the Fischer 344/NNia x Brown Norway/BiNia rat.* Redox Rep, 2007. **12**(4): p. 167-80.

188. Sanz, A., et al., *Evaluation of sex differences on mitochondrial bioenergetics and apoptosis in mice.* Exp Gerontol, 2007. **42**(3): p. 173-82.

189. Borras, C., et al., *Mitochondria from females exhibit higher antioxidant gene expression and lower oxidative damage than males.* Free Radic Biol Med, 2003. **34**(5): p. 546-52.

190. Jang, Y.M., et al., *Doxorubicin treatment in vivo activates caspase-12 mediated cardiac apoptosis in both male and female rats.* FEBS Lett, 2004. **577**(3): p. 483-90.

191. Strniskova, M., M. Barancik, and T. Ravingerova, *Mitogen-activated protein kinases and their role in regulation of cellular processes.* Gen Physiol Biophys, 2002. **21**(3): p. 231-55.

192. Garrington, T.P. and G.L. Johnson, *Organization and regulation of mitogen-activated protein kinase signaling pathways.* Curr Opin Cell Biol, 1999. **11**(2): p. 211-8.

193. House, S.L., et al., *Fibroblast Growth Factor 2 Mediates Isoproterenol-induced Cardiac Hypertrophy through Activation of the Extracellular Regulated Kinase.* Mol Cell Pharmacol, 2010. **2**(4): p. 143-154.

194. Lemke, L.E., et al., *Decreased p38 MAPK activity in end-stage failing human*

myocardium: p38 MAPK alpha is the predominant isoform expressed in human heart. J Mol Cell Cardiol, 2001. **33**(8): p. 1527-40.

195. Communal, C., et al., *Reciprocal modulation of mitogen-activated protein kinases and mitogen-activated protein kinase phosphatase 1 and 2 in failing human myocardium.* J Card Fail, 2002. **8**(2): p. 86-92.

196. Peart, J.N., et al., *Impaired p38 MAPK/HSP27 signaling underlies aging-related failure in opioid-mediated cardioprotection.* J Mol Cell Cardiol, 2007. **42**(5): p. 972-80.

197. Kakarla, S.K., et al., *Chronic acetaminophen attenuates age-associated increases in cardiac ROS and apoptosis in the Fischer Brown Norway rat.* Basic Res Cardiol, 2010. **105**(4): p. 535-44.

198. Izumi, Y., et al., *Cardiac mitogen-activated protein kinase activities are chronically increased in stroke-prone hypertensive rats.* Hypertension, 1998. **31**(1): p. 50-6.

199. Aoyagi, T. and S. Izumo, *Hemodynamic Overload-Induced Activation of Myocardial Mitogen-Activated Protein Kinases In Vivo : Augmented Responses in Young Spontaneously Hypertensive Rats and Diminished Responses in Aged Fischer 344 Rats.* Hypertension, 2001. **37**(1): p. 52-57.

200. Yeo, E.J. and S.C. Park, *Age-dependent agonist-specific dysregulation of membrane-mediated signal transduction: emergence of the gate theory of aging.* Mech Ageing Dev, 2002. **123**(12): p. 1563-78.

201. Knowlton, A.A., P. Brecher, and C.S. Apstein, *Rapid expression of heat shock protein in the rabbit after brief cardiac ischemia.* J Clin Invest, 1991. **87**(1): p. 139-47.

202. Benjamin, I.J. and D.R. McMillan, *Stress (heat shock) proteins: molecular chaperones in cardiovascular biology and disease.* Circ Res, 1998. **83**(2): p. 117-32.

203. Tatar, M., A.A. Khazaeli, and J.W. Curtsinger, *Chaperoning extended life.* Nature, 1997. **390**(6655): p. 30.

204. Balch, W.E., et al., *Adapting proteostasis for disease intervention.* Science, 2008. **319**(5865): p. 916-9.

205. Swindell, W.R., et al., *Endocrine regulation of heat shock protein mRNA levels in long-lived dwarf mice.* Mech Ageing Dev, 2009. **130**(6): p. 393-400.

206. Westerheide, S.D. and R.I. Morimoto, *Heat shock response modulators as therapeutic tools for diseases of protein conformation.* J Biol Chem, 2005. **280**(39): p. 33097-100.

207. Morimoto, R.I., *Proteotoxic stress and inducible chaperone networks in*

neurodegenerative disease and aging. Genes Dev, 2008. **22**(11): p. 1427-38.

208. Morley, J.F. and R.I. Morimoto, *Regulation of longevity in Caenorhabditis elegans by heat shock factor and molecular chaperones.* Mol Biol Cell, 2004. **15**(2): p. 657-64.

209. Morrow, G., et al., *Overexpression of the small mitochondrial Hsp22 extends Drosophila life span and increases resistance to oxidative stress.* FASEB J, 2004. **18**(3): p. 598-9.

210. Starnes, J.W., et al., *Myocardial heat shock protein 70 expression in young and old rats after identical exercise programs.* J Gerontol A Biol Sci Med Sci, 2005. **60**(8): p. 963-9.

211. Lawler, J.M., et al., *Exercise training inducibility of MnSOD protein expression and activity is retained while reducing prooxidant signaling in the heart of senescent rats.* Am J Physiol Regul Integr Comp Physiol, 2009. **296**(5): p. R1496-502.

212. Kregel, K.C., et al., *HSP70 accumulation in tissues of heat-stressed rats is blunted with advancing age.* J Appl Physiol, 1995. **79**(5): p. 1673-8.

213. Chandrasekar, B. and G.L. Freeman, *Induction of nuclear factor kappaB and activation protein 1 in postischemic myocardium.* FEBS Lett, 1997. **401**(1): p. 30-4.

214. Li, C., W. Browder, and R.L. Kao, *Early activation of transcription factor NF-kappaB during ischemia in perfused rat heart.* Am J Physiol, 1999. **276**(2 Pt 2): p. H543-52.

215. Wong, S.C., et al., *Induction of cyclooxygenase-2 and activation of nuclear factor-kappaB in myocardium of patients with congestive heart failure.* Circulation, 1998. **98**(2): p. 100-3.

216. Frantz, S., et al., *Sustained activation of nuclear factor kappa B and activator protein 1 in chronic heart failure.* Cardiovasc Res, 2003. **57**(3): p. 749-56.

217. Valen, G., *Innate immunity and remodelling.* Heart Fail Rev, 2011. **16**(1): p. 71-8.

218. Yndestad, A., et al., *Role of inflammation in the progression of heart failure.* Curr Cardiol Rep, 2007. **9**(3): p. 236-41.

219. Pelletier, D.A., et al., *Effects of engineered cerium oxide nanoparticles on bacterial growth and viability.* Appl Environ Microbiol, 2010. **76**(24): p. 7981-9.

220. May, M.J. and S. Ghosh, *Signal transduction through NF-kappa B.* Immunol Today, 1998. **19**(2): p. 80-8.

221. Baeuerle, P.A. and D. Baltimore, *NF-kappa B: ten years after.* Cell, 1996. **87**(1): p. 13-20.
222. Bonizzi, G. and M. Karin, *The two NF-kappaB activation pathways and their role in innate and adaptive immunity.* Trends Immunol, 2004. **25**(6): p. 280-8.
223. Damgaard, R.B. and M. Gyrd-Hansen, *Inhibitor of apoptosis (IAP) proteins in regulation of inflammation and innate immunity.* Discov Med, 2011. **11**(58): p. 221-31.
224. Lawrence, T. and C. Fong, *The resolution of inflammation: anti-inflammatory roles for NF-kappaB.* Int J Biochem Cell Biol, 2010. **42**(4): p. 519-23.
225. Frantz, S., et al., *Absence of NF-kappaB subunit p50 improves heart failure after myocardial infarction.* FASEB J, 2006. **20**(11): p. 1918-20.
226. Timmers, L., et al., *Targeted deletion of nuclear factor kappaB p50 enhances cardiac remodeling and dysfunction following myocardial infarction.* Circ Res, 2009. **104**(5): p. 699-706.
227. Wang, M., et al., *Estrogen receptor-alpha mediates acute myocardial protection in females.* Am J Physiol Heart Circ Physiol, 2006. **290**(6): p. H2204-9.
228. Meldrum, D.R., et al., *Intracellular signaling mechanisms of sex hormones in acute myocardial inflammation and injury.* Front Biosci, 2005. **10**: p. 1835-67.
229. Wang, M., et al., *17-beta-Estradiol decreases p38 MAPK-mediated myocardial inflammation and dysfunction following acute ischemia.* J Mol Cell Cardiol, 2006. **40**(2): p. 205-12.
230. Cheng, W., et al., *Puerarin suppresses proliferation of endometriotic stromal cells partly via the MAPK signaling pathway induced by 17ss-estradiol-BSA.* PLoS One, 2012. **7**(9): p. e45529.
231. Nuedling, S., et al., *Differential effects of 17beta-estradiol on mitogen-activated protein kinase pathways in rat cardiomyocytes.* FEBS Lett, 1999. **454**(3): p. 271-6.
232. Watson, C.S., et al., *Rapid actions of estrogens in GH3/B6 pituitary tumor cells via a plasma membrane version of estrogen receptor-alpha.* Steroids, 1999. **64**(1-2): p. 5-13.
233. Song, R.X., et al., *Linkage of rapid estrogen action to MAPK activation by ERalpha-Shc association and Shc pathway activation.* Mol Endocrinol, 2002. **16**(1): p. 116-27.

234. Borras, C., et al., *17beta-oestradiol up-regulates longevity-related, antioxidant enzyme expression via the ERK1 and ERK2[MAPK]/NFkappaB cascade.* Aging Cell, 2005. **4**(3): p. 113-8.

235. van Eickels, M., et al., *17beta-estradiol attenuates the development of pressure-overload hypertrophy.* Circulation, 2001. **104**(12): p. 1419-23.

236. Patten, R.D., et al., *17 Beta-estradiol differentially affects left ventricular and cardiomyocyte hypertrophy following myocardial infarction and pressure overload.* J Card Fail, 2008. **14**(3): p. 245-53.

237. Voss, M.R., et al., *Gender differences in the expression of heat shock proteins: the effect of estrogen.* Am J Physiol Heart Circ Physiol, 2003. **285**(2): p. H687-92.

238. Knowlton, A.A. and L. Sun, *Heat-shock factor-1, steroid hormones, and regulation of heat-shock protein expression in the heart.* Am J Physiol Heart Circ Physiol, 2001. **280**(1): p. H455-64.

239. Rayner, K., et al., *Heat shock protein 27 protects against atherogenesis via an estrogen-dependent mechanism: role of selective estrogen receptor beta modulation.* Arterioscler Thromb Vasc Biol, 2009. **29**(11): p. 1751-6.

240. Al-Madhoun, A.S., et al., *The interaction and cellular localization of HSP27 and ERbeta are modulated by 17beta-estradiol and HSP27 phosphorylation.* Mol Cell Endocrinol, 2007. **270**(1-2): p. 33-42.

241. Yu, H.P., et al., *Mechanism of cardioprotection following trauma-hemorrhagic shock by a selective estrogen receptor-beta agonist: up-regulation of cardiac heat shock factor-1 and heat shock proteins.* J Mol Cell Cardiol, 2006. **40**(1): p. 185-94.

242. Al-Khlaiwi, T., et al., *Estrogen protects cardiac myogenic (H9c2) rat cells against lethal heat shock-induced cell injury: modulation of estrogen receptor alpha, glucocorticoid receptors, heat shock protein 70, and iNOS.* J Cardiovasc Pharmacol, 2005. **45**(3): p. 217-24.

243. Borras, C., J. Gambini, and J. Vina, *Mitochondrial oxidant generation is involved in determining why females live longer than males.* Front Biosci, 2007. **12**: p. 1008-13.

244. Helenius, M., et al., *Aging-induced up-regulation of nuclear binding activities of oxidative stress responsive NF-kB transcription factor in mouse cardiac muscle.* J Mol Cell Cardiol, 1996. **28**(3): p. 487-98.

245. Dannels, E., *Neuropathic foot ulcer prevention in diabetic American Indians with hallux limitus.* J Am Podiatr Med Assoc, 1989. **79**(9): p. 447-50.

246. Dorn, G.W., 2nd, *Apoptotic and non-apoptotic programmed cardiomyocyte*

death in ventricular remodelling. Cardiovasc Res, 2009. **81**(3): p. 465-73.

247. Hotchkiss, R.S., et al., *Cell death.* N Engl J Med, 2009. **361**(16): p. 1570-83.

248. Narula, J., et al., *Apoptosis in myocytes in end-stage heart failure.* N Engl J Med, 1996. **335**(16): p. 1182-9.

249. Olivetti, G., et al., *Apoptosis in the failing human heart.* N Engl J Med, 1997. **336**(16): p. 1131-41.

250. Mallat, Z., et al., *Evidence of apoptosis in arrhythmogenic right ventricular dysplasia.* N Engl J Med, 1996. **335**(16): p. 1190-6.

251. Hein, S., et al., *Progression from compensated hypertrophy to failure in the pressure-overloaded human heart: structural deterioration and compensatory mechanisms.* Circulation, 2003. **107**(7): p. 984-91.

252. Gallogly, M.M., et al., *Glutaredoxin regulates apoptosis in cardiomyocytes via NFkappaB targets Bcl-2 and Bcl-xL: implications for cardiac aging.* Antioxid Redox Signal, 2010. **12**(12): p. 1339-53.

253. Ljubicic, V., K.J. Menzies, and D.A. Hood, *Mitochondrial dysfunction is associated with a pro-apoptotic cellular environment in senescent cardiac muscle.* Mech Ageing Dev, 2010. **131**(2): p. 79-88.

254. Kakarla, S.K., et al., *Possible molecular mechanisms underlying age-related cardiomyocyte apoptosis in the F344XBN rat heart.* J Gerontol A Biol Sci Med Sci, 2010. **65**(2): p. 147-55.

255. Mallat, Z., et al., *Age and gender effects on cardiomyocyte apoptosis in the normal human heart.* J Gerontol A Biol Sci Med Sci, 2001. **56**(11): p. M719-23.

256. Biondi-Zoccai, G.G., et al., *Female gender, myocardial remodeling and cardiac failure: are women protected from increased myocardiocyte apoptosis?* Ital Heart J, 2004. **5**(7): p. 498-504.

257. Guerra, S., et al., *Myocyte death in the failing human heart is gender dependent.* Circ Res, 1999. **85**(9): p. 856-66.

258. Lakatta, E.G. and D. Levy, *Arterial and cardiac aging: major shareholders in cardiovascular disease enterprises: Part II: the aging heart in health: links to heart disease.* Circulation, 2003. **107**(2): p. 346-54.

259. Qiu, H., et al., *Sex-specific regulation of gene expression in the aging monkey aorta.* Physiol Genomics, 2007. **29**(2): p. 169-80.

260. Lusis, A.J., *Atherosclerosis.* Nature, 2000. **407**(6801): p. 233-41.

261. Challah, M., et al., *Circulating and cellular markers of endothelial dysfunction with aging in rats.* Am J Physiol, 1997. **273**(4 Pt 2): p. H1941-8.

262. Li, M. and N.K. Fukagawa, *Age-related changes in redox signaling and VSMC*

function. Antioxid Redox Signal, 2010. **12**(5): p. 641-55.

263. O'Leary, D.H., et al., *Carotid-artery intima and media thickness as a risk factor for myocardial infarction and stroke in older adults. Cardiovascular Health Study Collaborative Research Group.* N Engl J Med, 1999. **340**(1): p. 14-22.

264. Ferrari, A.U., A. Radaelli, and M. Centola, *Invited review: aging and the cardiovascular system.* J Appl Physiol, 2003. **95**(6): p. 2591-7.

265. Sprott, R.L. and I. Ramirez, *Current Inbred and Hybrid Rat and Mouse Models for Gereontological Research.* ILAR J, 1997. **38**(3): p. 104-109.

266. van der Heijden-Spek, J.J., et al., *Effect of age on brachial artery wall properties differs from the aorta and is gender dependent: a population study.* Hypertension, 2000. **35**(2): p. 637-42.

267. Elliott, H.L., et al., *Effect of age on the responsiveness of vascular alpha-adrenoceptors in man.* J Cardiovasc Pharmacol, 1982. **4**(3): p. 388-92.

268. Miller, S.J., et al., *Development of progressive aortic vasculopathy in a rat model of aging.* Am J Physiol Heart Circ Physiol, 2007. **293**(5): p. H2634-43.

269. Moon, S.K., et al., *Age-related changes in matrix metalloproteinase-9 regulation in cultured mouse aortic smooth muscle cells.* Exp Gerontol, 2004. **39**(1): p. 123-31.

270. Spinetti, G., et al., *Rat aortic MCP-1 and its receptor CCR2 increase with age and alter vascular smooth muscle cell function.* Arterioscler Thromb Vasc Biol, 2004. **24**(8): p. 1397-402.

271. Zhang, W., X. Zhang, and Y. Zhang, *[Evaluation of thoracic aortic anatomy and function with transesophageal echocardiography].* Zhonghua Yi Xue Za Zhi, 1998. **78**(9): p. 666-9.

272. Albaladejo, P., et al., *Influence of sex on the relation between heart rate and aortic stiffness.* J Hypertens, 2003. **21**(3): p. 555-62.

273. Ross, R., *Atherosclerosis--an inflammatory disease.* N Engl J Med, 1999. **340**(2): p. 115-26.

274. Gennaro, G., et al., *Role of p44/p42 MAP kinase in the age-dependent increase in vascular smooth muscle cell proliferation and neointimal formation.* Arterioscler Thromb Vasc Biol, 2003. **23**(2): p. 204-10.

275. Hariri, R.J., et al., *Aging and arteriosclerosis. Cell cycle kinetics of young and old arterial smooth muscle cells.* Am J Pathol, 1988. **131**(1): p. 132-6.

276. Porreca, E., et al., *Protein kinase C pathway and proliferative responses of aged and young rat vascular smooth muscle cells.* Atherosclerosis, 1993. **104**(1-2): p. 137-45.

277. Stemerman, M.B., et al., *Vascular smooth muscle cell growth kinetics in vivo in aged rats.* Proc Natl Acad Sci U S A, 1982. **79**(12): p. 3863-6.

278. Hariri, R.J., et al., *Aging and arteriosclerosis. I. Development of myointimal hyperplasia after endothelial injury.* J Exp Med, 1986. **164**(4): p. 1171-8.

279. Vanhoutte, P.M., *Endothelial dysfunction and atherosclerosis.* Eur Heart J, 1997. **18 Suppl E**: p. E19-29.

280. Marin, J. and J. Redondo, *Vascular sodium pump: endothelial modulation and alterations in some pathological processes and aging.* Pharmacol Ther, 1999. **84**(3): p. 249-71.

281. Sagach, V., et al., *Endothelial dysfunction: Possible mechanisms and ways of correction.* Exp Clin Cardiol, 2006. **11**(2): p. 107-10.

282. Neumann, P., N. Gertzberg, and A. Johnson, *TNF-alpha induces a decrease in eNOS promoter activity.* Am J Physiol Lung Cell Mol Physiol, 2004. **286**(2): p. L452-9.

283. Dimmeler, S., et al., *Activation of nitric oxide synthase in endothelial cells by Akt-dependent phosphorylation.* Nature, 1999. **399**(6736): p. 601-5.

284. Drummond, G.R., et al., *Transcriptional and posttranscriptional regulation of endothelial nitric oxide synthase expression by hydrogen peroxide.* Circ Res, 2000. **86**(3): p. 347-54.

285. Hayashi, T. and A. Iguchi, *Possibility of the regression of atherosclerosis through the prevention of endothelial senescence by the regulation of nitric oxide and free radical scavengers.* Geriatr Gerontol Int, 2010. **10**(2): p. 115-30.

286. Dudzinski, D.M. and T. Michel, *Life history of eNOS: partners and pathways.* Cardiovasc Res, 2007. **75**(2): p. 247-60.

287. Ho, F.M., et al., *High glucose-induced apoptosis in human vascular endothelial cells is mediated through NF-kappaB and c-Jun NH2-terminal kinase pathway and prevented by PI3K/Akt/eNOS pathway.* Cell Signal, 2006. **18**(3): p. 391-9.

288. Boo, Y.C. and H. Jo, *Flow-dependent regulation of endothelial nitric oxide synthase: role of protein kinases.* Am J Physiol Cell Physiol, 2003. **285**(3): p. C499-508.

289. Dohi, Y., et al., *Age-related changes in vascular smooth muscle and endothelium.* Drugs Aging, 1995. **7**(4): p. 278-91.

290. Zeiher, A.M., et al., *Endothelium-mediated coronary blood flow modulation in humans. Effects of age, atherosclerosis, hypercholesterolemia, and hypertension.* J Clin Invest, 1993. **92**(2): p. 652-62.

291. Tschudi, M.R., et al., *Effect of age on kinetics of nitric oxide release in rat aorta and pulmonary artery.* J Clin Invest, 1996. **98**(4): p. 899-905.

292. Hoffmann, J., et al., *Aging enhances the sensitivity of endothelial cells toward apoptotic stimuli: important role of nitric oxide.* Circ Res, 2001. **89**(8): p. 709-15.

293. Gryglewski, R.J., R.M. Palmer, and S. Moncada, *Superoxide anion is involved in the breakdown of endothelium-derived vascular relaxing factor.* Nature, 1986. **320**(6061): p. 454-6.

294. Azhar, S., L. Cao, and E. Reaven, *Alteration of the adrenal antioxidant defense system during aging in rats.* J Clin Invest, 1995. **96**(3): p. 1414-24.

295. Shigenaga, M.K., T.M. Hagen, and B.N. Ames, *Oxidative damage and mitochondrial decay in aging.* Proc Natl Acad Sci U S A, 1994. **91**(23): p. 10771-8.

296. Stadtman, E.R., et al., *Age-related oxidation reaction in proteins.* Toxicol Ind Health, 1993. **9**(1-2): p. 187-96.

297. Reckelhoff, J.F., et al., *Changes in nitric oxide precursor, L-arginine, and metabolites, nitrate and nitrite, with aging.* Life Sci, 1994. **55**(24): p. 1895-902.

298. Barton, M., et al., *Anatomic heterogeneity of vascular aging: role of nitric oxide and endothelin.* Hypertension, 1997. **30**(4): p. 817-24.

299. Brandes, R.P., I. Fleming, and R. Busse, *Endothelial aging.* Cardiovasc Res, 2005. **66**(2): p. 286-94.

300. Kim, J.H., et al., *Arginase inhibition restores NOS coupling and reverses endothelial dysfunction and vascular stiffness in old rats.* J Appl Physiol, 2009. **107**(4): p. 1249-57.

301. Cernadas, M.R., et al., *Expression of constitutive and inducible nitric oxide synthases in the vascular wall of young and aging rats.* Circ Res, 1998. **83**(3): p. 279-86.

302. Chou, T.C., et al., *Alterations of nitric oxide synthase expression with aging and hypertension in rats.* Hypertension, 1998. **31**(2): p. 643-8.

303. Kokoszka, J.E., et al., *Increased mitochondrial oxidative stress in the Sod2 (+/-) mouse results in the age-related decline of mitochondrial function culminating in increased apoptosis.* Proc Natl Acad Sci U S A, 2001. **98**(5): p. 2278-83.

304. Xu, D., R. Neville, and T. Finkel, *Homocysteine accelerates endothelial cell senescence.* FEBS Lett, 2000. **470**(1): p. 20-4.

305. van der Loo, B., et al., *Enhanced peroxynitrite formation is associated with*

vascular aging. J Exp Med, 2000. **192**(12): p. 1731-44.

306.   Rajapakse, A.G., et al., *Hyperactive S6K1 mediates oxidative stress and endothelial dysfunction in aging: inhibition by resveratrol.* PLoS One, 2011. **6**(4): p. e19237.

307.   Takenouchi, Y., et al., *Gender differences in age-related endothelial function in the murine aorta.* Atherosclerosis, 2009. **206**(2): p. 397-404.

308.   Chakrabarti, S., et al., *17beta-Estradiol induces protein S-nitrosylation in the endothelium.* Cardiovasc Res, 2010. **85**(4): p. 796-805.

309.   Widder, J., et al., *Improvement of endothelial dysfunction by selective estrogen receptor-alpha stimulation in ovariectomized SHR.* Hypertension, 2003. **42**(5): p. 991-6.

310.   MacRitchie, A.N., et al., *Estrogen upregulates endothelial nitric oxide synthase gene expression in fetal pulmonary artery endothelium.* Circ Res, 1997. **81**(3): p. 355-62.

311.   Lantin-Hermoso, R.L., et al., *Estrogen acutely stimulates nitric oxide synthase activity in fetal pulmonary artery endothelium.* Am J Physiol, 1997. **273**(1 Pt 1): p. L119-26.

312.   Caulin-Glaser, T., et al., *17 beta-estradiol regulation of human endothelial cell basal nitric oxide release, independent of cytosolic Ca2+ mobilization.* Circ Res, 1997. **81**(5): p. 885-92.

313.   Hulley, S., et al., *Randomized trial of estrogen plus progestin for secondary prevention of coronary heart disease in postmenopausal women. Heart and Estrogen/progestin Replacement Study (HERS) Research Group.* JAMA, 1998. **280**(7): p. 605-13.

314.   Cherry, N., et al., *Oestrogen therapy for prevention of reinfarction in postmenopausal women: a randomised placebo controlled trial.* Lancet, 2002. **360**(9350): p. 2001-8.

315.   Rossouw, J.E., *Hormones, genetic factors, and gender differences in cardiovascular disease.* Cardiovasc Res, 2002. **53**(3): p. 550-7.

316.   Angerer, P., et al., *Effect of oral postmenopausal hormone replacement on progression of atherosclerosis : a randomized, controlled trial.* Arterioscler Thromb Vasc Biol, 2001. **21**(2): p. 262-8.

317.   Ling, S., et al., *Endogenous estrogen deficiency reduces proliferation and enhances apoptosis-related death in vascular smooth muscle cells: insights from the aromatase-knockout mouse.* Circulation, 2004. **109**(4): p. 537-43.

318.   Wenger, N.K., L. Speroff, and B. Packard, *Cardiovascular health and disease in women.* N Engl J Med, 1993. **329**(4): p. 247-56.

319. Espinosa, E., B.S. Oemar, and T.F. Luscher, *17 beta-Estradiol and smooth muscle cell proliferation in aortic cells of male and female rats.* Biochem Biophys Res Commun, 1996. **221**(1): p. 8-14.

320. Suzuki, A., et al., *Effects of 17 beta-estradiol and progesterone on growth-factor-induced proliferation and migration in human female aortic smooth muscle cells in vitro.* Cardiovasc Res, 1996. **32**(3): p. 516-23.

321. Dubey, R.K., et al., *Methoxyestradiols mediate the antimitogenic effects of estradiol on vascular smooth muscle cells via estrogen receptor-independent mechanisms.* Biochem Biophys Res Commun, 2000. **278**(1): p. 27-33.

322. Lee, W.S., et al., *Progesterone inhibits arterial smooth muscle cell proliferation.* Nat Med, 1997. **3**(9): p. 1005-8.

323. Bolego, C., et al., *Diabetes abolishes the vascular protective effects of estrogen in female rats.* Life Sci, 1999. **64**(9): p. 741-9.

324. Rubanyi, G.M., et al., *Vascular estrogen receptors and endothelium-derived nitric oxide production in the mouse aorta. Gender difference and effect of estrogen receptor gene disruption.* J Clin Invest, 1997. **99**(10): p. 2429-37.

325. Iafrati, M.D., et al., *Estrogen inhibits the vascular injury response in estrogen receptor alpha-deficient mice.* Nat Med, 1997. **3**(5): p. 545-8.

326. Chen, Q.W., L. Edvinsson, and C.B. Xu, *Role of ERK/MAPK in endothelin receptor signaling in human aortic smooth muscle cells.* BMC Cell Biol, 2009. **10**: p. 52.

327. Pearson, G., et al., *Mitogen-activated protein (MAP) kinase pathways: regulation and physiological functions.* Endocr Rev, 2001. **22**(2): p. 153-83.

328. Guyton, K.Z., et al., *Activation of mitogen-activated protein kinase by H2O2. Role in cell survival following oxidant injury.* J Biol Chem, 1996. **271**(8): p. 4138-42.

329. Zou, T., et al., *Homocysteine enhances cell proliferation in vascular smooth muscle cells: role of p38 MAPK and p47phox.* Acta Biochim Biophys Sin (Shanghai), 2010. **42**(12): p. 908-15.

330. Bhattacharya, I., et al., *Inhibition of activated ERK1/2 and JNKs improves vascular function in mouse aortae in the absence of nitric oxide.* Eur J Pharmacol, 2011. **658**(1): p. 22-7.

331. Rice, K.M., et al., *Fluprostenol-induced MAPK signaling is independent of aging in Fischer 344/NNiaHSd x Brown Norway/BiNia rat aorta.* Ann Clin Lab Sci, 2010. **40**(1): p. 26-31.

332. Rice, K.M., et al., *Effects of aging on pressure-induced MAPK activation in the rat aorta.* Pflugers Arch, 2005. **450**(3): p. 192-9.

333. Fukagawa, N.K., et al., *Modulation of cell injury and survival by high glucose and advancing age.* Free Radic Biol Med, 2001. **31**(12): p. 1560-9.

334. Sharma, R.V., M.V. Gurjar, and R.C. Bhalla, *Selected contribution: estrogen receptor-alpha gene transfer inhibits proliferation and NF-kappaB activation in VSM cells from female rats.* J Appl Physiol, 2001. **91**(5): p. 2400-6; discussion 2389-90.

335. Xing, D., et al., *Estrogen and mechanisms of vascular protection.* Arterioscler Thromb Vasc Biol, 2009. **29**(3): p. 289-95.

336. Speir, E., et al., *Antioxidant effect of estrogen on cytomegalovirus-induced gene expression in coronary artery smooth muscle cells.* Circulation, 2000. **102**(24): p. 2990-6.

337. Colditz, G.A., et al., *Menopause and the risk of coronary heart disease in women.* N Engl J Med, 1987. **316**(18): p. 1105-10.

338. Gordon, T., et al., *Menopause and coronary heart disease. The Framingham Study.* Ann Intern Med, 1978. **89**(2): p. 157-61.

339. Rosamond, W., et al., *Heart disease and stroke statistics--2007 update: a report from the American Heart Association Statistics Committee and Stroke Statistics Subcommittee.* Circulation, 2007. **115**(5): p. e69-171.

340. Sohal, R.S. and R. Weindruch, *Oxidative stress, caloric restriction, and aging.* Science, 1996. **273**(5271): p. 59-63.

341. Finkel, T. and N.J. Holbrook, *Oxidants, oxidative stress and the biology of ageing.* Nature, 2000. **408**(6809): p. 239-47.

342. Lakatta, E.G., *Cardiovascular Aging: Perspectives From Humans to Rodents.* Am J Geriatr Cardiol, 1998. **7**(6): p. 32-45.

343. Ubaque, C.A., A.G. Hassig, and C.A. Mendoza, *Stack emissions tests in a brick manufacturing Hoffmann kiln: firing of municipal solid waste.* Waste Manag Res, 2010. **28**(7): p. 596-608.

344. Blough, E.R., et al., *Aging alters mechanical and contractile properties of the Fisher 344/Nnia X Norway/Binia rat aorta.* Biogerontology, 2007. **8**(3): p. 303-13.

345. Rice, K.M., et al., *Aging influences multiple incidices of oxidative stress in the aortic media of the Fischer 344/NNiaxBrown Norway/BiNia rat.* Free Radic Res, 2006. **40**(2): p. 185-97.

346. Rice, K.M., M. Wu, and E.R. Blough, *Aortic aging in the Fischer 344 / NNiaHSd x Brown Norway / BiNia Rat.* J Pharmacol Sci, 2008. **108**(4): p. 393-8.

347. Phaneuf, S. and C. Leeuwenburgh, *Cytochrome c release from mitochondria*

in the aging heart: a possible mechanism for apoptosis with age. Am J Physiol Regul Integr Comp Physiol, 2002. **282**(2): p. R423-30.

348. Anversa, P., et al., *Myocyte cell loss and myocyte hypertrophy in the aging rat heart.* J Am Coll Cardiol, 1986. **8**(6): p. 1441-8.

349. Patten, R.D., et al., *17beta-estradiol reduces cardiomyocyte apoptosis in vivo and in vitro via activation of phospho-inositide-3 kinase/Akt signaling.* Circ Res, 2004. **95**(7): p. 692-9.

350. Doublier, S., et al., *Testosterone and 17beta-estradiol have opposite effects on podocyte apoptosis that precedes glomerulosclerosis in female estrogen receptor knockout mice.* Kidney Int, 2010.

351. Barp, J., et al., *Myocardial antioxidant and oxidative stress changes due to sex hormones.* Braz J Med Biol Res, 2002. **35**(9): p. 1075-81.

352. Kaprielian, R.R. and N.J. Severs, *Dystrophin and the cardiomyocyte membrane cytoskeleton in the healthy and failing heart.* Heart Fail Rev, 2000. **5**(3): p. 221-38.

353. Rice, K.M. and E.R. Blough, *Sarcopenia-related apoptosis is regulated differently in fast- and slow-twitch muscles of the aging F344/N x BN rat model.* Mech Ageing Dev, 2006. **127**(8): p. 670-9.

354. Arvapalli, R.K., et al., *Deferasirox decreases age-associated iron accumulation in the aging F344XBN rat heart and liver.* Cardiovasc Toxicol, 2010. **10**(2): p. 108-16.

355. Wang, Y., et al., *Iron-induced cardiac damage: role of apoptosis and deferasirox intervention.* J Pharmacol Exp Ther, 2011. **336**(1): p. 56-63.

356. Misra, M.K., et al., *Oxidative stress and ischemic myocardial syndromes.* Med Sci Monit, 2009. **15**(10): p. RA209-219.

357. Pompeia, C., M.F. Cury-Boaventura, and R. Curi, *Arachidonic acid triggers an oxidative burst in leukocytes.* Braz J Med Biol Res, 2003. **36**(11): p. 1549-60.

358. Ghanizadeh, A., et al., *Glutathione-related factors and oxidative stress in autism, a review.* Curr Med Chem, 2012. **19**(23): p. 4000-5.

359. Judge, S., et al., *Age-associated increases in oxidative stress and antioxidant enzyme activities in cardiac interfibrillar mitochondria: implications for the mitochondrial theory of aging.* FASEB J, 2005. **19**(3): p. 419-21.

360. Ramesh, T., et al., *Effect of fermented Panax ginseng extract (GINST) on oxidative stress and antioxidant activities in major organs of aged rats.* Exp Gerontol, 2012. **47**(1): p. 77-84.

361. Escobales, N. and M.J. Crespo, *Oxidative-nitrosative stress in hypertension.* Curr Vasc Pharmacol, 2005. **3**(3): p. 231-46.

362. Leeuwenburgh, C., et al., *Markers of protein oxidation by hydroxyl radical and reactive nitrogen species in tissues of aging rats.* Am J Physiol, 1998. **274**(2 Pt 2): p. R453-61.

363. McLain, A.L., P.A. Szweda, and L.I. Szweda, *alpha-Ketoglutarate dehydrogenase: a mitochondrial redox sensor.* Free Radic Res, 2011. **45**(1): p. 29-36.

364. Anderson, E.J., L.A. Katunga, and M.S. Willis, *Mitochondria as a source and target of lipid peroxidation products in healthy and diseased heart.* Clin Exp Pharmacol Physiol, 2012. **39**(2): p. 179-93.

365. Smith, M.A. and R.G. Schnellmann, *Calpains, mitochondria, and apoptosis.* Cardiovasc Res, 2012. **96**(1): p. 32-7.

366. Kawara, T., et al., *Activation delay after premature stimulation in chronically diseased human myocardium relates to the architecture of interstitial fibrosis.* Circulation, 2001. **104**(25): p. 3069-75.

367. El-Sherif, N. and G. Turitto, *Electrolyte disorders and arrhythmogenesis.* Cardiol J, 2011. **18**(3): p. 233-45.

368. Nattel, S., et al., *Arrhythmogenic ion-channel remodeling in the heart: heart failure, myocardial infarction, and atrial fibrillation.* Physiol Rev, 2007. **87**(2): p. 425-56.

369. Litwin, S.E., et al., *Serial echocardiographic assessment of left ventricular geometry and function after large myocardial infarction in the rat.* Circulation, 1994. **89**(1): p. 345-54.

370. Litwin, S.E., et al., *Serial echocardiographic-Doppler assessment of left ventricular geometry and function in rats with pressure-overload hypertrophy. Chronic angiotensin-converting enzyme inhibition attenuates the transition to heart failure.* Circulation, 1995. **91**(10): p. 2642-54.

371. Aigbe, I.F., P.M. Kolo, and A.B. Omotoso, *Left ventricular structure and function in black normotensive type 2 diabetes mellitus patients.* Ann Afr Med, 2012. **11**(2): p. 84-90.

372. Drexler, E., et al., *An experimental method for measuring mechanical properties of rat pulmonary arteries verified with latex.* J Res Natl Stand Technol, 2003. **108**: p. 183-191.

373. Tsika, R.W., et al., *TEAD-1 overexpression in the mouse heart promotes an age-dependent heart dysfunction.* J Biol Chem, 2010. **285**(18): p. 13721-35.

374. Singh, P.N. and M. Sajjad Athar, *Simplified Calculation of Mean QRS Vector (Mean Electrical Axis of Heart) of Electrocardiogram.* Indian J Physiol Pharmacol, 2003. **47**(2): p. 212-216.

375. Hamlin, S.K., et al., *Role of diastole in left ventricular function, II: diagnosis and treatment.* Am J Crit Care, 2004. **13**(6): p. 453-66; quiz 467-8.

376. Sone, K., et al., *Changes of estrous cycles with aging in female F344/n rats.* Exp Anim, 2007. **56**(2): p. 139-48.

377. Wu, J.M., et al., *Ovarian aging and menopause: current theories, hypotheses, and research models.* Exp Biol Med (Maywood), 2005. **230**(11): p. 818-28.

378. Bestetti, R.B. and J.S. Oliveira, *The surface electrocardiogram: a simple and reliable method for detecting overt and latent heart disease in rats.* Braz J Med Biol Res, 1990. **23**(12): p. 1213-22.

379. Hayashi, H., et al., *Aging-related increase to inducible atrial fibrillation in the rat model.* J Cardiovasc Electrophysiol, 2002. **13**(8): p. 801-8.

380. Berta, E., et al., *Evaluation of the metabolic changes during hemodialysis by signal averaged ECG.* Pharmazie, 2012. **67**(5): p. 380-3.

381. Tong, Y. and H. Hou, *The alteration of QT dispersion in hemodialysis subjects.* Kidney Blood Press Res, 2006. **29**(4): p. 231-6.

382. Grandi, N.C., et al., *Calcium, phosphate and the risk of cardiovascular events and all-cause mortality in a population with stable coronary heart disease.* Heart, 2012. **98**(12): p. 926-33.

383. Sabir, I.N., et al., *Restitution analysis of alternans and its relationship to arrhythmogenicity in hypokalaemic Langendorff-perfused murine hearts.* Pflugers Arch, 2008. **455**(4): p. 653-66.

384. Yang, X.P. and J.F. Reckelhoff, *Estrogen, hormonal replacement therapy and cardiovascular disease.* Curr Opin Nephrol Hypertens, 2011. **20**(2): p. 133-8.

385. Sprott, R.L., *Development of animal models of aging at the National Institute of Aging.* Neurobiol Aging, 1991. **12**(6): p. 635-8.

386. Michel, T. and P.M. Vanhoutte, *Cellular signaling and NO production.* Pflugers Arch, 2010. **459**(6): p. 807-16.

387. Soucy, K.G., et al., *Impaired shear stress-induced nitric oxide production through decreased NOS phosphorylation contributes to age-related vascular stiffness.* J Appl Physiol, 2006. **101**(6): p. 1751-9.

388. Spier, S.A., et al., *Effects of ageing and exercise training on endothelium-dependent vasodilatation and structure of rat skeletal muscle arterioles.* J Physiol, 2004. **556**(Pt 3): p. 947-58.

389. Sun, D., et al., *Reduced release of nitric oxide to shear stress in mesenteric arteries of aged rats.* Am J Physiol Heart Circ Physiol, 2004. **286**(6): p. H2249-56.

390. White, A.R., et al., *Knockdown of arginase I restores NO signaling in the vasculature of old rats.* Hypertension, 2006. **47**(2): p. 245-51.

391. Muslin, A.J., *MAPK signalling in cardiovascular health and disease: molecular mechanisms and therapeutic targets.* Clin Sci (Lond), 2008. **115**(7): p. 203-18.

392. Xia, Z., et al., *Opposing effects of ERK and JNK-p38 MAP kinases on apoptosis.* Science, 1995. **270**(5240): p. 1326-31.

393. Xu, H., et al., *A heat shock protein 90 binding domain in endothelial nitric-oxide synthase influences enzyme function.* J Biol Chem, 2007. **282**(52): p. 37567-74.

394. Madrigal-Matute, J., et al., *Heat-shock proteins in cardiovascular disease.* Adv Clin Chem, 2011. **54**: p. 1-43.

395. Ghayour-Mobarhan, M., H. Saber, and G.A. Ferns, *The potential role of heat shock protein 27 in cardiovascular disease.* Clin Chim Acta, 2012. **413**(1-2): p. 15-24.

396. Rayner, K., et al., *Extracellular release of the atheroprotective heat shock protein 27 is mediated by estrogen and competitively inhibits acLDL binding to scavenger receptor-A.* Circ Res, 2008. **103**(2): p. 133-41.

397. Yu, Y.M., H.C. Lin, and W.C. Chang, *Carnosic acid prevents the migration of human aortic smooth muscle cells by inhibiting the activation and expression of matrix metalloproteinase-9.* Br J Nutr, 2008. **100**(4): p. 731-8.

398. Obata, H., et al., *NF-kappa B is induced in the nuclei of cultured rat aortic smooth muscle cells by stimulation of various growth factors.* Biochem Biophys Res Commun, 1996. **224**(1): p. 27-32.

399. Forman, K., et al., *Beneficial effects of melatonin on cardiological alterations in a murine model of accelerated aging.* J Pineal Res, 2010. **49**(3): p. 312-20.

400. Tanaka, S., et al., *Establishment of an Aging Farm of F344/N Rats and C57BL/6 Mice at the National Institute for Longevity Sciences (NILS).* Arch Gerontol Geriatr, 2000. **30**(3): p. 215-223.

401. Baba, T., et al., *Estrogen, insulin, and dietary signals cooperatively regulate longevity signals to enhance resistance to oxidative stress in mice.* J Biol Chem, 2005. **280**(16): p. 16417-26.

402. Sverko, V., et al., *Age-associated alteration of lipid peroxidation and superoxide dismutase activity in CBA and AKR mice.* Exp Gerontol, 2002. **37**(8-9): p. 1031-9.

403. Sverko, V., et al., *Age and gender differences in antioxidant enzyme activity: potential relationship to liver carcinogenesis in male mice.* Biogerontology,

2004. **5**(4): p. 235-42.

404. Zorov, D.B., M. Juhaszova, and S.J. Sollott, *Mitochondrial ROS-induced ROS release: an update and review.* Biochim Biophys Acta, 2006. **1757**(5-6): p. 509-17.

405. Juhaszova, M., et al., *Protection in the aged heart: preventing the heart-break of old age?* Cardiovasc Res, 2005. **66**(2): p. 233-44.

406. Datta, S.R., et al., *Akt phosphorylation of BAD couples survival signals to the cell-intrinsic death machinery.* Cell, 1997. **91**(2): p. 231-41.

407. del Peso, L., et al., *Interleukin-3-induced phosphorylation of BAD through the protein kinase Akt.* Science, 1997. **278**(5338): p. 687-9.

408. Cardone, M.H., et al., *Regulation of cell death protease caspase-9 by phosphorylation.* Science, 1998. **282**(5392): p. 1318-21.

409. Gelov, N., *[Diagnosis and treatment of closed abdominal wounds].* Khirurgiia (Sofiia), 1976. **29**(2): p. 116-8.

410. Report, T.W.H. and 1997, *Conquering, Suffering, Enriching Humanity*, 1997, World Health Organization: Geneva.

411. Thomas, D.P., et al., *Collagen gene expression in rat left ventricle: interactive effect of age and exercise training.* J Appl Physiol, 2000. **89**(4): p. 1462-8.

412. Kasi, V.S., et al., *Cardiac-restricted angiotensin-converting enzyme overexpression causes conduction defects and connexin dysregulation.* Am J Physiol Heart Circ Physiol, 2007. **293**(1): p. H182-92.

413. Walker, K.E., E.G. Lakatta, and S.R. Houser, *Age associated changes in membrane currents in rat ventricular myocytes.* Cardiovasc Res, 1993. **27**(11): p. 1968-77.

414. Fleg, J.L., et al., *Age-associated changes in the components of atrioventricular conduction in apparently healthy volunteers.* J Gerontol, 1990. **45**(3): p. M95-100.

415. Craft, N. and J.B. Schwartz, *Effects of age on intrinsic heart rate, heart rate variability, and AV conduction in healthy humans.* Am J Physiol, 1995. **268**(4 Pt 2): p. H1441-52.

416. Cranefield, P.F., A.L. Wit, and B.F. Hoffman, *Conduction of the cardiac impulse. 3. Characteristics of very slow conduction.* J Gen Physiol, 1972. **59**(2): p. 227-46.

417. Cole, W.C., J.B. Picone, and N. Sperelakis, *Gap junction uncoupling and discontinuous propagation in the heart. A comparison of experimental data with computer simulations.* Biophys J, 1988. **53**(5): p. 809-18.

418. Rohr, S., J.P. Kucera, and A.G. Kleber, *Slow conduction in cardiac tissue, I:*

effects of a reduction of excitability versus a reduction of electrical coupling on microconduction. Circ Res, 1998. **83**(8): p. 781-94.

419. Gardner, P.I., et al., *Electrophysiologic and anatomic basis for fractionated electrograms recorded from healed myocardial infarcts.* Circulation, 1985. **72**(3): p. 596-611.

420. Adiga, I.K. and R.R. Nair, *Multiple signaling pathways coordinately mediate reactive oxygen species dependent cardiomyocyte hypertrophy.* Cell Biochem Funct, 2008. **26**(3): p. 346-51.

421. Brunk, U.T. and A. Terman, *The mitochondrial-lysosomal axis theory of aging: accumulation of damaged mitochondria as a result of imperfect autophagocytosis.* Eur J Biochem, 2002. **269**(8): p. 1996-2002.

422. Muscari, C., C.M. Caldarera, and C. Guarnieri, *Age-dependent production of mitochondrial hydrogen peroxide, lipid peroxides and fluorescent pigments in the rat heart.* Basic Res Cardiol, 1990. **85**(2): p. 172-8.

423. Sohal, R.S. and B.H. Sohal, *Hydrogen peroxide release by mitochondria increases during aging.* Mech Ageing Dev, 1991. **57**(2): p. 187-202.

424. Han, L., et al., *Gender differences in the relationship between age-related carotid intima-media thickness and cardiac diastolic function in a healthy Chinese population.* J Card Fail, 2013. **19**(5): p. 325-32.

425. Albu, A., et al., *Arterial stiffness, carotid atherosclerosis and left ventricular diastolic dysfunction in postmenopausal women.* Eur J Intern Med, 2013. **24**(3): p. 250-4.

426. Wu, G., et al., *[An antihypertensive factor in the erythrocytes of essential hypertensive subjects].* Chin Med Sci J, 1991. **6**(2): p. 122.

427. Spinale, F.G., *Myocardial matrix remodeling and the matrix metalloproteinases: influence on cardiac form and function.* Physiol Rev, 2007. **87**(4): p. 1285-342.

428. Louch, W.E., et al., *No rest for the weary: diastolic calcium homeostasis in the normal and failing myocardium.* Physiology (Bethesda), 2012. **27**(5): p. 308-23.

429. Bers, D.M., *Altered cardiac myocyte Ca regulation in heart failure.* Physiology (Bethesda), 2006. **21**: p. 380-7.

430. Virmani, R., et al., *Effect of aging on aortic morphology in populations with high and low prevalence of hypertension and atherosclerosis. Comparison between occidental and Chinese communities.* Am J Pathol, 1991. **139**(5): p. 1119-29.

431. Smith, A.R., F. Visioli, and T.M. Hagen, *Plasma membrane-associated*

endothelial nitric oxide synthase and activity in aging rat aortic vascular endothelia markedly decline with age. Arch Biochem Biophys, 2006. **454**(1): p. 100-5.

432. Fulton, D., et al., *Regulation of endothelium-derived nitric oxide production by the protein kinase Akt.* Nature, 1999. **399**(6736): p. 597-601.

433. Ward, N.C., et al., *Chronic activation of AMP-activated protein kinase prevents 20-hydroxyeicosatetraenoic acid-induced endothelial dysfunction.* Clin Exp Pharmacol Physiol, 2011. **38**(5): p. 328-33.

434. Yetik-Anacak, G., et al., *Effects of hsp90 binding inhibitors on sGC-mediated vascular relaxation.* Am J Physiol Heart Circ Physiol, 2006. **291**(1): p. H260-8.

435. Schulz, E., et al., *Estradiol-mediated endothelial nitric oxide synthase association with heat shock protein 90 requires adenosine monophosphate-dependent protein kinase.* Circulation, 2005. **111**(25): p. 3473-80.

436. Takahashi, S. and M.E. Mendelsohn, *Synergistic activation of endothelial nitric-oxide synthase (eNOS) by HSP90 and Akt: calcium-independent eNOS activation involves formation of an HSP90-Akt-CaM-bound eNOS complex.* J Biol Chem, 2003. **278**(33): p. 30821-7.

437. Harris, M.B., et al., *Heat-induced increases in endothelial NO synthase expression and activity and endothelial NO release.* Am J Physiol Heart Circ Physiol, 2003. **285**(1): p. H333-40.

438. Bauer, P.M., et al., *Compensatory phosphorylation and protein-protein interactions revealed by loss of function and gain of function mutants of multiple serine phosphorylation sites in endothelial nitric-oxide synthase.* J Biol Chem, 2003. **278**(17): p. 14841-9.

439. Bucci, M., et al., *17-beta-oestradiol-induced vasorelaxation in vitro is mediated by eNOS through hsp90 and akt/pkb dependent mechanism.* Br J Pharmacol, 2002. **135**(7): p. 1695-700.

440. Jacobsen, B.K., et al., *Does age at natural menopause affect mortality from ischemic heart disease?* J Clin Epidemiol, 1997. **50**(4): p. 475-9.

441. Morrow, D., et al., *Cyclic strain inhibits Notch receptor signaling in vascular smooth muscle cells in vitro.* Circ Res, 2005. **96**(5): p. 567-75.

442. Rivard, A., N. Principe, and V. Andres, *Age-dependent increase in c-fos activity and cyclin A expression in vascular smooth muscle cells. A potential link between aging, smooth muscle cell proliferation and atherosclerosis.* Cardiovasc Res, 2000. **45**(4): p. 1026-34.

443. Moon, S.K., et al., *Aging, oxidative responses, and proliferative capacity in cultured mouse aortic smooth muscle cells.* Am J Physiol Heart Circ Physiol,

2001. **280**(6): p. H2779-88.

444. Roy, J., et al., *Phenotypic modulation of arterial smooth muscle cells is associated with prolonged activation of ERK1/2.* Differentiation, 2001. **67**(1-2): p. 50-8.

445. Hayashi, K., et al., *Changes in the balance of phosphoinositide 3-kinase/protein kinase B (Akt) and the mitogen-activated protein kinases (ERK/p38MAPK) determine a phenotype of visceral and vascular smooth muscle cells.* J Cell Biol, 1999. **145**(4): p. 727-40.

446. Li, M., et al., *Age-related differences in MAP kinase activity in VSMC in response to glucose or TNF-alpha.* J Cell Physiol, 2003. **197**(3): p. 418-25.

447. Miller, H., et al., *Modulation of estrogen signaling by the novel interaction of heat shock protein 27, a biomarker for atherosclerosis, and estrogen receptor beta: mechanistic insight into the vascular effects of estrogens.* Arterioscler Thromb Vasc Biol, 2005. **25**(3): p. e10-4.

APPENDIX

LETTER FROM INSTITUTIONAL RESEARCH BOARD

MARSHALL UNIVERSITY®

www.marshall.edu

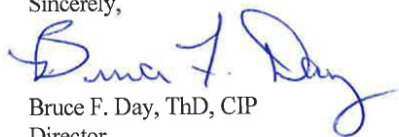Office of Research Integrity

October 23, 2012

Jacqueline Fannin
11101 Indian Legends Dr., Apt. 202
Louisville, KY 40241

Dear Ms. Fannin:

This letter is in response to the submitted dissertation abstract titled "Age-Associated Alterations in the Female F344XBN Rat Heart and Aorta." After assessing the abstract it has been deemed not to be human subject research and therefore exempt from oversight of the Marshall University Institutional Review Board (IRB). The Institutional Animal Care and Use Committee (IACUC) has reviewed and approved the study under protocol #367. The applicable human and animal federal regulations have set forth the criteria utilized in making this determination. If there are any changes to the abstract you provided then you would need to resubmit that information to the Office of Research Integrity for review and a determination.

I appreciate your willingness to submit the abstract for determination. Please feel free to contact the Office of Research Integrity if you have any questions regarding future protocols that may require IRB review.

Sincerely,

Bruce F. Day, ThD, CIP
Director
Office of Research Integrity

WE ARE... MARSHALL®

401 11th Street, Suite 1300 • Huntington, West Virginia 25701 • Tel 304/696-7320
A State University of West Virginia • An Affirmative Action/Equal Opportunity Employer

CURRICULUM VITAE

Jacqueline C. Fannin BS

1539 Thompson Road Culloden, WV 25510
Phone: (606)-225-0344
Email: decker8@marshall.edu

Career Objective

To work as a postdoctoral research assistant to further my research skills, gain grant writing in addition to teaching experience in order to prepare for a future assistant professor position.

Education

Aug 2003-Jun 2007   BS, Biological Sciences (Molecular Physiology) College of Science, Marshall University, Huntington, WV

July 2007-Present   Ph.D., Biomedical Sciences (Cardiovascular Disease, Obesity, and Diabetes) Joan C Edward School of Medicine, Marshall University, Huntington, WV

Dissertation Project – "Cardiovascular Aging in the Female F344xBN Rat Model"
Advisor: Dr. Eric Blough

Objectives:
  i.   To investigate the age-associated alterations in the cardiovascular structure, function, and protein signaling in the female F344xBN rat

Results:
  i.   Aging in the female F344xBN rat heart is associated with increased oxidative-nitrosative stress and mitochondrial-mediated apoptosis (manuscript in preparation).

  ii.   The aging female F344xBN heart was associated with slight evidence of diastolic dysfunction, arrhythmias, heart rhythm alterations, in addition to increases in connexin 43 heterogeneity and spatial variable redistribution (manuscript in review).

  iii. The female F344xBN aorta exhibited increased medial thickness and activation of p44/42 with age (manuscript in preparation).

Professional Experience

Graduate Research Assistant – (July 2007- May 2012)

Joan C Edward School of Medicine, Marshall University, Huntington, WV

  ➢ Investigated and implemented research projects on the aging cardiovascular system in an aging rodent model
  ➢ Responsible for the maintenance, treatment, and biochemical in addition to physiological monitoring of laboratory animals
  ➢ Assisted veterinarians in euthanizing and collection of tissues from laboratory animals
  ➢ Used immunohistochemistry and histological stains to determine alterations in animal tissue sections
  ➢ Mentored graduate and undergraduate students in methodology and analysis of microRNA isolation/expression, protein signaling, quantitative real time PCR, and echocardiogram parameters in rodents
  ➢ Assisted in preparation, readings, and analysis of echocardiograms in addition to electrocardiograms of aging rodents
  ➢ Isolation and quantification of microRNAs involved in cardiovascular aging
  ➢ Involved in the design and development of microRNA isolation and quantitative real time PCR protocols for skeletal muscle, cardiac muscle and serum
  ➢ Investigated different statistical analysis methods for miRNA expression
  ➢ Preparation of manuscripts for publication

Research Assistant – (May 2007 – Aug 2007)

Laboratory of Molecular Physiology, Marshall University, Huntington, WV

  ➢ Isolation and quantification of microRNAs involved in cardiovascular aging, skeletal muscle hind limb suspension models, animal cell cultures, and serum
  ➢ Maintained and treated animal cell cultures in order to isolate microRNA and protein expression

Research Student Assistant – (May 2006 –Aug 2007)

Department of Biological Science, Marshall University, Huntington, WV

- ➢ Investigated the effects of microgravity using bioreactors on protein expression in plant cell cultures
- ➢ Implemented standard protocols for the maintenance and operation of a NASA microgravity bioreactor
- ➢ Micropropagation and maintenance of callus in addition to liquid sandalwood, soybean, and periwinkle plant cell cultures
- ➢ Investigated the effects of microgravity on plant cell culture morphology using fluorescence confocal microscopy
- ➢ Mentored undergraduate students in plant cell culture techniques in addition NASA microgravity bioreactor assembly, operation, and maintenance

Skills and Techniques

- ➢ Laboratory animal husbandry and maintenance
- ➢ Biochemical and physiological monitoring of lab animals
- ➢ Electrocardiography of rodents
- ➢ Plant and animal cell cultures
- ➢ Immunohistochemistry
- ➢ Immunoblotting
- ➢ DNA, RNA, and miRNA isolation/quantitation
- ➢ PCR and Quantitative Real Time PCR

Familiarity of Techniques

- ➢ Echocardiography of rodents
- ➢ Microarray
- ➢ Confocal microscopy

Computer Skills

- ➢ Sigma Stat
- ➢ Alpha Ease and Image J
- ➢ Adobe
- ➢ MS Office

Awards and Honors

July 2007 – Jan 2012: Marshall University, NSFEPSCoR Graduate Assistantship

May 2006 – May 2007: NASA Undergraduate Research Fellowship

Extracurricular Activities

Graduate Student Organization (July 2007 – July 2011)

Marshall University Brain Expo (March 2009 and March 2010)

Publications in Peer-Reviews Journals

Fannin J, Wang Y, Arvapalli R, Wehner, Rice K, and Blough ER. The Effects of Aging on Indices of Oxidative Stress and Apoptosis in the Female Fischer 344/Nnia x Brown Norway/BiNia Rat Heart. Open Cardiovasc Med J. 2013 Nov 29;7:113-21.

Wang Y, Wu M, Al-Rousan R, Liu H, **Fannin J**, Paturi S, Arvapalli R, Katta A, Kakarla SK, Rice K, Triest WE, Blough ER. Iron-induced cardiac damage: role of apoptosis and deferasirox intervention. J Pharmacol Exp Ther. 2011 Jan;336[410]:56-63

Katta A, Kundla S, Kakarla SK, Wu M, **Fannin J**, Paturi S, Liu H, Addagarla HS, Blough ER. Impaired overload-induced hypertrophy is associated with diminished mTOR signaling in insulin resistant skeletal muscle of the obese Zucker rat. Am J Physiol Regul Integr Comp Physiol. 2010 Dec; 299(6):R1666-75.

Wu M, Liu H, **Fannin J**, Katta A, Wang Y, Arvapalli RK, Paturi S, Kakarla SK, Rice KM, Blough ER. Acetaminophen Improves Protein Translational Signaling in Aged Skeletal Muscle. Rejuvenation Res. 2010 Oct; 13(5):571-9

Kakarla SK, **Fannin J**, Keshavarzian S, Katta A, Paturi S, Nalabotu SK, Wu M, Rice KM, Manzoor K, Walker EM Jr, Blough ER; Chronic acetaminophen attenuates age-associated increases in cardiac ROS and apoptosis in the Fischer Brown Norway Hybrid Rat. Basic Res Cardiol. 2010 Jul; 105(4):535-44

Wu M, Katta A, Gadde MK, Liu H, Kakarla SK, **Fannin J**, Paturi S, Arvapalli RK, Rice KM, Wang Y, Blough ER. Aging-associated dysfunction of Akt / protein kinase B: S-nitrosylation and acetaminophen intervention. PLoS One. 2009 Jul 29; 4[410]:e6430.

Wu M, **Fannin J**, Rice KM, Wang B, Blough ER. Effect of aging on cellular mechanotransduction. Aging Res Rev. 2011 Jan; 10[410]-15.

Manuscripts in Review

Fannin J, Thulluri S, Dornon L, Arvapalli R, Paturi S, Gadde M, Khitan F, Wehner P, Rice K, and Blough ER. Age-associated Alterations of Cardiac Structure and Function in the Female F344xBN Rat Heart.

Manuscripts in Preparation

Fannin J, Para R, Thulluri S, Triest W, Rice K, and Blough ER. Age-associated Alterations of Morphology and Protein Signaling in the Female F344xBN Rat Aorta.

Abstracts and Presentations

Fannin J, Neal M, Kakarla S, Katta A, Paturi S, Gutta A, Wu M, Dornon L, Rice K, Santanam N, and Blough ER. The Effects of Aging in MicroRNA Expression in the Fischer 344/NNia x Brown Norway/BiNia Female Rat Heart. Journal of the American College of Cardiology. 2009. 53; A144-A197.

Fannin J, University of Kentucky Cardiovascular Research Day. 2008. Lexington, KY

References

Dr. Eric R. Blough, Ph.D.
Ph.D. Advisor
Associate Professor
Department of Pharmaceutical Science Research
Center for Diagnostic Nanosystems
Marshall University, Huntington, WV
Phone: (304) 696-2708
E-mail: blough@marshall.edu

Dr. Richard Egleton Ph.D.
Associate Professor
Dept. of Physiology, Pharmacology and Toxicology
Joan C Edward School of Medicine
Marshall University, Huntington, WV
Phone: (304) 696-3523
E-mail: egelton@marshall.edu,

Dr. Todd L. Green, Ph.D.
Associate Professor and Director of Graduate Studies of Biomedical Sciences Graduate Program
Dept. of Pharmacology, Physiology and Toxicology
Phone: (304) 696-3531
E-mail: green@marshall.edu